INFORMATION TO USERS

The most advanced technology has been used to photograph and reproduce this manuscript from the microfilm master. UMI films the original text directly from the copy submitted. Thus, some dissertation copies are in typewriter face, while others may be from a computer printer.

In the unlikely event that the author did not send UMI a complete manuscript and there are missing pages, these will be noted. Also, if unauthorized copyrighted material had to be removed, a note will indicate the deletion.

Oversize materials (e.g., maps, drawings, charts) are reproduced by sectioning the original, beginning at the upper left-hand corner and continuing from left to right in equal sections with small overlaps. Each oversize page is available as one exposure on a standard 35 mm slide or as a 17″ × 23″ black and white photographic print for an additional charge.

Photographs included in the original manuscript have been reproduced xerographically in this copy. 35 mm slides or 6″ × 9″ black and white photographic prints are available for any photographs or illustrations appearing in this copy for an additional charge. Contact UMI directly to order.

Accessing the World's Information since 1938

300 North Zeeb Road, Ann Arbor, MI 48106-1346 USA

Order Number 8801698

Mitochondrial metabolism of 3-mercaptopropionic acid; aspects of the β-oxidation of unsaturated fatty acids; steady-state kinetics of coupled enzyme reactions

Cuebas, Dean Anthony, Ph.D.

City University of New York, 1987

U·M·I
300 N. Zeeb Rd.
Ann Arbor, MI 48106

PLEASE NOTE:

In all cases this material has been filmed in the best possible way from the available copy. Problems encountered with this document have been identified here with a check mark __✓__.

1. Glossy photographs or pages _____
2. Colored illustrations, paper or print _____
3. Photographs with dark background _____
4. Illustrations are poor copy _____
5. Pages with black marks, not original copy __✓__
6. Print shows through as there is text on both sides of page _____
7. Indistinct, broken or small print on several pages __✓__
8. Print exceeds margin requirements _____
9. Tightly bound copy with print lost in spine _____
10. Computer printout pages with indistinct print _____
11. Page(s) _____ lacking when material received, and not available from school or author.
12. Page(s) _____ seem to be missing in numbering only as text follows.
13. Two pages numbered _____. Text follows.
14. Curling and wrinkled pages _____
15. Dissertation contains pages with print at a slant, filmed as received _____
16. Other _____

_____

_____

University
Microfilms
International

MITOCHONDRIAL METABOLISM OF 3-MERCAPTOPROPIONIC ACID; ASPECTS OF THE β-OXIDATION OF UNSATURATED FATTY ACIDS; STEADY-STATE KINETICS OF COUPLED ENZYME REACTIONS

by

Dean Cuebas

A dissertation submitted to the Graduate Faculty in Biochemistry
in partial fulfillment of the requirements for the degree of
Doctor of Philosophy, The City University of New York.

1987

This manuscript has been read and accepted for the Graduate Faculty in Biochemistry in satisfaction of the dissertation requirement for the degree of Doctor of Philosophy.

1/23/1987
Date

Chair of Examing Committee

1/23/1987
Date

Executive Officer

Supervisory Committee

The City University of New York

ABSTRACT

MITOCHONDRIAL METABOLISM OF 3-MERCAPTOPROPIONIC ACID; ASPECTS OF THE β-OXIDATION OF UNSATURATED FATTY ACIDS; STEADY-STATE KINETICS OF COUPLED ENZYME REACTIONS

by

Dean Cuebas

Advisor: Dr. Horst Schulz

The metabolism of 3-mercaptopropionic acid in mitochondria was studied by use of purified mitochondrial enzymes and rat heart mitochondria. Metabolites of 3-mercaptopropionic acid were separated by high performance liquid chromatography and identified by comparing them with chemically synthesized derivatives of 3-mercaptopropionic acid. The initial step in the metabolism of 3-mercaptopropionic acid is its conversion to a CoA thioester, most likely catalyzed by medium-chain acyl-CoA synthetase. The resulting 3-mercaptopropionyl-CoA is a poor substrate of acyl-CoA dehydrogenase but substitutes effectively for CoASH in reactions catalyzed by 3-ketoacyl-CoA thiolase and acetoacetyl-CoA thiolase. S-Acyl-3-mercaptopropionyl-CoA thioesters formed in the thiolase-catalyzed reactions are not at all or only poorly acted upon by acyl-CoA dehydrogenases. However, they are hydrolyzed by thioesterase(s) to CoASH and S-acyl-3-mercaptopropionic acid. The hydrolysis of S-acyl-3-mercaptopropionyl-CoA thioesters proceeds more rapidly than the hydrolysis of fatty acyl-CoA thioesters of comparable chain lengths. Free CoASH is also regenerated from S-acetyl-3-mercaptopropionyl-CoA and more rapidly from 3-mercaptopropionyl-CoA as a result of their reactions with carnitine catalyzed by carnitine acetyltransferase.

These findings lead to the suggestion that the major mitochondrial CoA-containing metabolites of 3-mercaptopropionic acid are S-acyl-3-mercaptopropionyl-CoA thioesters.

Using coupled rat heart mitochondria, previous work in our laboratory found 3-mercaptopropionic acid to be a potent inhibitor of respiration sustained by palmitoylcarnitine, whereas under identical conditions respiration with pyruvate as a substrate was unaffected. Since 3-mercaptopropionic acid did not inhibit β-oxidation in uncoupled mitochondria, it appears that this compound must first be metabolized in an energy-dependent reaction before it becomes inhibitory. With this knowledge, 3-mercaptopropionyl-CoA and three of its S-acyl derivatives, all of which are likely mitochondrial metabolites of 3-mercaptopropionic acid , were tested for their capacity to inhibit the individual enzymes of β-oxidation. 3-Mercaptopropionyl-CoA inhibits only acyl-CoA dehydrogenase, whereas S-myristoyl-3-mercaptopropionyl-CoA inhibits reversibly several β-oxidation enzymes. All observations together lead to the suggestion that the inhibition of β-oxidation by 3-mercaptopropionic acid in coupled rat heart mitochondria is most likely a consequence of the reversible inhibition of acyl-CoA dehydrogenase by long-chain S-acyl-3-mercaptopropionyl-CoA thioesters and possibly by 3-mercaptopropionyl-CoA.

A collaborative investigation of the metabolism of 2,4-decadienoyl-CoA, a presumed metabolite in the oxidation of linoleic acid, necessitated the synthesis of various geometric isomers of 2,4-decadienoic acid and their respective CoA derivatives. Additionally, geometrically and optically pure 3-hydroxy-4-decenoic acids and their CoA thioesters were prepared. The characterization of these materials is presented , as well the comparisons of the electronic spectra of three of the four possible geometric isomers of 2,4-decadienoyl-CoA. The equilibrium constant of the 3-hydroxyacyl-CoA dehydrogenase catalyzed oxidation of L-3-hydroxy-4-*trans*-decenoyl-CoA was determined and found to be 1.1×10^{-8} M, which is significantly higher than the equilibrium constant that had been previously determined for saturated 3-hydroxyacyl-CoA's.

A mathematical analysis of the steady state kinetics of coupled enzyme reactions is presented, where the primary reaction is thermodynamically very unfavored. The model assumes the primary enzyme to obey a uni uni reversible mechanism and the coupling enzyme to follow a uni irreversible mechanism. The simplifying assumptions which are made for such systems allow the determination of the equilibrium constant of the primary reaction with only the knowledge of the forward kinetic parameters of the coupling enzyme. The derivation of several equations that take into account high concentrations of primary and coupling enzymes is presented, as well as an analysis of the error associated with the use of simple rate equations that do not take into account the binding of substrates due to high enzyme concentrations. The results of the error analysis show that under most circumstances the use of simplified equations that do not take into account substrate depletion leads to errors in initial rate predictions that are insignificant, even at infinite concentration of coupling enzyme, although it is shown that under unusual circumstances, it may not be possible to construct a coupled enzyme system where the rate limiting steps are independent of coupling enzyme, even at infinite concentrations of the the latter.

ACKNOWLEDGEMENTS

I would first like to thank the people at MIT for developing MACSYMA, without which the kinetic analyses would not have been possible. Secondly, I would like to express my appreciation to Dr. Leslie Kushner for the innumerable discussions we had concerning our related research projects. Much thanks also goes to Emily Sabbagh for her initial studies on 3-mercaptopropionic acid, and to Dr. Song-Yu Yang for a productive collaboration which forced me to learn something about enzyme kinetics. I also wish to thank all the members of the biochemistry faculty at City College and the thesis committee members for their encouragement and also the Minority Biomedical Research Support Program for their financial support. I would like to thank my family for their constant support throughout the years, and lastly my deepest appreciation goes to my mentor, friend, and colleague, Dr. Horst Schulz.

TABLE OF CONTENTS

LIST OF TABLES

LIST OF FIGURES

ABBREVIATIONS

ADP adenosine 5'-diphosphate
ATP adenosine 5'-triphosphate
BSA bovine serum albumin
CoA coenzyme A
CoASH coenzyme A
DEAE diethylamino ethyl
E. coli Escherichia coli
EDTA ethylene diamine tetraacetic acid
EGTA ethylene glycol bis -(β-aminoethyl ether)N,N'-tetraacetic acid
HPLC high performance liquid chromatography
NAD nicotinamide adenine dinucleotide
NADP nicotinamide adenine dinucleotide phosphate
NADPH reduced nicotinamide adenine dinuleotide phosphate
tms tetramethyl silane
Tris tris(hydroxymethyl)amino methane
UV ultraviolet

INTRODUCTION

A major catabolic pathway in most living systems is the degradation of fatty acids. Many tissues normally derive their metabolic energy from the extremely thermodynamically favored oxidation of fatty acids (resting skeletal muscle and heart tissue), and therefore a competent fatty acid degrading system is essential for these tissues to sustain a normal level of metabolic activity. Also, ketogenesis in liver requires an active β-oxidation system. Recent work has shown that inherited defects in one or more of the enzymes required for this process can result in diseased states that vary from mild muscle weakness to death.[1, 2] Tissues that do not rely heavily on fatty acid degradation for the production of metabolic energy still contain measureable levels of β-oxidation activity which is most probably required for the turnover of fatty acids that are components of membrane phospholipids. In prokaryotes such as *E. coli*, fatty acids can be utilized as the sole carbon source, and therefore all carbon containing cellular constituents can be synthesized from the oxidation products of fatty acids. Thus, the catabolism of fatty acids is an important intracellular process that is common to essentially all forms of living systems and much effort has gone into investigating the details of this process on the molecular level.

The basic scheme for the degradation of the carbon skeleton of fatty acids in eukaryotes was elucidated several decades ago by various groups,[3, 4] and was found to occur in the mitochondrial fraction obtained by differential centrifugation of rat liver homogenates. It involves the stepwise removal of two-carbon units from a fatty acid that is thioesterified to coenzyme A. Figure 1 shows the four reactions involved in the β-oxidation cycle. The enzymes of β-oxidation have been purified from a variety of sources and a recent review describes the history as well as the current understanding of many of the molecular details of fatty acid oxidation.[5]

In addition to understanding the molecular transformations and characterizing the enzymes involved in a metabolic pathway, an important aspect of intermediary metabolism involves the elucidation of the regulation of metabolic pathways. Glycolysis, gluconeogenesis, glycogenolysis, and many other important intermediary metabolic pathways are controlled by a variety of mechanisms to insure proper control of fluxes through these pathways. In contrast, evidence for the regulation of β-oxidation by hormones via second messengers, by covalent modification, or allosteric control of enzymes is lacking, and therefore a major thrust of our laboratory has been the search for factors that control rates of β-oxidation. Our laboratory [6] has found no effect of many of the important hormones on the rates of β-oxidation in rat heart cells, and despite an extensive search for allosteric modulators of β-oxidation enzymes, none have been found. The only reported modulatory effect which could possibly be of importance in the control of fatty acid oxidation is the finding that malonyl-CoA, an endogenous cytosolic metabolite of *de novo* fatty acid synthesis, is a potent reversible inhibitor of carnitine palmitoyltransferase, the enzyme system responsible for the interconversion of acyl-CoA's and acyl-carnitines necessary for the import and export of long- and medium-chain acyl groups between the intramitochondrial space and the cytosol.[7] With regard to the β-oxidation cycle itself, our laboratory has investigated the possibility of product inhibition of β-oxidation enzymes by the various intermediates formed during this process. This work has led to the conclusions shown in Figure 2; the rate of β-oxidation is tuned to the rate of the tricarboxylic acid cycle primarily by the inhibition of 3-ketoacyl-CoA thiolase by acetyl-CoA. In order for the above hypothesis to be valid, the rate of the 3-ketoacyl-CoA thiolase reaction should be rate limiting for the overall process, and evidence for this has been obtained by the use of 4-bromocrotonic acid, a synthetic irreversible inhibitor of this enzyme in a study with coupled rat heart mitochondria.[8]

Other inhibitors of β-oxidation include 4-pentenoate[9] , hypoglycin[10] , 2-bromopalmitate[11, 12] , 2{5(4-chlorophenyl)pentyl}oxirane-2-carboxylate[13, 14] , and 2-tetradecylglycidic acid.[15, 16] Almost invariably, a necessary condition for a compound to be a potent inhibitor of a β-oxidation enzyme is the prior activation to its

respective CoA thioester. This is not so surprising since a reasonably productive binding event between substrate and a β-oxidation enzyme occurs only when the fatty acyl substrate is covalently attached to the multifunctional CoA moiety. Subsequent to activation, many known oxidation inhibitors must also be further metabolized by one or more β-oxidation steps to yield an acyl-CoA intermediate that is the actual inhibitory species. Such is the case for 4-bromocrotonic acid, which subsequent to its activation, is metabolized by two β-oxidation steps to yield 4-bromo-3-keto-butyryl-CoA which appears to inactivate 3-ketoacyl-CoA thiolase by covalent modification of one of the sulfhydryl groups at the active site.[8]

It is obvious from the above, that the identification or design of synthetic enzyme inhibitors can greatly aid the study of metabolic regulation by providing the tool for specifically inhibiting a given pathway or enzymatic activity. We were, therefore, very interested when Sabourault, *et al.*,[17] and Bauche, *et al.*,[18-20] reported that β-oxidation in rat liver is inhibited by 2-mercaptoacetic acid. Using liver mitochondria from 2-mercaptoacetic acid treated rats, these workers found that the inhibition of β-oxidation was not due to impaired fatty acid uptake by mitochondria, or to impaired respiratory-chain and citrate-cycle activities or to impaired coupling of oxidation to phosphorylation, but was apparently caused by the inhibition of long-chain acyl-CoA dehydrogenase activity. Subsequent *in vitro* experiments with mitochondria isolated from the livers of normal rats led to the conclusions that (a), 2-mercaptoacetic acid is able to enter the mitochondrial matrix, (b), inhibition of fatty acid oxidation requires the activation of 2-mercaptoacetic acid through an energy-dependent process, and (c) a metabolite of 2-mercaptoacetic acid (probably 2-mercaptoacetyl-CoA) inhibits reversibly the three acyl-CoA dehydrogenases (long-chain, general-chain, and short-chain), as well as the branched-chain dehydrogenase.

In light of the above findings, our laboratory decided to further investigate the effects of 2-mercaptoacetic acid in a rat heart mitochondrial system, and in addition, test the effects of various commercially available short-chain

mercaptoacids on β-oxidation. 3-Mercaptopropionic acid was found to be a potent inhibitor of respiration sustained by palmitoylcarnitine or octanoate, whereas under identical conditions, respiration with pyruvate was unaffected.[21] 2-Mercaptoacetic acid also inhibited palmitoylcarnitine supported respiration, but only at much higher concentrations of the inhibitor, whereas 2-mercaptopropionic acid was without effect. Since 3-mercaptopropionic acid was the most effective of the three short-chain mercaptoacids tested, further work in our laboratory concentrated on further characterizing the inhibition of β-oxidation by this compound. Interestingly, 3-mercaptopropionic acid causes convulsions in mice[22], presumably by lowering the concentration of γ-aminobutyric acid in brain.[23] It has also been suggested that 3-mercaptopropionic acid interferes with energy metabolism in brain mitochondria, possibly by affecting the utilization or formation of ATP.[24]

Since incubation of mitochondria with 3-mercaptopropionic acid did not cause the irreversible inactivation of any β-oxidation enzyme,[21] an understanding of the mechanism of β-oxidation inhibition by this compound required elucidating its metabolism and a substantial portion of this thesis describes the work performed toward this end.

Another area of recent interest is the β-oxidation of unsaturated fatty acids. Most naturally occurring unsaturated fatty acids contain *cis* double bonds and these can extend from either odd or even numbered carbon atoms of the fatty acid. Degradation of an unsaturated fatty acid containing an odd numbered double bond can proceed via β-oxidation until a 3-enoyl-CoA derivative is obtained. This intermediate is not a substrate for any of the four β-oxidation enzymes and the enzyme *3-cis,2-trans*-enoyl-CoA isomerase transforms this intermediate to a *2-trans*-enoyl-CoA which can now proceed through the β-oxidation cycle. This activity was reported by several groups[25-27] and has since been purified and characterized.[28, 29]

In the case of double bonds extending from even-numbered carbons, normal β-oxidation would yield a 2-*cis*-enoyl-CoA which is hydrated by enoyl-CoA hydratase to a D-3-hydroxyacyl-CoA. The latter compound is not a substrate for 3-hydroxyacyl-CoA dehydrogenase since this enzyme is absolutely specific for the L isomer. The discovery of a 3-hydroxyacyl-CoA epimerase activity by Stoffel[30], which interconverts D-, and L-3-hydroxyacyl-CoA's in the absence of exogenously added NAD led to the conclusion that the epimerase activity is absolutely required for the complete degradation of unsaturated fatty acids with double bonds extending from even numbered carbons.

More recently, a reductase activity was reported that is capable of reducing 2,4-dienoyl-CoA's to 3-*trans*-enoyl-CoA's[31-35] Work by Kunau and others[36, 37] has provided convincing evidence for the participation of the enzyme in the degradation of 2,4-dienoyl-CoA intermediates arising from the β-oxidation of polyunsaturated fatty acids. Figure 3 shows the epimerase and reductase pathways.

Since the two pathways diverge at the level of the dienoyl-CoA intermediate, Cuebas and Schulz[38] investigated the ability of these type of compounds to participate in both pathways. Using a rat heart mitochondrial extract and a system reconstituted from purified mitochondrial β-oxidation enzymes, it was found that 2-*trans*,4-*trans*-dienoyl-CoA, 2-*trans*,4-*cis*-dienoyl-CoA, and 2-*cis*,4-*cis*-dienoyl-CoA are all reduced by the reductase at comparable rates, whereas only the 2-*trans*,4-*trans* isomer is capable of sustaining measurable rates of β-oxidation via the old pathway. It was therefore concluded that the reductase is required for the complete degradation of unsaturated fatty acids containing even numbered *cis* double bonds, whereas the complete degradation of unsaturated fatty acids containing even numbered *trans* double bonds can probably procede via both pathways.

It has recently been found that in addition to the classic β-oxidation system of mitochondria there exits a β-oxidation system associated with peroxisomes.[39-41]

Although the peroxisomal β-oxidative scheme is essentially identical to that found in mitochondria and *E. coli*, the first dehydrogenation step utilizes an oxidase which directly transfers electrons to oxygen, whereas this step is catalyzed by a flavin-linked dehydrogenases in mitochondria and *E. coli*. With regard to the β-oxidation of unsaturated fatty acids, a more relevant distinction between these systems is the degree to which there exists multifunctional complexing. In mitochondria the enzymes are all separable (unlinked), whereas in mammalian peroxisomes the enoyl-CoA hydratase and 3-hydroxyacyl-CoA dehydrogenase activities reside on a single 80,000 Da protein[42] and these two activities as well as the isomerase and epimerase activities appear to reside on one of the two different subunits of the fatty acid oxidation complex of *E. coli*.[43, 44]

Although it is well established that the equilibrium of the hydration of dienoyl-CoA's is far to the side of the diene[38, 45, 46] the question arose as to why only the *trans,trans* isomer was directly β-oxidized by a reconstituted mitochondrial system used by Cuebas and Schulz. Furthermore, the question was asked whether there is any kinetic advantage to having 2-enoyl-CoA hydratase and 3-hydroxyacyl-CoA dehydrogenase physically linked. This question is especially significant in view of the unfavorable hydration of conjugated diene thioesters, and in view of a recent transient kinetic study which provided evidence for a channeling mechanism associated with these activities on the *E. coli* fatty acid oxidation complex.[47]

To provide quantitative answers to these questions, a detailed steady-state kinetic analysis was undertaken in collaboration with Dr. Song-Yu Yang[48] which required the chemical synthesis of the following CoA derivatives: 2-*trans*,4-*trans*-decadienoyl-CoA, 2-*trans*,4-*cis*-decadienoyl-CoA, D-3-hydroxy-4-*trans*-decenoyl-CoA, L-3-hydroxy-4-*trans*-decenoyl-CoA, and D,L-3-hydroxy-4-*cis*-decenoyl-CoA.

The availability of these geometrically and optically pure materials has made it possible for us to study the flux of conjugated diene CoA derivatives through β-oxidation systems reconstituted from purified enzymes of β-oxidation from rat liver mitochondria, rat liver peroxisomes, and *E. coli*. The geometric configuration of the double bonds and the structural assignment of the optical isomers of the hydroxy derivatives were important factors for this work and therefore a significant portion of this thesis details the synthesis, purification, and partial characterization of these compounds.

The detailed kinetic study of the metabolism of 2,4-decadienoyl-CoA's revealed several major implications regarding the β-oxidation of unsaturated fatty acids. The first major conclusion is that regardless of the geometry of the double bonds, 2,4-decadienoyl-CoAs are mostly metabolized via the NADPH-dependent 2,4-dienoyl-CoA reductase pathway in all three reconstituted systems. The major reason for this is the extremely unfavorable equilibrium of the hydration of these conjugated systems, and it therefore appears that reduction of the conjugated diene system coupled to the aromatization of the nicotinamide ring in NADP is nature's way of bypassing the thermodynamic block in the hydration reaction. Secondly, there exist subtle differences between the geometric isomers with respect to the rates of hydration in the reconstituted systems. These differences are due to large differences in the kinetic parameters (Km's and Vmax's), even though the equilibrium constants for the hydration of the different stereoisomers are of the same order of magnitude. Thirdly, for both the peroxisomal and *E. coli* systems, both of which harbor the hydratase and dehydrogenase activities on the same polypeptide, convincing evidence was obtained for the direct transfer of the product of hydration reaction to the active site of the dehydrogenase, whereas the kinetics of the mitochondrial system behaved essentially as predicted for a free-diffusion unlinked coupled enzyme system. Additional details of the kinetic study can be found in the publication by Yang, *et al.*.[48]

For the kinetic analysis of the above described systems, rate equations were derived which take into account the very high concentrations of enzymes needed to observe measurable reaction rates. The fact that high enzyme concentrations were required is not unexpected, since the catalytic rate constant in the forward direction for the primary enzyme is extremely low (100 sec^{-1}) and the extremely high reverse reaction rate at high concentrations of primary enzyme can only be suppressed by using high concentrations of coupling enzyme. Several treatments of irreversible uni enzyme mechanism have appeared,[49-53] yet no formal treatment of coupled enzyme kinetics at high enzyme concentration is available. This situation prompted me to examine in detail some of the simplifications and complications that arise in initial rate predictions of coupled enzyme systems where the primary enzyme catalyzes a thermodynamically very unfavorable reaction. The results and conclusions of this work constitute the final topic of this thesis.

EXPERIMENTAL

Materials—

NAD, NADH, CoASH and CoA derivatives of saturated fatty acids were purchased from P-L Biochemicals. Aldrich was the source of diketene, 2,6-dichlorophenolindophenol, 2-*trans*-decenoic acid, 2-*trans*-octenal, methyl bromoacetate, and di-(2-ethylhexyl) phthalate. Crotonic anhydride was obtained from Eastman Kodak Co. ICN Pharmaceuticals was the source of 2-*trans*,4-*trans*-decadienal, 4-*trans*-decenal, and 4-*cis*-decenal. Phenazine methosulfate, ATP, N-ethylmaleimide, 3-mercaptopropionic acid, 3-hydroxyacyl-CoA dehydrogenase, lactate dehydrogenase, carnitine acetyltransferase, caproyl chloride, myristoyl chloride, D,L-3-hydroxybutyric acid, D(+)-α-phenylethylamine, L(-)-α-phenylethylamine, catalase, as well as all other standard biochemicals, were obtained from Sigma. Palmitoyl-L-carnitine was generously provided by Dr. K. Brendel, University of Arizona, College of Medicine. 3-Ketoacyl-CoA thiolase and acetoacetyl-CoA thiolase from pig heart mitochondria,[54] beef liver crotonase,[55] and acyl-CoA dehydrogenases[56] were purified as described previously. The peroxisomal acyl-CoA oxidase [57] and enoyl-CoA hydratase/3-hydroxyacyl-CoA dehydrogenase [58] were purified from rat liver as previously described by Osumi and Hashimoto.

Isolation of Mitochondria and Oxygen Uptake Measurements—

Rat heart mitochondria were isolated from male Sprague-Dawley rats (240-260 g) by the procedure of Chappell and Hansford.[59] The isolation buffer

contained 0.21 M mannitol, 0.07 M sucrose, 5 mM Tris-HCl (pH 7.4), and 1 mM EGTA. Protein concentrations were determined by the biuret method.[60] For oxygen uptake measurements, mitochondria (0.5-1.0 mg/ml) were incubated in 1.9 ml of a basal isotonic medium containing 0.11 M KCl, 33 mM Tris-HCl (pH 7.4), 2 mM KP_i, 2 mM $MgCl_2$, and 0.1 mM EGTA. To this suspension were added bovine serum albumin (0.5 mg/ml) and 0.5 mM L-malate. Respiration was initiated by the simultaneous addition of ADP (2 μmol) and either palmitoyl-L-carnitine (60 nmol) or pyruvate (5 μmol). Rates of respiration were measured polarographically with a Clark oxygen electrode attached to a Gilson oxygraph. For the preparation of a soluble mitochondrial extract, mitochondria (11 mg/ml) were suspended in 0.1 M Tris-HCl (pH 8.0) and were sonicated at 5°C five times for 5 sec each with a Branson Sonifier (model W-185E) equipped with a microtip. The resulting mixture was centrifuged at 100,000 x g for 1 hr, and the supernatant was collected.

Synthesis of Substrates—

The CoA derivatives of 2-*trans*-decenoic acid, S-acyl-3-mercaptopropionic acids, and DL-3-hydroxybutyric acid were synthesized from their corresponding free acids and CoA by the method of Goldman and Vagelos.[61] Crotonyl-CoA[62] and acetoacetyl-CoA[63] were prepared according to standard procedures. 3-Ketodecanoyl-CoA was prepared enzymatically from 2-*trans*-decenoyl-CoA by the procedure of Seubert et al.[64] The concentrations of all CoA derivatives except for 3-ketodecanoyl-CoA were determined by the method of Ellman[65] after cleaving the thioester bond with neutral hydroxylamine. The concentration of 3-ketodecanoyl-CoA was measured by following the oxidation of NADH at 340 nm in the presence of 3-hydroxyacyl-CoA dehydrogenase at pH 7.

Synthesis of 3-Mercaptopropionyl-CoA—

Bis(2-carboxyethyl)disulfide was prepared from 3-mercaptopropionic acid by oxidation with bromine[66] and was twice recrystallized from hot methanol. The resulting solid had a melting point of 155°C (lit. 154-156°C[67]). It was converted mainly to its mono-CoA thioester by using one equivalent of ethyl chloroformate in the mixed anhydride method of Goldman and Vagelos.[61] The resulting material (40 mg) was subjected to chromatography on a DEAE-cellulose column (2.5 x 60 cm) which was equilibrated with 5 mM HCl. The column was developed with a gradient made up of 1 liter of 5 mM HCl and 1 liter of 5 mM HCl containing 0.3 M LiCl. Fractions of 20 ml were collected. Material which absorbed light at 260 nm emerged from the column in three major peaks (see Fig. 4). Only the materials corresponding to peaks II and III gave positive spot tests for both thioester and disulfide linkages. Since the position of peak II is close to where CoASH would appear and peak III was eluted where dimeric CoA would appear, we assumed that the materials corresponding to peaks II and III were the mono-CoA thioester and di-CoA thioester of bis(2-carboxyethyl)disulfide, respectively. Fractions 51-55 corresponding to peak II were pooled and concentrated in an Amicon concentrator (YC-05 membrane). The pH of the concentrate was adjusted to 1 with 1 N HCl. Zinc dust (150 mg) was added, and the solution was vortexed for approximately 10 min until the free sulfhydryl was twice that of thioester. The pH was adjusted to 3 and the zinc dust was filtered off. The solution was applied to a DEAE-cellulose column (2.5 x 60 cm) previously equilibrated with 5 mM HCl. The column was developed with a gradient made up of 500 ml of 5 mM HCl and 500 ml of 5 mM HCl containing 0.3 M LiCl. The solvent reservoirs were kept equilibrated with nitrogen, and fractions of 22.5 ml were collected. As shown in Fig. 5, only one UV-light absorbing compound, presumably 3-mercaptopropionyl-CoA, emerged from the column (peak II). 3-Mercaptopropionic acid, the other reaction product, was eluted in earlier fractions (peak I). Fractions corresponding to peak II were pooled and concentrated in an Amicon concentrator (YC-05 membrane). The final solution was stored under nitrogen at -78°C. The material thus obtained contained the following structural moieties in the indicated quantities:

free sulfhydryl, 2.215 mM; thioester, 2.215 mM; adenosine, 2.15 mM. The ratio of free sulfydryl/thioester/adenosine of 1:1:0.97 agrees with the structure of 3-mercaptopropionyl-CoA. To provide proof for the assigned structure of synthetic 3-mercaptopropionyl-CoA, the compound (33.3 nmol) in 32 μl of H_2O was reacted with an approximately equimolar amount of N-ethylmaleimide in the presence of $KHCO_3$ (0.4 mg). The reaction mixture was kept for 1 hr at 25°C during which time the pH increased to 10 due to loss of CO_2. At that time a molar excess of N-ethylmaleimide was added to the solution. Samples of the reaction mixture were analyzed by HPLC.

Synthesis of S-Acetyl-3-mercaptopropionic Acid —

3-Mercaptopropionic acid (1 g) in 100 ml of H_2O was adjusted to pH 6 with KOH and then to pH 8.2 with $KHCO_3$. Acetic anhydride was added dropwise under constant stirring while the pH was maintained between 8.0 and 8.2 by addition of 2N KOH. After 1.1 mol eq of acetic anhydride had been added, the reaction was complete as judged by the absence of sulfhydryl group determined with Ellman's reagent. The pH of the solution was adjusted to 2 with concentrated HCl and extracted four times with ether. The combined etheral extracts were dried over anhydrous Na_2SO_4, and the ether was evaporated. Remaining acetic acid was removed under a stream of nitrogen until the crude product began to crystallize. After two recrystallizations from petroleum ether at 4°C, 100 mg of long white needles were obtained which had a melting point of 51.5-53°C (lit. 52-54°C[68]).

Synthesis of S-Caproyl-3-mercaptopropionic Acid and S-Myristoyl-3-mercaptopropionic Acid —

3-Mercaptopropionic acid (500 mg) was added to 25 ml of 0.04 M KOH under constant stirring. The pH of this solution was adjusted to 8.3 with $KHCO_3$, and 35 ml of tetrahydrofuran were added after which the pH was 9.3. The appropriate acid chloride (caproyl chloride or myristoyl chloride) was added dropwise, and the pH was maintained at 9.0-9.2 by the dropwise addition of 2 M KOH until 95% of the sulfhydryl content was consumed as determined by the use of Ellman's reagent. The mixture was acidified to pH 2, and the tetrahydrofuran was removed by evaporation. The precipitated S-myristoyl-3-mercaptopropionic acid was then isolated by filtration, washed several times with distilled water, dried under reduced pressure, and recrystallized several times from hexane. S-Myristoyl-3-mercaptopropionic acid (500 mg) was obtained as shiny curved plates with a melting point of 80.5-81°C. The following was obtained by elemental analysis:

$$C_{17}H_{32}O_3S$$

Calculated: C,64.51; H, 10.19; S,10.13
Found: C,64.56; H,10.24; S,10.15

After removal of the tetrahydrofuran by evaporation, S-caproyl-3-mercaptopropionic acid was separated from the aqueous layer by extraction with ether. The combined etheral extracts were dried over anhydrous sodium sulfate. After removal of the ether by evaporation the liquid residue was dissolved in hexane with a trace of ether and cooled in a dry ice-acetone bath. The resulting crystals were rapidly filtered on a Buchner funnel and recrystallized twice from hexane at 4°C to yield S-caproyl- 3-mercaptopropionic acid (200 mg) as shiny white plates with a melting point of 41-42.5°C. The following was obtained by elemental analysis:

$$C_9H_{16}O_3S$$

Calculated: C,52.92; H,7.89; S,15.7
Found: C,52.91; H,7.86; S,15.8

Enzymatic Formation of 3-Mercaptopropionyl-CoA—

The reaction mixture contained ATP (0.5 μmol), $MgCl_2$ (1.5 μmol), 3-mercaptopropionic acid (0.5 μmol), and CoASH (0.21 μmol) in 250 μl of 20 mM Tris-HCl (pH 8.0). The reaction was started by the addition of soluble proteins (0.25 mg) extracted from rat heart mitochondria. After 50 min at room temperature, the mixture was acidified with 0.1 N HCl (50 μl), filtered, and EDTA was added to a final concentration of 6.25 mM. The resulting mixture (25 μl) was analyzed by HPLC.

Synthesis of 2-trans,4-trans-Decadienoyl-CoA—

2-*trans*,4-*trans*-Decadienoic acid was prepared from 2-*trans*,4-*trans*-decadienal by oxidation with Ag_2O as described previously[38] 2-*trans*,4-*trans*-Decadienoyl-CoA was prepared by the method of Goldman and Vagelos[61] and was purified as described below. The product 68 (μmol) in 60 ml of 5 mM imidazole (pH 7.0) was applied to a DEAE cellulose column (2.5 x 30 cm) that had been pre-equilibrated with 5 mM imidazole-HCl (pH 7.0). The column was developed with a linear gradient made up of 1 liter of 5 mM imidazole-HCl (pH 7.0) and 1 liter of 5 mM imiadzole-HCl (pH 7.0) containing 0.3 M LiCl. Fractions of 10 ml were collected and monitored at 260 nm for adenine and 300 nm for the conjugated diene chromophore. The material which eluted in one large peak contained both chromophores, the ratio of which was constant throughout the entire peak. The fractions containing the above material were pooled and concentrated on an Amicon concentrator (YC-05 membrane). The concentration of the product was determined by the method of Ellman[65] after cleaving the thioester bond with 1M hydroxylamine (pH 7). Although most CoA derivatives are completely cleaved by 1 M hydroxylamine (pH 7) within 5 min, conjugated diene thioesters must be reacted for 15 minutes before the cleavage is complete. The purified 2-*trans*,4-*trans*-decadienoyl-CoA had a 300/260 nm absorbance ratio of 0.97. The extinction

coefficient of the diene thioester chromophore at 300 nm was determined to be 27,800 M^{-1} cm^{-1}. Since this material has a strong tendency to polymerize, it was stored at a concentration of less than 1 mM in the dark at pH 3 and 4°C.

Synthesis of L-3-Hydroxy-4-trans-decenoyl-CoA—

2-*trans*-octenal and methyl bromoacetate were condensed by a Reformatzsky reaction using the zinc column procedure of Ruppert and White[69] to yield methyl-3-hydroxy-4-*trans*-decenoate. The product was purified by fractional distillation *in vacuo* , dissolved in methanol/H_2O (1:1), and hydrolyzed by reacting it for 24 hrs at 25°C with a slight molar excess of NaOH. The resulting D,L-hydroxy-4-*trans*-decenoic acid was obtained as a viscous oil. The proton nmr spectrum of this compound agreed with the assigned positions of the functional groups and the configuration of the double bond was consistent with the observed ir spectrum which showed a strong absorbance at 975 cm^{-1} characteristic of *trans* double bonds. The proton decoupled ^{13}C nmr spectrum gave the following resonances: (tms = 0 ppm), 177.3 (carboxyl); 133.5, 130.0 (olefinic); 69.0; 41.5; 32.1; 31.4; 28.7; 22.5; 14.0.

D,L-3-Hydroxy-4-*trans*-decenoic acid was resolved into its optical isomers by applying the procedure of Stoffel, Caesar and Ditzer[70] who resolved D,L-3-hydroxydodecanoic acid. The racemic acid (14.7 g) and D-(+)-α-phenylethylamine (9.62 g) were added to 150 ml of acetone and kept at -20°C for 3 hrs. The resulting crystals were collected by filtration and recrystallized seven times from acetone at -20°C. The product (1 g) was acidified with HCl and extracted three times with ether. After evaporation of the ether, (+)-3-hydroxy-4-*trans*-decenoic acid, which had an $[\alpha]_D^{25}$ of +12.8 (C = 1, $CHCl_3$), was obtained. The (-) isomer of the acid was obtained by the same procedure except that L(-)-α-phenylethylamine was used. Its $[\alpha]_D^{25}$ was -13.9 (C = 1,$CHCl_3$). The CoA derivatives of both optical isomers were prepared by the method of Goldman and

Vagelos[61] and their concentrations were determined by the method of Ellman[65] after cleaving the thioester bond with 1 M hydroxylamine (pH 7). The absolute specificity of 3-hydroxyacyl-CoA dehydrogenase for the L isomers of 3-hydroxyacyl-CoA thioesters, permitted the determination of the absolute configuration of the optical isomers. By this approach, the (-) isomer and the (+) isomer were determined to have the D-configuration and the L-configuration, respectively. When L-3-hydroxy-4-*trans*-decenoyl-CoA was quantitatively dehydrogenated by 3-hydroxyacyl-CoA dehydrogenase coupled to 3-ketoacyl-CoA thiolase, it was found to contain 93% of the L isomer and thus 7% of the D isomer. Similarly, the CoA derivative of the D isomer was found to contain approximately 3% of the L isomer.

Synthesis of 3-Hydroxy-4-cis-Decenoic Acid—

3-Hydroxy-4-*cis*-decenoic acid was prepared as described previously[38] The proton nmr spectrum of the product agreed with the assigned positions of the functional groups, and the proton decoupled ^{13}C nmr spectrum gave the following resonances: (tms = 0 ppm); 177.1 (carboxyl); 133.7, 129.7 (olefinic); 64.3; 41.5; 31.5; 29.2; 27.7; 22.5; 14.0. By comparing the ^{13}C nmr spectrum of the *cis*- isomer with that of the *trans*- isomer, the contamination of the *cis*- isomer with the *trans*- isomer was estimated to be 3%.

Synthesis of 4-trans-Decenoic Acid and 4-*cis*-Decenoic Acid—

4-*cis*-Decenoic acid was prepared from 4-*cis*-decenal by oxidation with Ag_2O as described principle by Thomason and Kubler.[71] The *trans* isomer was synthesized from the *trans* aldehyde by the same procedure. The proton-decoupled ^{13}C nmr spectra were obtained for both geometric isomers, and since the olefinic

resonances of the *trans* and the *cis* isomers were clearly resolved, it was possible to estimate that the *cis*- isomer contained less than 5% of the *trans*- isomer.

Enzymatic Synthesis of 2-trans,4-cis-Decadienoyl-CoA—

The reaction mixture which contained 4-*cis*-decenoyl-CoA (17 μmol), catalase (140 μg), and acyl-CoA oxidase (4.1 units) in 40 ml of 20 mM KP_i (pH 8.0), was incubated at 37°C. Aliquots of 90 μl were withdrawn at various time intervals and diluted to 1 ml with 0.1 KP_i (pH 8.0) and analyzed for their absorbance at 300 nm. When the absorbance at 300 nm did not further increase even upon the addition of more acyl-CoA oxidase and catalase, the reaction was judged complete and terminated by acidification to pH 3 with HCl. The precipitated protein was removed by filtration, and the resulting solution was concentrated in an Amicon concentrator (YC-05 membrane). Since the hydrogen peroxide produced in the reaction was destroyed by catalase, and since the formation of the conjugated diene thioester is a thermodynamically favorable reaction, it was assumed that 4-*cis*-decenoyl-CoA was completely converted to 2-*trans*,4-*cis*-decadienoyl-CoA.

Enzyme Assays—

All enzyme assays were performed at 25°C. Enzyme activities were determined spectrophotometrically on a Gilford recording spectrophotometer. Butyryl-CoA dehydrogenase (EC 1.3.99.2) and acyl-CoA dehydrogenase (EC 1.3.99.3) were assayed spectrophotometrically at 600 nm as described in principle by Hoskins[72] The assay mixture contained 0.1 M KP_i (pH 7.6), 28 μM 2,6-dichlorophenolindophenol, 0.2 mM N-ethylmaleimide, 30 μM acyl-CoA, and enzyme to give an ΔA/min of 0.08. The reaction was initiated by the addition of

phenazine methosulfate to a final concentration of 0.65 mM for the short and long chain enzymes and 3.3 mM for the medium chain acyl-CoA dehydrogenase. The dehydrogenation of 3-mercaptopropionyl-CoA by general chain acyl-CoA dehydrogenase from pig liver was assayed fluorometrically with electron-transferring flavoprotein as an electron acceptor as described by Beckman and Frerman.[73] Enoyl-CoA hydratase (EC 4.2.1.17) was measured spectrophotometrically at 280 nm as described by Steinman and Hill.[55] The assay mixture contained in 1 ml of 0.35 M Tris-HCl (pH 7.4), 85 μM crotonyl-CoA and crotonase (11 milliunits). 3-Hydroxyacyl-CoA dehydrogenase (EC 1.1.1.35) was assayed spectrophotometrically at 340 nm using a coupled assay containing 115 μM NAD, 113 μM CoASH, 3-hydroxyacyl-CoA dehydrogenase (19 milliunits), 3-ketoacyl-CoA thiolase (66 milliunits), and 60 μM DL-3-hydroxybutyryl-CoA in 1 ml of 0.2 M KP_i (pH 8.0). 3-Ketoacyl-CoA thiolase (EC 2.3.1.16) and acetoacetyl-CoA thiolase (EC 2.3.1.9) were measured spectrophotometrically by following the disappearance of the Mg^{2+}-enolate complex at 303 nm. The assay mixture contained 34 μM acetoacetyl-CoA or 22 μM 3-ketodecanoyl-CoA, 80 μM CoASH, 25 mM $MgCl_2$, and thiolase (6.6 milliunits) in 1 ml of 0.1 M Tris-HCl (pH 8.3). Molar extinction coefficients used to calculate rates were 21,400 M^{-1} cm^{-1} and 14,000 M^{-1} cm^{-1} for acetoacetyl-CoA and 3-ketodecanoyl-CoA, respectively.[74] When the effect of S-myristoyl-3-mercaptopropionyl-CoA on the activity of 3-ketoacyl-CoA thiolase was determined, Mg^{2+} was deleted from the assay mixture to avoid precipitation of the long-chain acyl-CoA. The assay mixture contained 0.1 M Tris-HCl (pH 8.3), 0.1 mM EDTA, 90 μM acetoacetyl-CoA, 178 μM CoASH, and 3-ketoacyl-CoA thiolase to obtain a ΔA/min of 0.08. The extinction coefficient used for calculating reaction rates in the absence of Mg^{2+} was 3,600 M^{-1} cm^{-1}.[75] Carnitine acetyltransferase (EC 2.3.1.7) was assayed spectrophotometrically by following the change in absorbance at 232 nm due to the appearance or disappearance of the thioester chromophore as described by Chase.[76] In the direction of acetyl-CoA formation, the assay mixture contained 400 μM L-acetylcarnitine and 158 μM CoASH in 0.2 M Tris-HCl (pH 7.4). In the direction of acetylcarnitine formation, the assay mixture contained 100 μM acetyl-CoA and 400 μM L-carnitine in the same buffer. The reactions were initiated by the addition of carnitine

acetyltransferase (1 μg). An extinction coefficient of 4500 M^{-1} cm^{-1} was used to calculate rates. Citrate synthase (EC 4.1.3.7) was assayed spectrophotometrically by following the release of free CoASH as measured with Ellman's reagent at 412 nm.[77] The assay mixture contained in 1 ml of 0.12 M KP_i (pH 8.0), 150 μM 5,5'-dithiobis(2-nitrobenzoic acid), 100 μM acetyl-CoA, and citrate synthase (7.5 milli-units). The reaction was initiated by the addition of oxaloacetate to a final concentration of 1 mM. Rat heart mitochondrial thioesterase activity was measured spectrophotometrically by following the release of free CoASH as determined by Ellman's reagent. The assay mixture contained in 0.175 M KP_i (pH 8.0), 200 μM 5,5'-dithiobis(2-nitrobenzoic acid), 0.06 % Triton X-100, 22 or 66 μM acyl-CoA or S-acyl-3-mercaptopropionyl-CoA, and freeze-thawed rat heart mitochondria (85-170 μg/ml). Assays with either palmitoyl-CoA or S-myristoyl-3-mercaptopropionyl-CoA as substrates did not contain Triton X-100. 3-Hydroxyacyl-CoA epimerase was measured by a coupled assay in which the formation of NADH was followed at 340 nm as described in detail by Binstock and Schulz.[78] The assay mixture contained 0.2 M Kp_i (pH 8), 0.33 mM NAD, 60 μM DL-3-hydroxydecanoyl-CoA, pig heart 3-hydroxyacyl-CoA dehydrogenase (0.3 U/ml), and pig heart 3-ketoacyl-CoA thiolase (33 mU/ml). For the determination of 3-hydroxyacyl-CoA epimerase activity in the enoyl-CoA hydratase and acyl-CoA oxidase preparations, the reaction was initiated by the addition of either of the above preparations after the oxidation of the L isomer 3-hydroxydecanoyl-CoA was complete. One unit of enzyme activity is defined as the amount that catalyzes the conversion of 1 μmol of substrate to product/min.

The Determination of the Equilibrium Constant of the Oxidation of L-3-Hydroxy-4-trans-decenoyl-CoA by NAD^+—

The assay mixture contained 0.2 M imidazole (pH 6.5), 65 to 100 μM L-3-hydroxy-4-*trans*-decenoyl-CoA, 58 μM NAD, and sufficient 3-hydroxyacyl-CoA dehydrogenase to reach equilibrium within 4 min. The concentration of NADH at

equilibrium was determined by monitoring the increase in absorbance at 340 nm after initiating the reaction with 3-hydroxyacyl-CoA dehydrogenase. After reaching equilibrium, the interfering absorbance at 340 nm due to the enolate form of 3-keto-4-*trans*-decenoyl-CoA was determined by the sequential addition of palmitoyl-CoA (50 nmoles, to reversibly inhibit 3-hydroxyacyl-CoA dehydrogenase), pyruvate (500 nmoles), and lactate dehydrogenase (500 mU), which quantitatively oxidized NADH to NAD. The remaining absorbance at 340 nm is taken as that due to the enolate form of 3-keto-4-*trans*-decenoyl-CoA.

HPLC Analyses—

All HPLC analyses were performed on a Waters Associates system consisting of two pumps (model 6000 A), one solvent programmer (model 660), an absorbance detector (model 441) set at 254 nm, and a μBondapak C_{18} column. Flow rates were between 2.0 and 3.0 ml/min. All separations were achieved with a solvent consisting of 0.05 M ammonium phosphate (pH 5.5) and between 15 and 30% methanol. The solvent gradient followed slope 7 of the solvent programmer and was complete within 7 min.

Derivation of Rate Equations and Computer Calculations—

Algebraic manipulations were performed with the aid of MACSYMA, a symbolic manipulation main-frame computer package (Symbolics, Inc.). All numerical calculations were performed with double precision programs written in Fortran on a VAX 780 computer. To minimize floating point error, coefficients of polynomial were represented in Horner notation when necessary, and a Port mathematical library subroutine (DPOLY) was used to solve higher order polynomials. Approximately 300 data points were calculated for each curve and then subject to

a spline curve fitting subroutine, to generate 1000 data points per curve. The following kinetic parameters were used for all computer calculations, and were those experimentally determined with 2-*trans*,4-*trans*-decadienoyl-CoA as substrate in the forward reaction of mitochondrial enoyl-CoA hydratase and L-3-hydroxy-4-*trans*-decenoyl-CoA as substrate for the reverse reaction of the hydratase and forward reaction of mitochondrial 3-hydroxyacyl-CoA dehydrogenase[48] :Km1f = 16.9 μM; Km1r = 12.1 μM; Km2 = 1.5 μM; kcat1r = 2.1×10^4 min^{-1}; kcat1f = 8.67×10^1 min^{-1}, and kcat2 = 1.26×10^3 min^{-1}, where Km refers to the Michaelis constant, and kcat refers to the catalytic rate constant. The numbers 1 and 2, and the letters f and r refer to the hydratase, dehydrogenase, and the forward and reverse reactions, respectively. The four individual rate constants for the primary enzyme were calculated by simultaneous solution of the above four kinetic parameters. The concentration of substrate for the primary enzyme in the coupled enzyme initial rate calculations was 20 μM and the concentration of the primary enzyme was 0.532 μM, unless stated otherwise.

MITOCHONDRIAL METABOLISM OF 3-MERCAPTOPROPIONIC ACID

RESULTS

Chemical Synthesis of 3-Mercaptopropionyl-CoA—

The observation that 3-mercaptopropionyl-CoA is a potent inhibitor of β-oxidation in coupled, but not uncoupled mitochondria, led to the hypothesis that the actual inhibitor is either 3-mercaptopropionyl-CoA or a derivative of it. To facilitate a study of the enzymatic formation of 3-mercaptopropionyl-CoA, this compound was chemically synthesized according to the scheme shown in Fig. 6. Oxidative dimerization of 3-mercaptopropionic acid with Br_2 gave bis(2-carboxyethyl)disulfide, a dicarboxylic acid that can be converted to its mono-CoA thioester or di-CoA thioester. The mono-CoA thioester was the better intermediate because it was easily separated by ion-exchange chromatography from oxidized CoA which is a contaminant of CoASH and which would have been reduced to CoASH in the last step of the synthesis. Finally, the mono-CoA thioester of bis(2-carboxyethyl)disulfide was reductively cleaved with Zn and HCl to yield 3-mercaptopropionic acid and 3-mercaptopropionyl-CoA which were separated by chromatography on DEAE-cellulose. The resulting 3-mercaptopropionyl-CoA contained adenosine, thioester, and sulfhydryl moities in equimolar amounts. Final proof for the structure of 3-mercaptopropionyl-CoA was obtained by the experiment summarized in Fig. 7. Synthetic 3-mercaptopropionyl-CoA gave one major peak on HPLC (see Fig. 7A). The addition of approximately 1 eq of N-ethylmaleimide to the synthetic material in the presence of $KHCO_3$ yielded the

more hydrophobic alkylation product of 3-mercaptopropionyl-CoA (see *peak II* in Fig. 7B). Upon standing, this sample became more alkaline due to the loss of CO_2, thereby causing the hydrolysis of the thioester bond. The resulting material co-migrated with CoASH and oxidized CoA (see *peaks III* and *IV* in Fig. 7C). The formation of free CoASH was confirmed by its reaction with N-ethylmaleimide to alkylated CoA which was co-eluted with authentic material on HPLC (see *peak V* in Fig. 7D). The material corresponding to *peak Va* in Fig. 7, B and C, is believed to be alkylated CoA formed from excess N-ethylmaleimide and free CoASH generated hydrolytically from alkylated 3-mercaptopropionyl-CoA.

This conclusion is based on the observed co-migration of this with authentic material (see *peak V* in Fig. 7). The small difference in elution time between *peaks V* and *Va* is believed to be the consequence of a slight change in the HPLC conditions. When synthetic 3-mercaptopropionyl-CoA was incubated for 4 min with a slight excess of N-methylmaleimide, the retention time of the alkylated product was less than that observed when N-ethylmaleimide was the alkylating agent, yet a peak was also present whose retention time matched that of *peak Va* described above. The above results clearly prove the sulfhydryl group of CoASH to participate in the thioester bond, whereas the free sufhydryl group of the material is that of the 3-mercaptopropionyl-CoA moiety. This conclusion strongly supports the structure assigned to the synthetic 3-mercaptopropionyl-CoA.

Activation of 3-Mercaptopropionic Acid—

The possible conversion of 3-mercaptopropionic acid to its CoA ester catalyzed by the mitochondrial medium-chain acyl-CoA synthetase (EC 6.2.1.2) was evaluated. The acid together with the necessary cofactors was incubated for 1 hr in the presence of a soluble extract from rat heart mitochondria, and the reaction products were analyzed by HPLC. The HPLC chromatrogram shown in Fig. 8 reveals the formation of 3-mercaptopropionyl-CoA (*peak IV*). In addition, nonspecific oxidation led to the formation of oxidized CoA (*peak III*) and a

presumed mixed disulfide between CoASH and 3-mercaptopropionic acid (*peak II*). Since the amount of 3-mercaptopropionyl-CoA detected was small, the hydrolysis of 3-mercaptopropionyl-CoA by the soluble mitochondrial extract was measured. A comparison of the chromatograms shown in Fig. 8, B and C, clearly demonstrates the extensive hydrolysis of 3-mercaptopropionyl-CoA by the mitochondrial extract, whereas little nonenzymatic hydrolysis was observed. Consequently, the rate of 3-mercaptopropionyl-CoA formation is significantly higher than can be estimated from its accumulation over a longer time period. When n-butyric acid was incubated under identical conditions, a small peak was observed corresponding to n-butyryl-CoA, which was quantitatively similar to the amount of 3-mercaptopropionyl-CoA formed during the same length of incubation time. Consequently, the presence of a terminal sulfhydryl moiety does not seem to influence the pseudo-steady-state level of short-chain CoA derivatives formed by free acid activation, although the relative rates of activation and thioester hydrolysis may be different for the two substrates.

Metabolism of 3-Mercaptopropionyl-CoA—

3-Mercaptopropionyl-CoA, a structural analog of 3-hydroxypropionyl-CoA, was neither a substrate of enoyl-CoA-hydratase (EC 4.2.1.17) nor of 3-hydroxyacyl-CoA dehydrogenase (EC 1.1.1.35). However, it was found to substitute for CoASH in the thiolytic cleavage of acetoacetyl-CoA catalyzed by 3-ketoacyl-CoA thiolase (EC 2.3.1.16). Since 3-mercaptopropionyl-CoA might be hydrolyzed to CoASH which would participate in the thiolytic cleavage of acetoacetyl-CoA, it was necessary to determine the structure of the reaction products. The HPLC chromatogram presented in Fig. 9A shows the good separation of the reactants acetoacetyl-CoA (*peak I*) and 3-mercaptopropionyl-CoA (*peak II*). Addition of 3-ketoacyl-CoA thiolase to the reactants resulted in the disappearance of 3-mercaptopropionyl-CoA (*peak II* in Fig. 9B) and the appearance of S-acetyl-3-mercaptopropionyl-CoA (*peak IV* in Fig. 9B) which was identified by co-chromatography with authentic material obtained by chemical synthesis. The

disappearance of acetoacetyl-CoA was masked by the formation of acetyl-CoA which was eluted from the column together with acetoacetyl-CoA. This experiment proves the participation of 3-mercaptopropionyl-CoA in the reaction catalyzed by 3-ketoacyl-CoA thiolase. The kinetic efficiency of 3-mercaptopropionyl-CoA in the thiolase catalyzed reaction was determined. The results shown in Fig. 10 demonstrate 3-mercaptopropionyl-CoA to be nearly as efficient as is CoASH. K_m values obtained from the Hanes-Woolf plot shown in Fig. 10 were 21 μM for CoASH and 36 μM for 3-mercaptopropionyl-CoA. Maximal velocity values of 10 units/mg and 7 units/mg were calculated for the reactions with CoASH and the analog, respectively. When 3-ketodecanoyl-CoA instead of acetoacetyl-CoA served as a substrate the substitution of 3-mercaptopropionyl-CoA for CoASH resulted in 10% higher reaction rates (data not shown). A comparison of 3-mercaptopropionyl-CoA with CoASH in the reaction catalyzed by the mitochondrial acetoacetyl-CoA thiolase (EC 2.3.1.9) proved them to be equally effective (data not shown). Thus, 3-mercaptopropionyl-CoA is an excellent analog of CoASH in all thiolase-catalyzed reactions studied so far.

Finally, the possible metabolism of 3-mercaptopropionyl-CoA by acyl-CoA dehydrogenase was evaluated. Since the standard assay for this enzyme contains an artificial electron acceptor, as for example 2,6-dichlorophenolindophenol, which reacts nonenzymatically with sulfhydryl groups, a fluorimetric assay using substrate-level amounts of electron-transferring flavoprotein was utilized.[73] 3-Mercaptopropionyl-CoA was slowly acted upon by general acyl-CoA dehydrogenase (EC 1.3.99.3) from pig liver. The kinetic constants obtained with either 3-mercaptopropionyl-CoA or butyryl-CoA are presented in Table 1. 3-Mercaptopropionyl-CoA is a poor substrate of the enzyme when compared with butyryl-CoA which is turned over 20 times faster than is 3-mercaptopropionyl-CoA. However, the K_m value for 3-mercaptopropionyl-CoA is only half of that determined for butyryl-CoA.

Metabolism of S-Acyl-3-mercaptopropionyl-CoAs—

Substituting 3-mercaptopropionyl-CoA for CoASH in thiolase-catalyzed reactions results in the formation of S-acyl-3-mercaptopropionyl-CoAs, in which the acyl group can be either an acetyl residue or any other acyl group derived from fatty acids by β-oxidation. After having provided evidence for the formation of S-acyl-3-mercaptopropionyl-CoAs in mitochondria, the further metabolism of these compounds needed to be elucidated. To facilitate such a study, the following compounds were obtained by chemical synthesis: S-acetyl-3-mercaptopropionyl-CoA, S-caproyl-3-mercaptopropionyl-CoA, and S-myristoyl-3-mercaptopropionyl-CoA. These compounds were synthesized by preparing first the desired S-acyl-3-mercaptopropionic acids from the appropriate acid chlorides and 3-mercaptopropionic acid. The resulting S-acyl-3-mercaptopropionic acids were then converted to their CoA derivatives by the mixed anhydride procedure of Goldman and Vagelos.[61] The three S-acyl-3-mercaptopropionyl-CoAs were tested for their ability to serve as substrates of either butyryl-CoA dehydrogenase (EC 1.3.99.2), medium-chain acyl-CoA dehydrogenase, or long-chain acyl-CoA dehydrogenase (EC 1.3.99.3). All three CoA derivatives were either not acted upon by the dehydrogenases or were very poor substrates with activities of less than 3% compared to those measured with the regular substrates. No attempt was made to determine kinetic parameters for these very slow reactions. Since the S-acyl-3-mercaptopropionyl-CoAs are apparently not further metabolized via β-oxidation, their breakdown with the concomitant release of CoASH was investigated. Shown in Table 2 are the rates for the reaction between carnitine and either 3-mercaptopropionyl-CoA or S-acetyl-3-mercaptopropionyl-CoA catalyzed by carnitine acetyltransferase (EC 2.3.1.7). The rates observed with 3-mercaptopropionyl-CoA, the better of the two substrate analogs, was approximately 25% of that obtained with acetyl-CoA. Since 3-mercaptopropionyl-CoA does not substitute for CoASH in the reverse reaction, the S-acetyl-3-mercaptopropionyl group and not the acetyl group seems to be transferred from CoA to carnitine in the forward reaction. S-acetyl-3-mercaptopropionyl-CoA did not substitute for acetyl-CoA in the reaction catalyzed by citrate synthase (EC 4.1.3.7). Finally, we have measured the hydrolysis of the three synthetic S-acyl-3-mercaptopropionyl-CoAs by thioesterase(s) present in rat heart mitochondria.

All three CoA thioesters were hydrolyzed at substantial rates which were higher than the rates observed with comparable acyl-CoAs (see Table 3). Since the rates were obtained by measuring the appearance of sulfhydryl groups, it remained to be established which of the two thioester bonds present in S-acyl-3-mercaptopropionyl-CoAs was hydrolyzed. For this purpose S-myristoyl-3-mercaptopropionyl-CoA was incubated with rat heart mitochondria, and the resulting acid was isolated by extraction. The product was identified as S-myristoyl-3-mercaptopropionic acid based on the presence of a thioester group and on its co-chromatography with authentic material on thin layer silica gel plates. This finding proves the hydrolysis to occur between the S-acyl-3-mercaptopropionyl moiety and CoA with the resultant regeneration of free CoA.

Inhibition of β-Oxidation in Rat Heart Mitochondria by Metabolites of 3-Mercaptopropionic acid—

Experiments performed by Emily Sabbagh in our laboratory characterized many aspects of the inhibition of β-oxidation in rat heart mitochondria by three commercially available short-chain mercaptoacids.[79] Of these, 3-mercaptopropionic acid was found to be the most effective and therefore efforts in our laboratory focused on elucidation of the mechanism by which 3-mercaptopropionic acid inhibits β-oxidation in coupled rat heart mitochondria. This was attempted by studying the effects of chemically synthesized metabolites of 3-mercaptopropionic acid on the activities of purified enzymes of β-oxidation. As expected, 3-mercaptopropionic acid itself at concentrations of up to 200 μmolar did not effect the activity of any of the β-oxidation enzymes. 3-Mercaptopropionyl-CoA, the first mitochondrial metabolite of 3-mercaptopropionic acid, had no effect on the activities of enoyl-CoA hydratase and 3-hydroxyacyl-CoA dehydrogenase. However, this compound is a good analog of CoASH in thiolase catalyzed reactions and a poor substrate of medium-chain acyl-CoA dehydrogenase. A kinetic study proved 3-mercaptopropionyl-CoA to be a competitive inhibitor (K_I = 5 μmolar) of medium-chain acyl-CoA dehydrogenase with respect to butyryl-CoA. Since 3-

mercaptopropionyl-CoA can substitute for CoASH in thiolase-catalyzed reactions it is expected to be converted intramitochondrially to S-acyl-3-mercaptopropionyl-CoA thioesters in which the acyl residue can be an acetyl group or any other acyl group derived from fatty acids by β-oxidation. We have studied the effects of three of these possible metabolites of 3-mercaptopropionyl-CoA on the activities of the enzymes of β-oxidation. The results presented in Table 4 show S-acetyl- 3-mercaptopropionyl-CoA and S-hexanoyl-3-mercaptopropionyl-CoA to have little or no effect on the β-oxidation enzymes. However, S-myristoyl-3-mercaptopropionyl-CoA, a long-chain acyl derivative of 3-mercaptopropionyl-CoA, inhibits enoyl-CoA hydratase (crotonase) moderately and is a strong inhibitor of 3-ketoacyl-CoA thiolase, 3-hydroxyacyl-CoA dehydrogenase, and long-chain as well as medium-chain acyl-CoA dehydrogenase.

Since S-myristoyl-3-mercaptopropionyl-CoA is a long-chain acyl-CoA thioester, it may be a nonspecific inhibitor of many enzymes as are the CoA derivatives of long-chain fatty acids. To evaluate the specificities of the observed inhibitions we have compared the effectiveness of S-myristoyl-3-mercaptopropionyl-CoA and palmitoyl-CoA as inhibitors of 3-ketoacyl-CoA thiolase and 3-hydroxyacyl-CoA dehydrogenase. Acyl CoA dehydrogenases were not included in this evaluation because palmitoyl-CoA is a good substrate of both the medium chain and long-chain enzyme.[56] As shown in Fig. 11 both 3-ketoacyl-CoA thiolase (Fig. 11A) and 3-hydroxyacyl-CoA dehydrogenase (Fig. 11B) are inhibited by both acyl-CoA thioesters with nearly equal effectiveness. At inhibitor concentrations of 10-20 μM, both enzymes are completely inhibited. However, the addition of bovine serum albumin to the inhibited enzymes resulted in their reactivation. Hence, the inhibitions are reversible. Since 3-hydroxyacyl-CoA dehydrogenase and 3-ketoacyl-CoA thiolase are strongly inhibited by palmitoyl-CoA, which is present at substantial concentrations in the matrix of mitochondria actively oxidizing fatty acids,[80] the inhibition of these two enzymes by S-myristoyl-3-mercaptopropionyl-CoA in whole mitochondria is unlikely.

In view of these findings, subsequent studies concentrated on the inhibition of medium-chain acyl-CoA dehydrogenase by S-myristoyl-3-mercaptopropionyl-CoA. As illustrated in Fig. 12, this compound is an effective inhibitor of the dehydrogenase. A kinetic study of this enzyme with octanoyl-CoA as a substrate yielded an inhibition constant of 0.8 μM for S-myristoyl-3-mercaptopropionyl-CoA (data not shown). It appears that long-chain derivatives of 3-mercaptopropionyl-CoA at low micromolar concentrations can effectively inhibit medium-chain acyl-CoA dehydrogenase.

Since 3-mercaptopropionic acid has only a slight effect on the respiration supported by pyruvate, it was concluded that the inhibition of β-oxidation by the same compound is not due to the inhibition of the tricarboxylic cycle, the respiratory chain, or oxidative phosphorylation. However, we have not ruled out the possibility that metabolic systems other than β-oxidation may be inhibited by S-acyl-3-mercaptopropionyl-CoA thioesters which are only formed when 3-mercaptopropionic acid and fatty acids are metabolized simultaneously.

Percent Inhibition of Respiration
with Various Substrates

	Palmitoylcarnitine	Pyruvate	Both
3-MPA	100	0	80
3-MPA + carnitine	100	0	45

where 3-MPA is 3-mercaptopropionic acid.

As shown in the above table, apparent evidence for such an inhibition is the observed 80% inhibition of respiration with pyruvate as a substrate in mitochondria preincubated with 0.5 mM 3-mercaptopropionic acid, malate, ADP, P_i, and palmitoylcarnitine. However, the addition of 50 mM L-carnitine restored pyruvate-dependent respiration to 45% of its control value, whereas respiration supported by palmitoylcarnitine was not stimulated by the addition of L-carnitine. We conclude that the inhibition of β-oxidation by long-chain S-acyl-3-mercaptopropionyl-CoA thioesters results in the sequestration of free CoASH as acyl-CoA, thereby preventing pyruvate metabolism. The addition of carnitine leads to the regeneration of CoASH and therefore results in the stimulation of pyruvate-supported respiration. Thus, none of the reactions subsequent to the β-oxidation cycle appears to be responsible for the inhibition of this pathway.

DISCUSSION

The observed enzymatic conversions of 3-mercaptopropionic acid are summarized in Fig. 13. Essential for its further metabolism is the conversion of the acid to its CoA derivative catalyzed by acyl-CoA synthetase, most likely medium-chain acyl-CoA synthetase, which is located in the mitochondrial matrix.[81] 3-Mercaptopropionyl-CoA thus formed intramitochondrially can participate in several reactions as outlined in Fig. 13. However, the respective contributions of these reactions to the overall metabolism of 3-mercaptopropionyl-CoA are different. The hydrolysis of 3-mercaptopropionyl-CoA by thioesterases does not need to be considered, because no new metabolite is being formed. If we assume that 3-mercaptopropionyl-CoA is an equally poor substrate of butyryl-CoA dehydrogenase and general (medium-chain) acyl-CoA dehydrogenase, its calculated rate of dehydrogenation would be only 4 nmol/min and mg of mitochondrial protein. This calculation is based on a reported total butyryl-CoA dehydrogenase activity of 72 nmol/min and mg of rat heart mitochondrial protein[8] and on the observed 20-fold slower rate of dehydrogenation of 3-mercaptopropionyl-CoA as compared to butyryl-CoA. Although the dehydrogenation product of 3-mercaptopropionyl-CoA has not been identified, it is expected to have the structure shown in Fig. 13. If so, it would be labile, and thus no attempt was made to isolate or synthesize it. Quantitatively of greater importance than the dehydrogenation is the transfer of the 3-mercaptopropionyl residue from CoA to carnitine catalyzed by carnitine acetyltransferase. Since the activity of this enzyme with acetyl-CoA as substrate is approximately 200 nmol/min and mg of heart mitochondrial protein,[82] its estimated activity with 3-mercaptopropionyl-CoA as a substrate is 60 nmol/min and mg of mitochondrial protein. The extent of the transfer reaction is limited by the availability of free carnitine. 3-Mercaptopropionyl-CoA is possibly regenerated from 3-mercaptopropionylcarnitine, because the reaction is freely reversible

and the latter compound is not known to be further metabolized. The most significant of all reactions in which 3-mercaptopropionyl-CoA can participate is its thiolase-catalyzed conversion to S-acyl-3-mercaptopropionyl-CoA. Since the total acetoacetyl-CoA thiolase activity is approximately 500 nmol/min and mg of rat heart mitochondrial protein[8] , and the thiolase activity with 3-mercaptopropionyl-CoA as a substrate is more than 50% of that observed with CoASH, the rate of the conversion of 3-mercaptopropionyl-CoA to S-acyl-3-mercaptopropionyl-CoA may be as high as 250 nmol/min and mg of mitochondrial protein. Consequently, 3-mercaptopropionyl-CoA is predicted to be converted intramitochondrially mostly to its S-acyl derivatives.. Since 3-mercaptopropionyl-CoA can substitute for CoASH in all thiolase-catalyzed reactions, a group of S-acyl-3-mercaptopropionyl-CoAs with different acyl groups is expected to be formed intramitochondrially. This situation has kept us from attempting to identify the mitochondrial metabolites of 3-mercaptopropionic acid directly. S-Acyl-3-mercaptopropionyl-CoAs are either very poorly or not at all dehydrogenated by acyl-CoA dehydrogenase and thus are not further degraded by β-oxidation. These compounds can, however, undergo reactions that will result in the regeneration of free CoASH. One of these reactions involves the transfer of the S-acyl-3-mercaptopropionyl groups from CoA to carnitine. In the case of S-acyl-3-mercaptopropionyl-CoA this reaction proceeds at only 10% of the rate observed with acetyl-CoA. Since these transfer reactions proceed slowly and since the activity of carnitine acyltransferase with long-chain substrates is low, the disappearance of long-chain S-acyl-3-mercaptopropionyl-CoA by this route is not expected to be significant. More important is the hydrolysis of S-acyl-3-mercaptopropionyl-CoA to CoASH and S-acyl-3-mercaptopropionic acid catalyzed by mitochondrial thioesterase(s). Interestingly, the hydrolysis of S-acyl-3-mercaptopropionyl-CoAs proceeds much faster than the hydrolysis of acyl-CoAs of comparable chain lengths. The further metabolism of S-acyl-3-mercaptopropionic acids thus formed are unknown.

This semi-quantitative evaluation of the mitochondrial metabolism of 3-mercaptopropionic acid leads to the conclusion that S-acyl-3-mercaptopropionyl-

CoA may accumulate in mitochondria in significant amounts. Hence, attempts to elucidate the effects of 3-mercaptopropionic acid on the energy metabolism of mitochondria have to focus on the question of how S-acyl-3-mercaptopropionyl-CoAs affect mitochondrial reactions in which CoASH or CoA derivatives participate.

Since 3-mercaptopropionic acid inhibits palmitoylcarnitine-supported respiration, but hardly affects respiration sustained by pyruvate, the inhibited reaction(s) must be one or several steps of β-oxidation. The inhibition of β-oxidation by 3-mercaptopropionic acid could be the consequence of (a) the depletion of mitochondrial coenzymes necessary for β-oxidation, (b) the irreversible inactivation of at least one β-oxidation enzyme, or (c) the reversible inhibition of at least one β-oxidation enzyme. Depletion of coenzymes cannot be the cause of the inhibition, because the degradations of pyruvate and fatty acids required the same coenzymes. Since all of the β-oxidation enzymes were fully active after their release from mitochondria preincubated with 3-mercaptopropionic acid, none was irreversibly inactivated by the inhibitor. It is therefore concluded that 3-mercaptopropionic acid or a compound derived from it inhibits one or several of the β-oxidation enzymes in a reversible manner. Since β-oxidation is not inhibited in uncoupled mitochondria, the inhibition is energy-dependent possibly because 3-mercaptopropionic acid must first be converted to its CoA derivative.

This study of the metabolism of 3-mercaptopropionic acid provides strong evidence for the formation of 3-mercaptopropionyl-CoA and S-acyl-3-mercaptopropionyl-CoA thioesters in the mitochondrial matrix. Since these metabolites are likely to be present at low concentrations only, no attempt was made to identify them directly and to quantitate them. Instead, chemically synthesized metabolites of 3-mercaptopropionic acid were prepared and tested for there ability to inhibit individual enzymes of β-oxidation. The conclusion of this evaluation is that 3-mercaptopropionyl-CoA is an inhibitor of medium-chain acyl-CoA dehydrogenase and presumably of butyryl-CoA dehydrogenase. More importantly, long-chain acyl derivatives of 3-mercaptopropionyl-CoA are effective inhibitors of

several enzymes of β-oxidation. The inhibitions of 3-ketoacyl-CoA thiolase and 3-hydroxyacyl-CoA dehydrogenase are not believed to be physiologically significant, because these two enzymes are inhibited to nearly the same extent by palmitoyl-CoA which is present at concentrations of 100μM and higher in mitochondria which actively oxidize fatty acids.[80] It seems likely that the inhibition of β-oxidation is a consequence of the inhibition of long-chain and medium-chain acyl-CoA dehydrogenase by long-chain S-acyl-3-mercaptopropionyl-CoA thioesters and 3-mercaptopropionyl-CoA. Although direct proof for the proposed mechanism by which 3-mercaptopropionic acid inhibits β-oxidation in coupled mitochondria is lacking, the data presented in this report agrees best with the suggestion that the inhibition of β-oxidation is a consequence of the reversible inhibition of the first step in the pathway.

It is of interest to note that 3-mercaptopropionic acid is a known convulsant agent[22] which has been suggested to cause seizures by depressing the levels of γ-aminobutyric acid in brain.[23] The data presented here greatly enhance our understanding of the metabolism and the biological activities of 3-mercaptopropionic acid and thus may aid future studies about the biochemistry of chemically induced convulsions.

ASPECTS OF THE β-OXIDATION OF UNSATURATED FATTY ACIDS

Synthesis and Characterization of Metabolites Formed During the Oxidation of Unsaturated Fatty Acids

Results and Discussion

It is well established that enzymes are very selective towards the structural features of the substrates upon which they act. Additionally, it is known that enzymes are capable of distinguishing between geometric and optical isomers, with the consequence that, (a) a substrate analogue may not bind to the enzyme active site, (b) the binding event takes place but catalytic turnover is minimal thereby resulting in competitive inhibition compared to the natural substrate, or (c) the enzyme catalyzes a reaction and yields product. With regard to the latter case, the product could possibly be identical with the product of the natural substrate or the enzyme may catalyze a stereoselective reaction where the product has different geometric or optical properties with respect to the product produced from the natural substrate.

Examples of all of the above possibilities can be found in enzymes involved in fatty acid oxidation. 3-Hydroxyacyl-CoA dehydrogenase is one of the four enzymes of the fatty acid oxidation cycle and is absolutely specific for the L isomer of 3-hydroxyacyl-CoA's. [83] The D isomer is neither a substrate for the enzyme nor does this isomer effectively compete with the natural substrate, which leads to the assumption that the D isomer does not bind effectively because of the geometric constraints of the active site of this enzyme. In contrast, carnitine palmitoyltransferase shows a different type of specificity for the geometry of its substrate. This enzyme is involved in the uptake of long-chain acyl groups into the mitochondria and the natural cofactor is the L isomer of carnitine. The D isomer is a potent competitive inhibitor with respect to the natural substrate, and therefore binds efficiently to the active site of the transferase. An example of the third type of response that an enzyme system can have towards its substrate is illustrated by the enzyme enoyl-CoA hydratase. This enzyme catalyses the stereoselective hydration of 2-enoyl-CoA's such that 2-*cis*-enoyl-CoA's are hydrated to the D-3-hydroxy stereoisomer and 2-*trans*-enoyl-CoA's are hydrated to the L-3-hydroxy stereoisomer, and the observed kinetic constants depend on the geometry or chirality of the substrate.

The above discussion serves to illustrate the importance of considering the optical as well as geometric properties of substrates utilized in metabolic studies. It is for this reason that strict attention to these factors was necessary in the syntheses of the various compounds outlined in the introduction which were utilized in the collaborative kinetic analysis of the β-oxidation of unsaturated fatty acids. The discussion that follows highlights some of the key features of the synthetic approaches to the syntheses of these compounds. In addition, the electronic spectral characteristics of three of the four possible geometric isomers of 2,4-decadienoyl-CoA are shown and discussed as well as the determination of the equilibrium constant of the 3-hydroxyacyl-CoA dehydrogenase catalyzed oxidation of L-3-hydroxy-4-*trans*-decenoyl-CoA to 3-keto-4-*trans*-decenoyl-CoA.

2-trans,4-trans-Decadienoyl-CoA—

The synthesis of this compound has been previously reported by several groups[31, 84] yet the purification procedure described below has not been previously reported. The synthesis starts with the oxidation of commercially available 2-*trans*,4-*trans*-decadienal to the carboxylic acid, followed by the preparation of the CoA derivative by the mixed anhydride method.[61] The preparation of the CoA derivative gives at best a 50-70% yield since the sulfhydryl group of CoA can nucleophilically attack carbon number 5 in a reaction analogous to a Michael addition. The yield is also poor because of the partial polymerization that occurs in aqueous media, which most probably is due to a Diels-Alder type of reaction. In fact, the fatty acid itself is very susceptible to polymerization if kept at room temperature and exposed to normal atmospheric humidity. Although a significant amount of polymerized CoA derivative can be removed by filtration since it is not soluble in aqueous media, further purification was desired and involved ion-exchange chromatography on DEAE-cellulose. A pH of 7 was chosen since this would ensure the ionization of carboxyl groups in contaminants that arise from the Michael addition. Elution with a LiCl gradient gave one major peak that contained significant UV absorbance at 260 nm (due to the adenine moiety) and 300 nm (due to the conjugated diene-thioester chromophore). The constant ratio of these two absorbances throughout the major peak indicates high purity of the material, since any disruption of the conjugated diene-thioester system would result in diminished absorbance at 300 nm.

The final product gave a UV spectrum whose 300/260 absorbance ratio was approximately 1.0, which implies a significant purification over the crude product obtained directly from the mixed anhydride reaction, where the 300/260 absorbance ratio was never greater than 0.7. The purification procedure described above appears to be superior to that reported by Kunau (personal communication), who has used preparative thin layer chromatography on cellulose plates according to the method of Pullman.[85] Kunau found that the center of the major band containing enzymatically active 2-*trans*,4-*trans*-decadienoyl-CoA contains a significant

amount of material that is not enzymatically active, and furthermore, this material has a reduced 300/260 nm absorbance ratio compared to material that migrates slightly ahead of or behind the center of the major band. The most probable explanation for this behavior is the increased susceptibility of the desired material to polymerize as the local concentration increases dramatically due to evaporation of the mobile phase. In contrast, the local concentration of the desired material is always very low during the ion-exchange procedure, and the possibility of polymerization is minimized. This conclusion is born out by the fact that the 300/260 nm absorbance ratio is constant throughout the major peak obtained by the ion-exchange method, and therefore this procedure is clearly superior to the method of Pullman, at least for CoA derivatives that have a strong tendency to undergo polymerization.

With regard to the geometry of the conjugated double bond system, it has been assumed throughout that the *trans,trans* configuration is maintained since it is thermodynamically the most stable of the four possible configurations.

2-trans,4-cis-Decadienoyl-CoA—

The synthesis of this compound has been previously reported, and has involved either the chemical synthesis of the parent fatty acid via a Wittig reaction,[86] or a combined chemical and enzymatic approach.[87] It has been shown by Stoffel *et. al.*,[70] that the preparation of CoA derivatives from fatty acids that contain a *cis* double bond in conjugation with the carboxyl group always leads to a significant amount of CoA derivative that has the *trans* configuration. As a result, the synthesis of 2-*trans*,4-*cis*-decadienoyl-CoA should not begin with the synthesis of the parent fatty acid. The best approach is via the synthesis of 4-*cis* decenoic acid, preparation of the CoA derivative by the mixed anhydride method, followed by introduction of the 2-*trans* double bond by the use of acyl-CoA oxidase, a peroxisomal enzyme that has been reported to introduce a *trans* unsaturation at the number 2 carbon of saturated fatty acyl-CoA's at the expense of the reduction of molecular oxygen to H_2O_2.[57]

Commercially available 4-*cis*-decenal was oxidized with Ag_2O to the carboxylic acid. By direct comparison with the *trans* isomer, the proton-decoupled ^{13}C spectrum of the 4-*cis*-aldehyde indicated a contamination of approximately 3-5% of the *trans* isomer, and the carboxylic acid product contained approximately the same percent contamination of *trans* isomer, indicating that the oxidation reaction did not result in any stereomutation. The CoA derivative of 4-*cis*-decenoic acid was prepared by the mixed anhydride procedure, and it was assumed that the 4-*cis* double bond retained its geometry since it is not conjugated to the carboxyl functionality.

The final step in the synthesis involves the introduction of the 2-*trans* double bond by acyl-CoA oxidase. Osumi, *et. al.*,[57] concluded that the oxidase specifically catalyzes the introduction of a *trans* double bond in the 2 position because the product of the reaction was completely oxidized by 3-hydroxyacyl-CoA dehydrogenase after prior hydration by enoyl-CoA hydratase. This conclusion is based on the established facts that the hydratase catalyses the formation of L-3-hydroxy-acyl-CoA's from 2-*trans*-enoyl-CoA's, and that 3-hydroxyacyl-CoA dehydrogenase is absolutely specific for the L isomer of 3-hydroxyacyl-CoA's. The authors did not consider, however, that a contamination with 3-hydroxyacyl-CoA epimerase, which catalyses the interconversion of D and L-3-hydroxyacyl-CoA's, would have yielded the same result even if the product of the acyl-CoA oxidase reaction would have been the 2-*cis* isomer. A rate study was therefore undertaken to determine the geometry of the product of the oxidase reaction by coupling it to enoyl-CoA hydratase and 3-hydroxyacyl-CoA dehydrogenase. It was observed that the rate of oxidation of the oxidase product was approximately 100 times faster than could be accounted for by the small amount of epimerase activity present in our enzyme preparations. It is thus concluded that the product of the acyl-CoA oxidase reaction is indeed the 2-*trans* isomer.

After having established the stereospecificity of the oxidase reaction, 4-*cis*-decenoyl-CoA was incubated with the oxidase and monitored for increases in absorbance at 300 nm. Since the reaction mixture contained catalase and since the

formation of the conjugated double bond system is thermodynamically favored, it was assumed that the reaction would go to completion, although it should be noted that the equilibrium of the acyl-CoA oxidase reaction with saturated acyl-CoA's is approximately 3:1 in favor of 2-enoyl-CoA.[57]

Although the use of acyl-CoA oxidase for the synthesis of 2-*trans*,4-*cis*-decadienoyl-CoA has been previously reported,[87] the work performed in this report conclusively demonstrates the specificity of the acyl-CoA oxidase reaction, and in addition, the kinetic parameters determined for this compound in the collaborative kinetic study of Yang, Cuebas, and Schulz[48] clearly distinguish this compound from the *trans,trans* isomer.

D-, and L-3-Hydroxy-4-trans-decenoyl-CoA—

The synthesis of the racemic mixture begins with the Reformatzky condensation of 2-*trans*-octenal and methyl bromoacetate to give methyl 3-hydroxy-4-*trans*-decenoate. The use of the zinc column procedure of Ruppert and White[69] afforded the desired material in high yield (85%) and was apparently free of any contaminant resulting from dehydration. Mild saponification of this material at room temperature gave 3-hydroxy-4-*trans*-decenoic acid, which surprisingly was a viscous oil that failed all attempts of crystallization. The proton nmr spectrum was indicative of the assigned structure.

The optical resolution of the above material was accomplished in a manner analogous to that used by Stoffel, *et. al.*,[70] where fractional crystallization of the diastereomeric phenylethylammonium salt of 3-hydroxy-dodecanoic acid resulted in the successful resolution of the optical isomers. Mild hydrolysis of the fractionally crystallized phenylethylammonium salts gave (+) and (-)-3-hydroxy-4-*trans*-decenoic acid. The optical purity of the isomers was estimated by the optical rotation, and showed that although complete resolution was not achieved, greater than 90% optical purity was obtained.

The CoA derivative was prepared by the usual mixed anhydride procedure to give (+)- and (-)-3-hydroxy-4-*trans*-decenoyl-CoA in good yield, and no further purification was necessary. Because the validity of the enzyme kinetic work critically depends on the knowledge of the absolute configuration of the substrate as well as its optical purity, the oxidation of the above materials by 3-hydroxyacyl-CoA dehydrogenase was used to accomplish both tasks. Since 3-hydroxyacyl-CoA dehydrogenase is absolutely specific for the L isomer of 3-hydroxyacyl-CoA's it was possible to assign the L-configuration to the (+)-optical isomer and the D-configuration to the (-) isomer. In addition, the same approach permitted us to estimate the extent of contamination of each of the isomers with the other, by quantitating the extent of the oxidation of the 3-hydroxyacyl-CoAs by 3-hydroxyacyl-CoA dehydrogenase coupled to 3-ketoacyl-CoA thiolase. The results of this quantitative analysis showed that L-3-hydroxy-4-*trans*-decenoyl-CoA was contaminated with 7% D isomer, and D-3-hydroxy-4-*trans*-decenoyl-CoA was contaminated with 3% of the L isomer. Although complete separation of the enantiomers was not achieved, the precise knowledge of the extent of contamination of each optical isomer with the other made it possible to account for discrepancies arising in the kinetic analyses due to this fact.

D,L-3-Hydroxy-4-cis-Decenoyl-CoA—

The synthesis of this material begins with the oxidation of commercially available 2-octyn-1-ol to the aldehyde with pyridinium chlorochromate. Condensation of the aldehyde with methyl bromoacetate by a Reformatzky reaction gave methyl 3-hydroxy-4-decynoate. Mild saponification followed by catalytic semihydrogenation afforded 3-hydroxy-4-*cis*-decenoic acid in good yield. To confirm the geometry of the double bond configuration, proton decoupled ^{13}C nmr spectra of the *cis* isomer was compared to the spectrum obtained with the *trans* isomer, and it was possible to estimate the contamination with *trans* material to be 3%.

The CoA derivative was prepared in the usual manner, to give D,L-3-hydroxy-4-*cis*-decenoyl-CoA in good yield and further purification was not

required. Although the optical resolution of this material would have been of some advantage, the practicality of this was hampered by the small scale of the catalytic hydrogenation reaction ($\simeq$ 200 mg), whereas the amount of material needed for the fractional crystallization of the phenylethylammonium salts requires several grams of material.

The Electronic Spectra of 2-trans,4-trans, 2-trans,4-cis, and *2-cis,4-trans*-Decadienoyl-CoA—

The selective syntheses of the four possible geometric isomers of 2,4-decadienoic acid was first accomplished by Crombie[88] and his report contains a detailed comparison of the electronic, and infrared spectra, as well as the boiling point and melting points of these compounds and various analogs obtained from them. The collaborative enzyme kinetics project required the synthesis of three of the four geometric isomers of 2,4-decadienoyl-CoA, and as a result, afforded the opportunity to examine the electronic spectra of these geometric isomers with respect to each other as well as with respect to the electronic spectral features reported by Crombie for the methyl esters of 2,4-decadienoic acid and the alcohol derivatives. The following summarizes the maximum absorbance wavelengths (λ_{max}) and the millimolar extinction coefficients for the methyl esters and alcohols reported by Crombie, and the CoA derivatives described in this report:

Isomer	Methyl Ester	Alcohol	CoA Derivative
2t,4t	260 (28.5)	230 (30.6)	298 (28.5)
2t,4c	265 (22.0)	232 (22.1)	300 (19.9)
2c,4t	263 (23.8)	232 (24.0)	301 (21.1)
2c,4c	263 (17.3)	233 (20.0)	n.d.

The numbers in the above listing refer to the maximum absorbance wavelength in nm, the numbers in parentheses refer to the extinction coefficients in units of mM^{-1} cm^{-1}, and t and c refer to the *trans* and *cis* isomers, respectively.

Noteworthy is the slightly lower maximum wavelength associated with the *trans,trans* isomer in all the derivatives, reflecting a higher excited state transition energy for this isomer. In addition, the values of the extinction coefficients are very similar irrespective of the derivative. Although data for the *cis,cis* isomer of the CoA derivative was not available, the wavelength of the maximum absorbance should be approximately 300 nm and the extinction coefficient approximately 60% of the value of the *trans,trans* isomer, 17.1 mM^{-1} cm^{-1}. The apparent consistency of the trends shown in the above table further supports the assigned structures of the various isomers and suggests that similar changes in electronic and steric factors are responsible for the patterns exhibited by the isomeric acids and their derivatives.

As not to repeat the detailed discussion offered by Crombie for these various effects, the interested reader is referred to his report.[88]

The availability of the above compounds enabled a detailed kinetic study of the degradation of unsaturated fatty acids in three β-oxidation systems. In all three systems, the equilibrium constant for the dehydration of 2-*trans*,4-*trans*-decadienoyl-CoA was found to be 0.003. Similarly, the 2-*trans*,4-*cis*-isomer was found to have an equilibrium constant of 0.001. The equilibrium constants of the two geometric isomers are similar, yet their rates of oxidation in the reconstituted β-oxidation systems are very different, and is a consequence of the different kinetic constants for the two isomers rather than any slight difference in their equilibrium constants.

Another interesting result of the kinetic study was the observation that a channeling mechanism must be operative in the bifunctional peroxisome system and the *E. coli* system, where direct transfer of the 3-hydroxy intermediate is possible. This conclusion is based upon the finding that the steady state rates of oxidation in these two reconstituted systems was much greater than the rates predicted from free-diffusion models.

Finally, it was also possible to estimate the flux of degradation of 2-*trans*,4-*cis*-decadienoyl-CoA in the original pathway described by Stoffel and the more recently described NADPH-dependent 2,4-dienoyl-CoA reductase pathway. These calculations indicate that a small fraction of the degradation of the 2-*trans*,4-*cis*-isomer (2%-3%) is possible via the original pathway in the two systems where the channeling mechanism is operative, whereas in the free-diffusion mitochondrial system, no more than 0.02% of the flux is possible via the original Stoffel pathway.

The Determination of the Equilibrium Constant for the Oxidation of L-3-Hydroxy-4-trans-decenoyl-CoA by NAD^+—

The general equation describing the oxidation of 3-hydroxyacyl-CoA's is shown in the equation below:

$$K_{eq} = \frac{(NADH)(3\text{-}ketoacyl\text{-}CoA)(H^+)}{(3\text{-}hydroxyacyl\text{-}CoA)(NAD)}$$

where the concentrations in the above equation are those obtained in the equilibrium state.

Since there is a 1:1 stoichiometry of NADH formation to 3-ketoacyl-CoA formation, the equation can be represented as follows:

$$K_{eq} = \frac{(NADH_{eq})^2 (H^+)}{(NAD_{in} - NADH_{eq})(3\text{-}hydroxyacyl\text{-}CoA_{in} - NADH_{eq})}$$

where the subscripts *in* and *eq* refer to the initial and equilibrium concentrations, respectively.

Since the initial concentrations of NAD and 3-hydroxyacyl-CoA are defined, and the reaction is carried out at a constant pH, the determination of the equilibrium constant is obtained by simply measuring the concentration of NADH at equilibrium.

Because of the availability of 3-hydroxy-4-*trans*-decenoyl-CoA, it was of interest to determine the equilibrium constant for the oxidation of this substrate by 3-hydroxyacyl-CoA dehydrogenase. Although the absorbance band of the enolate form of the 3-keto product overlaps with that of NADH, the contribution by the 3-keto product to the absorbance at 340 nm was reproducibly found to be 10% of the total absorbance under the conditions of the assay. Thus, the extinction coefficient of 3-keto-4-*trans*-decenoyl-CoA at 340 nm was estimated to be 620 M^{-1} cm^{-1} at pH 6.5. The equilibrium constant for the reaction was determined to be 1.10×10^{-8} M.

Fig. 14 (circles) shows the calculated percentage of 3-hydroxy substrate oxidized as the pH is varied between 5 and 10. The typical S-shaped curve has an

inflection at pH 7.0, which corresponds to the pH at which 50% of the substrate is oxidized under the specified concentrations of substrate and NAD. Wakil[83] has determined the equilibrium constant of the oxidation of 3-hydroxybutyryl-CoA to be 6.3×10^{-11}, and using the same concentrations of NAD and substrate, observed an inflection point at pH 8.2. The second curve in Figure 14 corresponds to the theoretical dependence of the percent oxidation of 3-hydroxybutyryl-CoA using the equilibrium constant and concentrations of 3-hydroxybutyryl-CoA and NAD used by Wakil. The plot predicts an inflection at pH 9.6, which significantly departs from the pH of the inflection point reported by Wakil (8.2). It is therefore obvious that either the equilibrium constant or the reported conditions of the assay are in error. Nevertheless, the equilibrium constant of the oxidation of 3-hydroxy-4-*trans*-decenoyl-CoA is significantly higher than that of 3-hydroxybutyryl-CoA. The explanation for this is most likely the increased stability provided by the additional double bond in conjugation with the enol or enolate form of the 3-keto-thioester, whereas the thermodynamic stability of the 3-hydroxyacyl-CoA's is not very much affected by the presence of the double bond in the 4-position. As a result, the percent of 3-hydroxy-4-*trans*-decenoyl-CoA oxidized at physiological pH is extremely sensitive to the concentration of NAD, and can easily be manipulated so that the compound exists mostly as the 3-keto derivative, whereas with saturated 3-hydroxyacyl-CoA's, either an unphysiologically high pH, or very high concentration of NAD is required to favor 3-ketoacyl-CoA formation.

STEADY STATE KINETICS OF COUPLED ENZYME REACTIONS

RESULTS AND DISCUSSION

The model shown below describes the simplest treatment of a coupled two-enzyme system:

$$S \xrightarrow[v_1]{E_1} P \xrightarrow[v_2]{E_2} Q$$

where S is the substrate for the primary reaction, P is the product of the primary reaction, Q is the product of the coupling enzyme, E_1 and E_2 are the primary and coupling enzymes, respectively, v_1 is the rate of the primary reaction, and v_2 is the rate of the coupling reaction.

The above model includes the assumptions that the coupling reaction, as well as the primary reaction, are irreversible and many treatments have appeared in the literature describing the pre-steady-state rate equations[89-91] , optimization of the coupled system with regard to coupling enzyme[92] , and limitations with respect to kinetic parameters of the enzymes in order for such systems to be capable of achieving a steady-state.[93, 94] If the kinetic parameters of the enzymes permit a steady-state to be achieved, then $v_1=v_2$ and the steady-state initial velocity rate equations can be solved.

Although the above model is sufficient to describe many coupled enzyme systems, it ignores the reverse reaction of the primary enzyme, a situation which is valid only when the removal of P by the coupling enzyme can completely suppress the reversal of the primary reaction. Irreversibility of the primary reaction can usually be achieved by the addition of a large excess of the coupling enzyme, so that the rate limiting step of the system is the formation of P.

For systems where the equilibrium of the primary reaction is not very unfavorable, transient and steady-state rate equations derived from the above model provide good approximations for the theoretical treatment of such systems. In contrast, systems where the primary reaction catalyzes a thermodynamically unfavorable reaction cannot be approximated by the above model since competition between the reverse reaction of the primary enzyme and the coupling reaction is significant. An additional complication is that the coupling of an unfavorable primary reaction requires high concentrations of coupling enzyme as well as primary enzyme (because the *kcat* of the forward reaction of the primary enzyme can be extremely low), and therefore Zone A kinetics[53], which assumes that the concentration of free substrate is approximately equal to the concentration of total substrate, may not hold under these conditions.

In light of the above, the model shown below represents a better approximation of a situation where the primary enzyme catalyzes a thermodynamically unfavorable reaction:

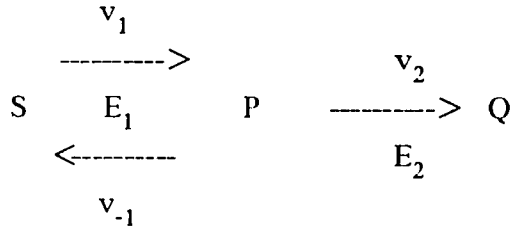

where v_{-1} is the rate of the reverse reaction of the primary enzyme.

In the following discussion, I will describe the properties of the steady-state kinetics of the the above model in which a reversible uni-uni primary enzyme mechanism is coupled to an irreversible uni enzyme reaction. It will be assumed throughout that a steady-state can always be reached, and that the lag time of the coupled system due to the time taken for the product of the primary reaction to reach steady-state is very short because the concentration of P is limited by the unfavorable equilibrium of the primary reaction.

The steady-state of the above model is achieved when

$$v_{1(net)} = v_2$$

where $v_{1(net)} = v_1 - v_{-1}$

For the enzyme mechanisms described above, the steady-state is described by equation (1):

$$\frac{V_{1f}\ K_{1r}\ S_t - K_{1f}\ V_{1r}\ P_{ss}}{K_{1r}\ S_t + K_{1f}\ P_{ss} + K_{1f}\ K_{1r}} = \frac{V_{2f}\ P_{ss}}{P_{ss} + K_{2f}} \qquad (1)$$

where S_t is the total substrate concentration, P_{ss} is the total steady-state concentration of intermediate P, the V terms are the V_{max} kinetic constants, the K terms are the Michaelis kinetic constants, and the subscripts refer to the primary (1) or coupling (2) enzymes and refer to the forward (f) or reverse (r) direction of the reaction. The assumptions are that $S_t \simeq S_f$, and that $P_{ss} \simeq P_{ss_f}$, where the subscripts (t) and (f) refer to the concentration of total (free plus bound) and free substrate or intermediate, respectively.

Since the two enzyme reactions are assumed to be at steady-state, the velocity of the coupled system is equal to the primary or coupling reaction velocity.

Elimination of P_{ss} from the two equations describing the coupled system gives the following quadratic equation (2):

$$((S_t + K_{1f})K_{1r} - K_{1f} K_{2f})vel^2 \qquad (2)$$
$$+ (((-V_{2f} - V_{1f})S_t - K_{1f} V_{2f})K_{1r} - K_{1f} V_{1r} K_{2f})vel + V_{1f} V_{2f} S_t K_{1r}$$
$$= 0$$

where vel is the velocity of the coupled reaction.

A simplifying assumption can be made if the primary enzyme catalyzes a reaction with a thermodynamically unfavorable solution equilibrium. The numerator of all linear rate equations describes the effect of product inhibition on the forward reaction with respect to the approach to equilibrium, and the denominator relates product inhibition to the decrease in the availability of free enzyme. Thus for a given concentration of S, if the equilibrium concentration of P in the absence of coupling enzyme is much less than K_{1r} and K_{2f}, then the terms containing P_{ss} in the denominator of equation (1) can be eliminated, resulting in a much simpler solution that resembles the Michaelis-Menton equation (Eq. (3)).

$$vel = \frac{V_{1f} S_t}{S_t + K_{1f}\left(\frac{V_{1r} K_{2f}}{K_{1r} V_{2f}} + 1\right)} \qquad (3)$$

It is readily apparent that the above equation reduces to the Michaelis-Menton equation at infinite concentrations of coupling enzyme, and that there is a rectangular hyperbolic dependency of the coupled reaction rate with respect to S_t. The apparent Km is a function of the kinetic constants of both the primary and and coupling enzyme. Rearrangement of Eq. 3 also predicts a rectangular hyberbolic dependency of the coupled reaction rate on the concentration of coupling enzyme (Eq. (4)),

$$vel = \frac{\frac{S_t \; V_{1f}}{S_t + K_{1f}} V_{2f}}{\frac{V_{1r} \; K_{2f}}{K_{1r} \left(\frac{S_t}{K_{1f}} + 1\right)} + V_{2f}} \tag{4}$$

Fig. 15 is a plot of coupled reaction velocity as a function of coupling enzyme concentration. When $V_{2f} = Km_{apparent}$, the rate of P_{ss} being converted to product exactly equals the rate of P_{ss} being converted to S. Eq. (3) can also be rearranged so that all kinetic constants of the primary reaction are substituted for by the equilibrium constant according to the Haldane relationship for a uni uni mechanism (Eq. (5)):

$$vel = \frac{vel_{\exp} K_{eq\,1} S_t \; V_{2f}}{K_{eq\,1} S_t \; V_{2f} + vel_{\exp} K_{2f}} \tag{5}$$

where $K_{eq\,1} = \frac{V_{1f} \; K_{1r}}{V_{1r} \; K_{1f}}$, and

$$vel_{\exp} = \frac{V_{1f} \; S_t}{K_{1f} + S_t}$$

is the highest expected velocity of the coupled system if the coupling reaction is not rate limiting.

Further rearrangement of Eq. 5 to a form that is analogous to the Eadie-Scatchard equation shows that the equilibrium constant of the primary reaction may be estimated with only the prior knowledge of the forward kinetic parameters of the coupling enzyme (Eq. (6)).

$$vel = -\frac{vel_{\exp}}{K_{eq\,1}} \frac{vel \; K_{2f}}{V_{2f} \; S_t} + vel_{\exp} \tag{6}$$

where the y-intercept = vel_{exp}

the x-intercept = $K_{eq\,1}$

and the slope = $-\frac{vel_{exp}}{K_{eq\,1}}$

Fig. 16 shows the characteristics of such a plot of *vel* versus *vel* ($\frac{K_{2f}}{S_t V_{2f}}$) for a coupled enzyme system where the primary enzyme has kinetic parameters that predict a $K_{eq\,1}$ of 2.8×10^{-3}. Lines 1-4 are are the theoretical predictions at various concentrations of primary enzyme, all of which intersect at a point on the x-axis that corresponds to the $K_{eq\,1}$ of the primary enzyme. Since the experimental determination of vel_{exp} and $K_{eq\,1}$ does not depend on the knowledge of the kinetic parameters of the primary enzyme in such an analysis, this method provides an independent check on the Haldane relationship if one already knows the four kinetic parameters of the primary enzyme. Conversely, this type of analysis can offer an independent check of the kinetic parameters of the coupling enzyme if the $K_{eq\,1}$ of the primary reaction is known with reasonable certainty. Another useful application of the above analysis is the simultaneous determination of the kinetic constants of the forward reaction catalyzed by the primary enzyme after independently determining the kinetic parameters of the primary reaction in the reverse direction and the coupling reaction in the forward direction. Rearrangement of Eq. (5) gives the following linear equation parameters for the Eadie-Scatchard plot:

$$\text{slope} = -\frac{S_t V_{1r}}{K_{1r}\left(\frac{S_t}{K_{1f}} + 1\right)}$$

$$\text{x-intercept} = \frac{V_{1f} K_{1r}}{V_{1r} K_{1f}}$$

and

$$\text{y-intercept} = \frac{S_t V_{1f}}{K_{1f} + S_t}$$

Deviation from linearity in the Eadie-Scatchard plot could possibly arise from the concentration of P_{ss} not satisfying the conditions stated above, or from the concentration of primary and/or coupling enzyme exceeding the limits that govern Zone A behavior ([E] $<<$ Km).

Although several thorough treatments of mutual depletion effects have been reported for the irreversible uni uni reaction,[49, 50, 53] none have appeared that dealt with the effects of high enzyme concentrations on coupled enzyme systems. It is well known that mutual depletion effects are maximal when [E] $\simeq Km$ *and* [S] $\simeq Km$. In other words, both enzyme and substrate are depleted under these conditions. If [E] $\simeq Km$ and [S] $<<$ Km, there is no mutual depletion since only the substrate is being depleted. This situation is referred to as Zone C, and for an irreversible uni uni mechanism the rate equation takes the form called the inverse Michaelis-Menton equation where the [S] term in the denominator is replaced by [E]. In the coupled enzyme systems described in this report, the intermediate concentration is assumed to be much lower than its Km for the coupling enzyme, yet the intermediate substrate is replenished by the forward reaction of the primary enzyme. Looked at in another way, high concentrations of coupling enzyme deplete the intermediate substrate for the reverse reaction of the primary enzyme. In addition, high concentrations of primary enzyme may satisfy Zone A kinetics

kinetics in the forward direction ($S_f >> [E_1]$), yet the depletion of free intermediate substrate by high concentrations of the primary enzyme will affect the availability of substrate for the coupling enzyme. Since all these effects occur simultaneously in a coupled enzyme system at steady state, it is clear that the conclusions of mathematical treatments describing single enzyme reactions cannot be applied to coupled enzyme systems, and the discussion that follows will attempt to develop a quantitative treatment of the kinetics of coupled enzyme systems at high enzyme concentrations.

The first analysis will examine effects of high concentrations of coupling enzyme with the assumption that the concentration of primary enzyme is always much less than the concentration of S. The above condition can be expressed mathematically as a conservation equation for total substrate of the primary enzyme ($[S_t]$) such that $[S_t] = [S_f] + [P_{ss_f}] + \Sigma$ [transitory complexes], where in the present case, Σ [transitory complexes] is the concentration of all transitory complexes associated with the coupling enzyme. If $[P_{ss_f}] << K_{2f}$ and K_{1r}, the following simultaneous equations can be used to derive the rate equation:

$$v_{1(net)} = \frac{\frac{S_f V_{1f}}{K_{1f}} - \frac{P_{ss_{free}} V_{1r}}{K_{1f}}}{\frac{S_f}{K_{1f}} + 1} \tag{7}$$

$$v_2 = kcat_{2f} X_2 \tag{8}$$

$$E_{2t} P_{ss_{free}} = K_{2f} X_2 \tag{9}$$

$$S_t = X_2 + S_f + P_{ss_{free}} \tag{10}$$

where X_2 is the sum of all coupling enzyme transitory complexes, $kcat_{2f}$ is the catalytic rate constant for the coupling enzyme, E_2 is the concentration of coupling enzyme, P_{ss_f} is the concentration of free intermediate, and the subscripts f and t refer to free and total, respectively.

When Eqs. 7-10 are at steady state, $v_{1(net)} = v_2 = vel$, and elimination of all unknown parameters gives the following steady state rate equation (Eq. (11)):

$$\left(\frac{E_{2t}}{K_{2f}} + 1\right) vel^2 \tag{11}$$

$$-\left(\frac{K_{1f}\, V_{1r}}{K_{1r}} + \frac{E_{2t}\,(V_{1f} + kcat_{2f}\,(S_t + K_{1f}))}{K_{2f}} + V_{1f}\right) vel$$

$$+ \frac{E_{2t}\, kcat_{2f}\, S_t\, V_{1f}}{K_{2f}} = 0$$

Although the above equation provides an accurate description of the coupled enzyme system given the restrictions mentioned above, it would be of interest to analyze the error associated with the use of Eq. (3) at high coupling enzyme concentrations. Fig. 17 is a plot of the percent error in the predicted coupled reaction rate vs. the log of the E_{2t} / K_{2f} ratio using typical values for the kinetic constants (Curve 1). The positive values for the percent error reflect the prediction of rates by Eq. (3) that are higher than the rates predicted by the more complete rate equation (Eq. (11)). Curve 2 shows the effect of increasing the substrate concentration ten-fold (from 20μM to 200μM), and it is obvious that at least with the kinetic parameters used in this plot, the percent error is not very responsive to large changes in the substrate concentration. Noteworthy is the decrease in error as the substrate concentration is increased. This behavior can be explained by the fact when the substrate is increased, the conditions of the system are approaching those for which the Zone A equation holds. In fact, the limit of the error function as the substrate concentration approaches infinity is zero, which is in accordance with the statement above.

In contrast, Fig. 18 shows the rather dramatic effect of various concentrations of primary enzyme on the percent error as a function of the E_{2t} / K_{2f} ratio. Curves 1-10 represent a linear increase in primary enzyme concentration from 0.53 μM to 5.3 μM. Regardless of the actual parameter values, the error function predicts a limiting fractional error at low concentrations of coupling enzyme and a limiting fractional error at high coupling enzyme concentrations. The limiting value of the error function as the E_{2t} / K_{2f} ratio approaches zero is equal to the solution equilibrium constant of the primary reaction. The limiting value of the error function at infinite concentration of the coupling enzyme can be obtained by taking the limit of the error function as the E_{2t} / K_{2f} ratio approaches infinity, and results in the following simple relationship between the independent variables and the fractional error (Eq. (12)):

$$V_{1f} = \frac{(S_t + K_{1f})^2 F_{E_{2t}\to\infty} kcat_{2f}}{\frac{S_t F_{E_{2t}\to\infty}}{F_{E_{2t}\to\infty} + 1} + K_{1f}} \qquad (12)$$

where $F_{E_{2t}\to\infty}$ is the limiting fractional error at infinite coupling enzyme concentration.

It is also apparent that under certain conditions, a subsidiary maximum occurs as the concentration of primary enzyme is increased. The equation describing this maximum can be found by partial differentiation of the implicit error function with respect to the E_{2t} / K_{2f} ratio, setting the numerator of the differential to zero, eliminating the E_{2t} / K_{2f} term from this equation and the implicit error function equation by taking successive resultants, and then factoring the resulting fourth order polynomial. The resulting equation relating the independent parameters and the subsidiary maximum is the following (Eq. (13)):

$$K_{eq\,1} = \frac{2^2 F_{max}(F_{max} + 1) kcat_{2f}\ S_t \left(\frac{K_{1f}\ V_{1r}}{K_{1r}} - kcat_{2f}\ (S_t + K_{1f})\right)}{((F_{max} + 1) K_{1f} \left(\frac{V_{1r}}{K_{1r}} - kcat_{2f}\right) - F_{max} kcat_{2f}\ S_t)^2} \qquad (13)$$

where F_{max} is the fractional error at the subsidiary maximum.

Both Eq. (12) and (13) can be solved for the fractional error by the quadratic formula, and only one of the two solutions gives a result that is positive. When the two roots of the quadratic solution for Eq. (13) are both negative, a subsidiary maximum does not exist; such is the situation for curves 1-4 in Fig. 18.

It is evident from the above analysis that the behavior of the error function is complex, yet the most notable observation is the that the error associated with the use of Eq. (3) is well below 1%, even when the concentration of coupling enzyme is extrapolated to infinity. Of course, this conclusion only applies to the parameters used for calculating the curves of Fig. 18, yet it is evident that for coupled enzyme systems where the primary reaction catalyzes a thermodynamically very unfavorable reaction, the error associated with the use of Eq. (3) is minimal if, and only if, the concentration of transitory complexes associated with the primary enzyme is insignificant.

Since the above rate equation describing the coupled system (Eq. (11)) is fairly complex, the availability of a simpler equation by approximation would be of considerable value. The following is a reasonable approximation to the true rate equation that was derived in a manner analogous to that used by Cha[49] to derive the "Cha-Cha" approximation to the total rate equation for the irreversible uni uni mechanism (Eq. 14):

$$vel = \frac{S_t V_{1f}}{K_{1f}\left(\frac{V_{1r} V_{2f}}{K_{1r} K_{2f}} + 1\right) + \frac{(K_{2f} + E_{2t})V_{1f}}{V_{2f}} + S_t} \qquad (14)$$

The above equation has the same form as Eq. (3) but includes an additional term in the denominator to account for the binding of intermediate P_{ss} at high concentrations of coupling enzyme. This equation shows that a significant error associated with the use of Eq. (3) occurs when the ratio V_{1f} / V_{2f} is significant,

and that this factor is modulated by the concentration of the coupling enzyme relative to its Km for the intermediate substrate.

As previously mentioned, high concentrations of primary enzyme may be required to observe measurable rates of coupled reactions for which the equilibrium constant and/or forward $kcat$ are extremely low. The mathematical model developed above is applicable to coupled systems that require high concentrations of coupling enzyme, but it does not account for mutual depletion effects with regard to the initial substrate, nor does it take into account the effect of high concentrations of primary enzyme on the coupling reaction. To account for these effects, the simultaneous equation system must include the following conservation equation:

$$S_t = S_f + X_1 + P_{ss_f} + X_2 \tag{15}$$

where X_1 is the concentration of transitory complexes associated with the primary enzyme.

After setting up the steady state relationships, partial elimination of unknowns, and partial grouping of rate constants into kinetic constants as defined by Cleland[95], the following three simultaneous equations are obtained:

$$vel = \frac{\frac{S_f V_{1f}}{K_{1f}} - \frac{P_{ss} V_{1r}}{K_{1r}}}{\frac{S_f}{K_{1f}} + \frac{P_{ss}}{K_{1r}} + 1} \tag{16}$$

$$P_{ss} = \frac{K_{2f} vel}{E_{2t} kcat_{2f}} \tag{17}$$

$$S_i = -\frac{K_{1f}\ vel - E_{1t}(kcat_{1r} + kcat_{1f})S_f}{(kcat_{1r} + kcat_{1f})S_f + K_{1f}\ kcat_{1r}} + \frac{vel}{kcat_{2f}} + S_f + P_{ss} \quad (18)$$

where vel is the coupled reaction rate, and $kcat_{1r}$ and $kcat_{1f}$ are the catalytic rate constants of the reverse and forward directions of the primary enzyme, respectively.

It should be noted that the above system of simultaneous equations makes only one limiting assumption; that $P_{ss_f} \ll K_{2f}$, which is less restricting than the system discussed previously which had the additional requirement that $P_{ss_f} \ll K_{1r}$. Elimination of all unknown parameters results in a complicated cubic rate equation. Nevertheless, it is still possible to numerically calculate the percent error between the use of this complex cubic and Eq. (3). Utilizing the same kinetic parameters as in the previous error analysis, the true initial velocity is solved numerically, and utilized in the following error equation:

$$\%error = \left(\frac{vel_{Eq.\ (3)}}{vel_{true}} - 1\right) \times 100 \quad (19)$$

Figure 19 shows the log of the percent error calculated by use of Eq. 19 as a function of the E_{2t} / K_{2f} ratio at logarithmically increasing ratios of E_{1t} / K_{1f} (see legend to Figure 19 for details). Curves 1-5 represent concentrations of primary enzyme that are 0.01, 0.1, 1, 10, and 100 times the K_{1f} value. Noteworthy is the dramatic effect of high concentrations of primary enzyme as these values approach and exceed the K_{1f} value. Since the concentration of substrate used for this plot is close to the values of K_{1f}, the error arises mainly from mutual depletion of substrate and primary enzyme, and it is not very responsive to changes in the concentration of coupling enzyme. Also noteworthy is the fact that this error function does not display a subsidiary maximum as did the

previous error function that did not take into consideration the concentration of transitory complexes associated with the primary enzyme.

To examine the effect of high concentrations of primary enzyme under conditions of non-mutual depletion with respect to the substrate of the forward reaction, high concentrations of primary enzyme (near K_{1f}) and substrate concentrations that are approximately ten times the K_{1f} value were used to generate the plot in Figure 20. Curves 1-3 represent the percent error at ratios of primary enzyme concentrations to K_{1f} of 0.01, 0.1, and 1, respectively. For curve 3, it is obvious that increasing the concentration of coupling enzyme can lower the percent error from a maximum of approximately 9% to a limiting error of approximately 0.7%. Regardless of the kinetic parameters, it is obvious that increasing concentrations of coupling enzyme always results in the decrease in error associated with the use of Eq. (3), which is in distinct contrast to conclusions drawn from the analysis of single enzyme catalyzed reactions at high concentrations of enzyme.

Again, it would be instructive to have an approximate rate equation for the coupled systems under consideration, since the true rate equation is a complex cubic polynomial. The equation shown below, which is a reasonable approximation of the true equation, was obtained by substituting zero for all higher order terms of P_{ss} during the elimination of unknown parameters (Eq. (20)):

$$vel = S_t \frac{V_{1f}}{\frac{K_{2f}}{V_{2f}} A + \frac{V_{1f}}{kcat_{2f}} + E_{1t} + S_t + K_{1f}} \qquad (20)$$

where A is defined as:

$$\frac{(V_{1r} + V_{1f})}{K_{1r}} (E_{1t} - S_t) + V_{1f} \left(\frac{1}{K_{eq\,1}} + 1\right)$$

The above equation should yield good values for situations where the concentration of intermediate P_{ss} is very low and the equation should more closely approximate the true cubic rate equation at increasing concentrations of primary and/or coupling enzyme. Equation (20) can be further simplified depending on the particular kinetic parameters of the coupled system under investigation.

One final point to consider is whether or not it is always possible to arrange a coupled enzyme system so that the rate limiting step is independent of the concentration of coupling enzyme. In other words, is there ever a situation where infinite concentration of coupling enzyme does not yield a rate that is solely dependent on the forward kinetic parameters of the primary enzyme? To answer this question, an equation is derived by taking the limit of the complete cubic rate equation as the concentration of coupling enzyme approaches infinity. For multivariate polynomial's, taking the limit as a variable approaches infinity can be accomplished by rationally substituting a dummy variable for the multiplicative inverse of the original variable, and then taking the limit of the equation as the dummy variable approaches zero. Solving for S_t and then performing partial fraction decomposition with respect to vel, gives the following equation relating the independent variables with the coupled reaction velocity when E_{2t} approaches infinity (Eq. (21)):

$$S_t = \frac{vel_{max}}{kcat_{2f}} + \frac{vel_{max}}{kcat_{1f}} + K_{1f}\left(\frac{V_{1f}}{V_{1f} - vel_{max}} - 1\right) \qquad (21)$$

where vel_{max} represents the maximum coupled velocity attainable at infinite concentration of coupling enzyme.

It is noteworthy that the form of the above equation is analogous to the partial fraction decomposition of the rate equation previously derived for the full solution of the irreversible uni mechanism.[96, 97] The $vel_{max}/kcat_{1f}$ and $vel/kcat\ 2f$ terms arise from the consideration of high concentrations of primary enzyme and coupling enzyme, respectively. If both of these terms are

significantly lower than the total concentration of substrate S_t, the equation reduces to the Michaelis-Menton equation for the forward direction of the primary enzyme. Situations that deviate from these conditions will probably occur very infrequently, yet it is instructive to point out that in a coupled enzyme assay where the equilibrium of the primary reaction is low and the *kcat* of the coupling enzyme is also very small, it is not impossible to find the system deviating from the expected first order behavior with respect to the concentration of primary enzyme. Under these circumstances it is impossible to accurately determine the forward kinetic constants of primary enzyme unless a coupling enzyme with a much larger *kcat* is available.

Finally, it is also possible to derive an exact relation between the fractional error associated with the use of Eq. (3) compared to the true cubic rate equation and the independent variables describing the coupled enzyme system at infinite concentrations of coupling enzyme (Eq. (22)):

$$E_{1t} = \frac{F_{E_{2t}\to\infty}(F_{E_{2t}\to\infty} + 1)kcat_{2f}\ (S_t + K_{1f})^2}{(kcat_{2f} + kcat_{1f})(F_{E_{2t}\to\infty}S_t + F_{E_{2t}\to\infty}K_{1f} + K_{1f})} \qquad (22)$$

In conclusion, the above analysis of coupled enzyme reactions for systems in which the primary enzyme catalyzes a thermodynamically unfavorable reaction provides a simple method to estimate the equilibrium constant of the primary reaction, or alternatively test the Haldane relationship between the four kinetic constants of the primary reaction. In addition, a mathematical analysis of such coupled systems examined the errors associated with the use of a simple equation that does not take into consideration the depletion of free substrates due to high concentrations of transitory complexes. Finally, some approximations to rate equations are provided that can be used when the concentrations of primary and/or coupling enzyme are significant.

TABLE 1

Kinetic parameters for general acyl-CoA dehydrogenase from pig liver.

Substrate	K_m [a]	K_m^{ETF} [b]	TN [a,c]
	μM	nM	s^{-1}
Butyryl-CoA	37.4 ± 6.4	72 ± 22	13.1 ± 0.7
3-Mercaptopropionyl-CoA	17.8 ± 1.7	39 ± 18	0.67 ± 0.05

[a] Initial rates were determined at five different concentrations of 3-mercaptopropionyl-CoA, and data were subjected to a weighted program for a Texas Instruments TI-59 calculator which provides values for K_m, V_{max}, and their standard errors (33).

[b] ETF, electron-transferring flavoprotein; values are means ± S.E. ($n = 5$).

[c] Turnover number.

TABLE 2

Activities of carnitine acetyltransferase with different acyl-CoA substrates.

For experimental details see Experimental section.

Substrate (100 μM)	Specific activity	Relative activity
	units/mg protein	%
Acetyl-CoA	40	100
S-Acetyl-3-mercapto-propionyl-CoA	4.4	11
3-Mercaptopropionyl-CoA	11.4	28.5

TABLE 3

Hydrolysis of acyl-CoA thioesters by rat heart mitochondria.

For experimental details see Experimental section.

Substrate	Specific activity	
	22 μM substrate	66 μM substrate
	milliunits/mg of mitochondria	
Acetyl-CoA	5	13
Octanoyl-CoA	7.1	11.5
Palmitoyl-CoA	25.3	20
S-Acetyl-3-mercapto-propionyl-CoA	18.4	40
S-Caproyl-3-mercapto-propionyl-CoA	31.6	41.5
S-Myristoyl-3-mercapto-propionyl-CoA	77	29.4

TABLE 4

The effects of S-acyl-3-mercaptopropionyl-CoA thioesters on the activities of β-oxidation enzymes.

The assay conditions are as described in the experimental section. The concentrations of all S-acyl-3-mercaptopropionyl-CoA thioesters were 20 μM. The substrates used for assaying the β-oxidation enzymes are: butyryl-CoA, octanoyl-CoA, and palmitoyl-CoA for the short-chain, medium-chain, and long-chain acyl-CoA dehydrogenases, respectively; crotonyl-CoA for crotonase; D,L-3-hydroxyoctanoyl-CoA for 3-hydroxyacyl-CoA dehydrogenase; and acetoacetyl-CoA for 3-ketoacyl-CoA thiolase.

Compound	Remaining activity					
	Acyl-CoA dehydrogenase			Crotonase	3-Hydroxyacyl-CoA dehydrogenase	3-Ketoacyl-CoA thiolase
	SC[a]	MC[a]	LC[a]			
	%					
S-Acetyl-3-mercaptopropionyl-CoA	100	100	100	96	100	92
S-Hexanoyl-3-mercaptopropionyl-CoA	100	100	100	94	100	86
S-Myristoyl-3-mercaptopropionyl-CoA	92	28	26	58	0	0

[a] SC, short-chain; MC, medium-chain; LC, long-chain.

Figure 1

The fatty acid oxidation cycle.

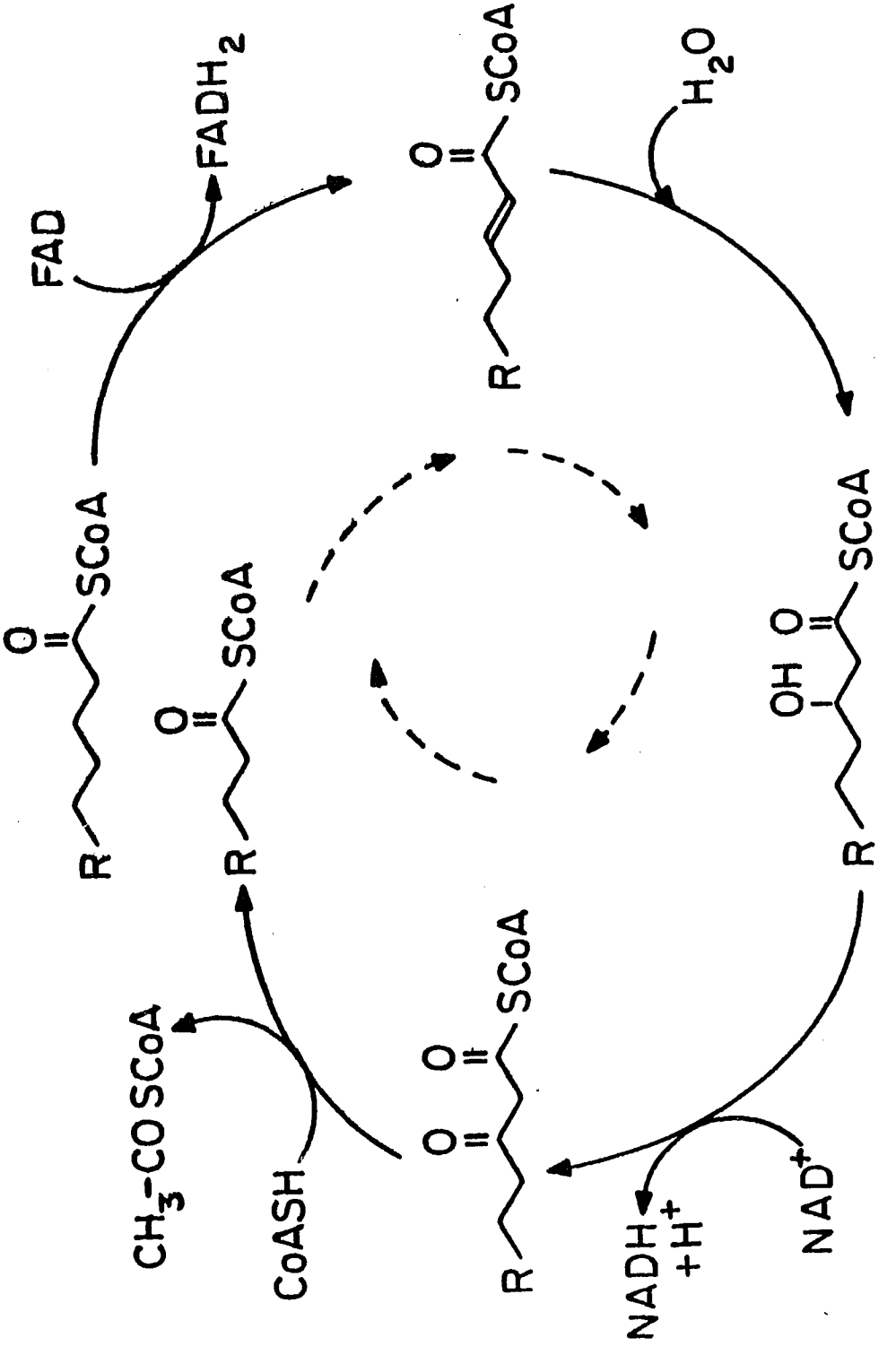

Figure 2

The regulation of fatty acid oxidation in heart.

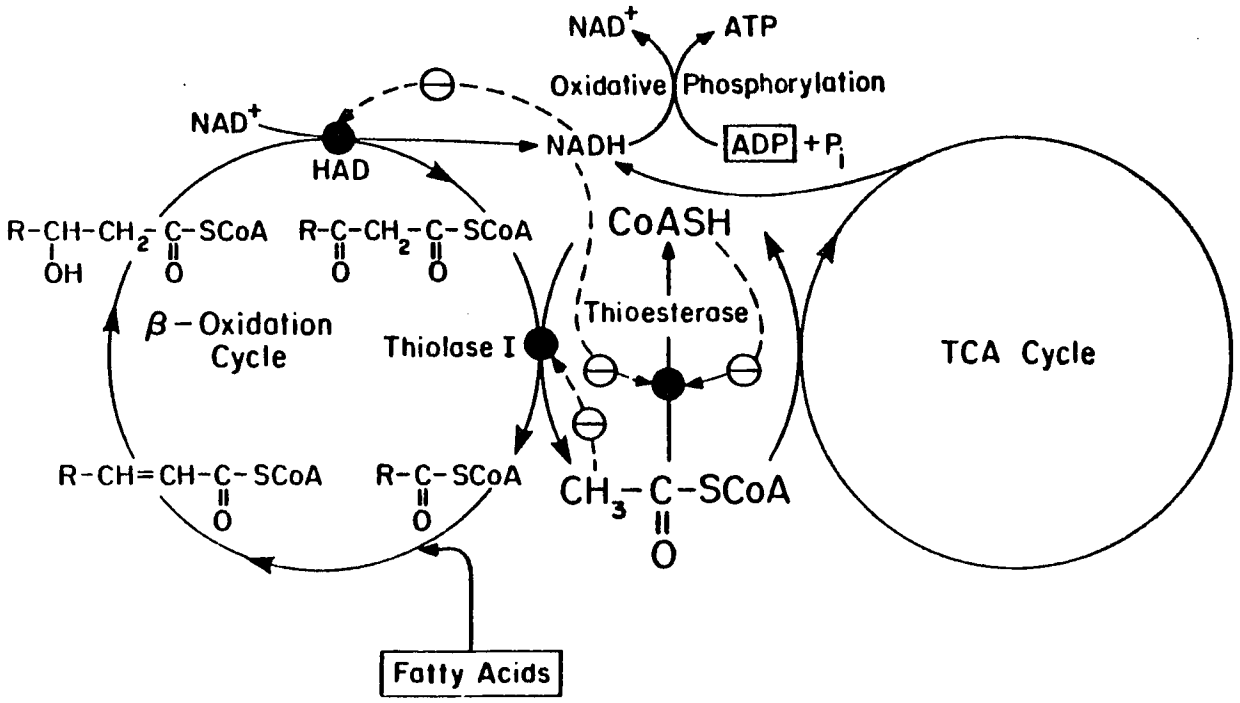

Figure 3

Pathway of linoleic acid degradation. A, pathway proposed by Stoffel and Caesar[30]. B, modified pathway supported by observations published by Cuebas and Schulz[38]. and by Kunau and Dommes[31]. Reactions catalyzed by: 1, acyl-CoA dehydrogenase; 2, enoyl-CoA hydratase; 3, L-3-hydroxyacyl-CoA dehydrogenase; 4, 3-ketoacyl-CoA thiolase; 5, 3-hydroxyacyl-CoA epimerase; 6, 3-cis,2-trans-enoyl-CoA isomerase; 7, 2,4-dienoyl-CoA reductase.

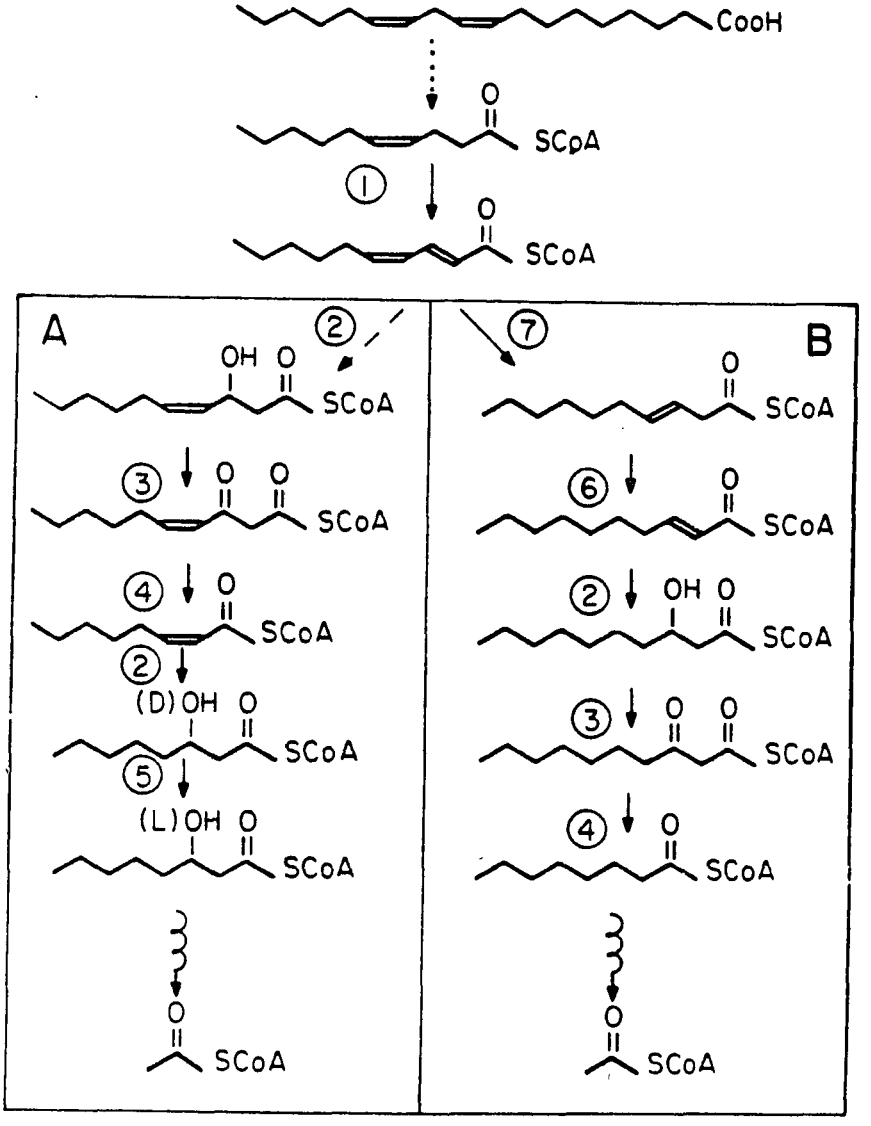

Figure 4

Purification of the mono-CoA thioester of bis(2-carboxyethyl)disulfide by chromatography on DEAE-cellulose.

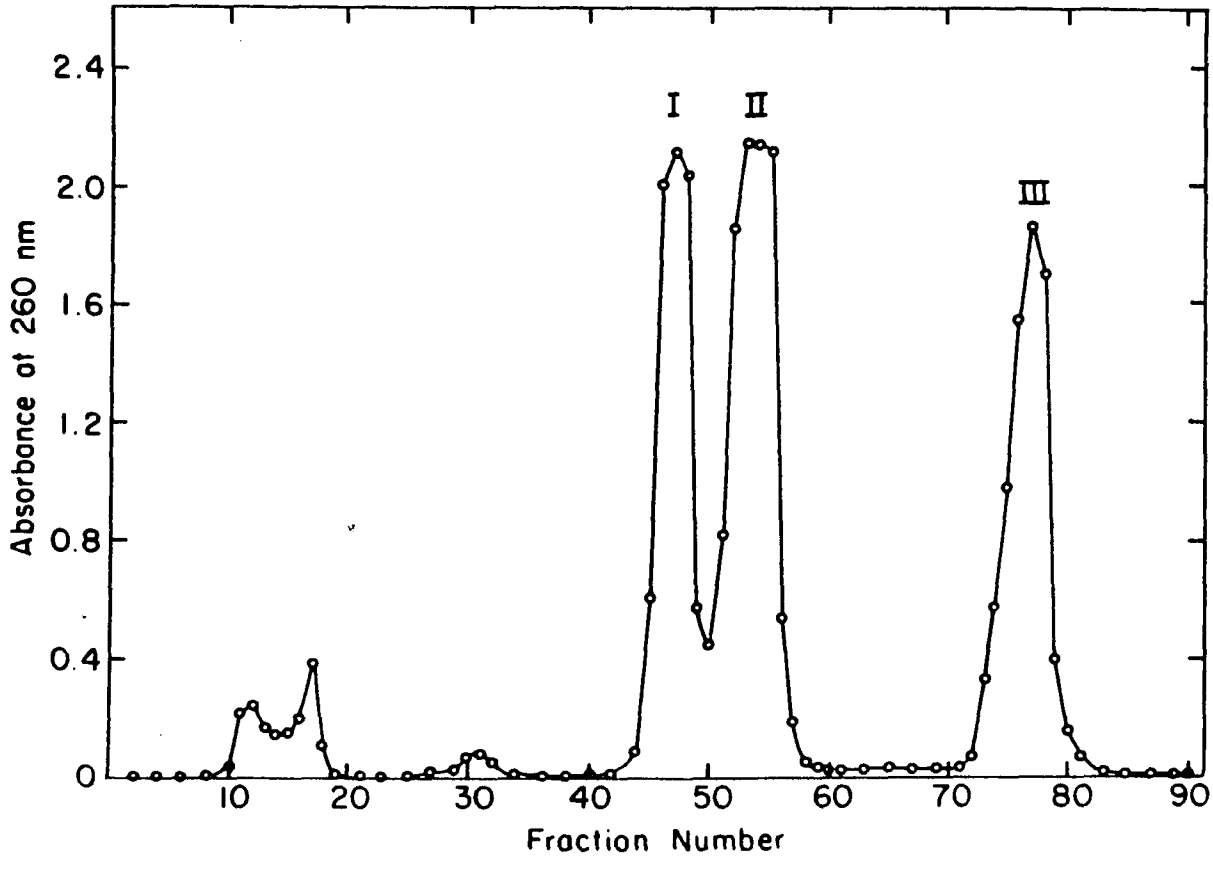

Figure 5

Purification of 3-mercaptopropionyl-CoA by chromatography on DEAE-cellulose. *Solid line* , absorbance at 260 nm; *dashed line* , sulfhydryl concentration. Only fractions 1-15 were tested for sulfhydryl groups.

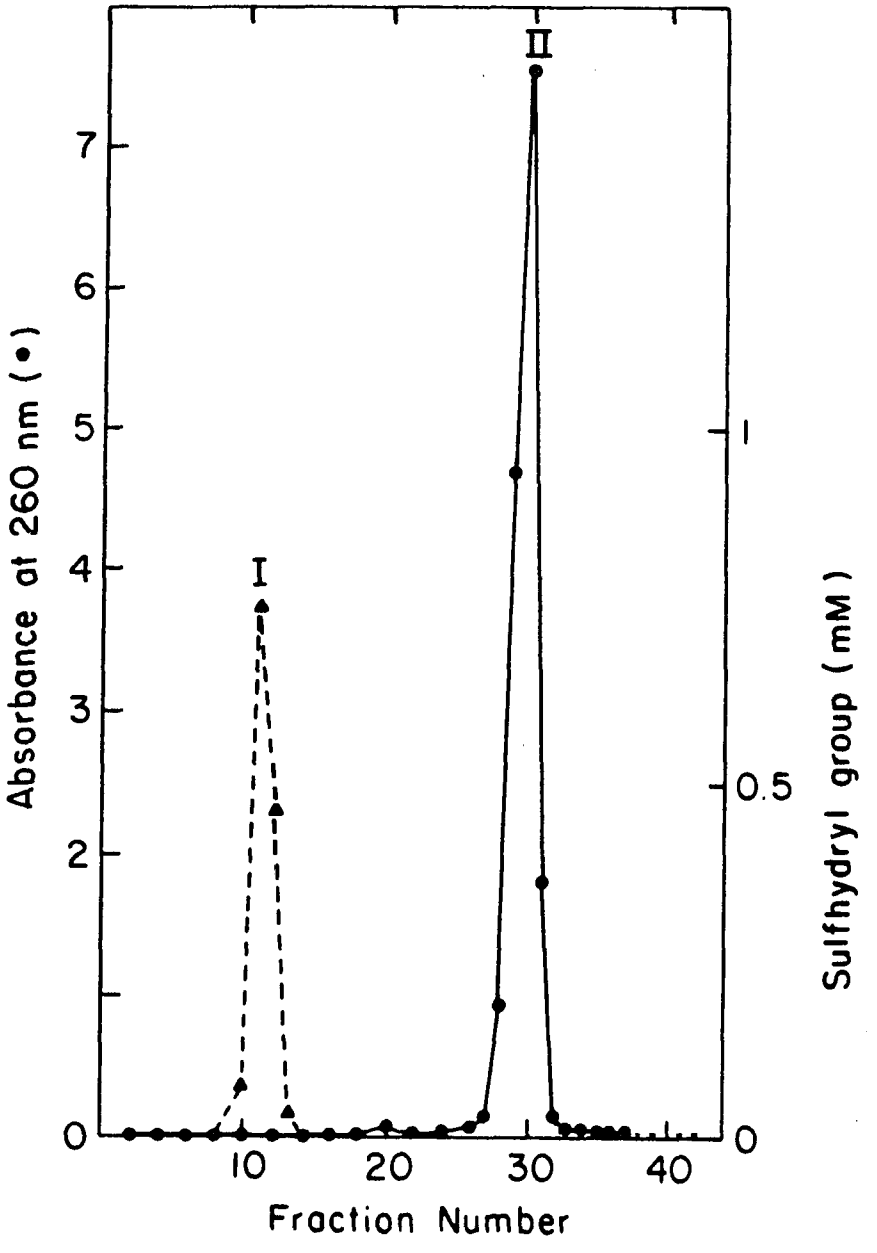

Figure 6

Chemical synthesis of 3-mercaptopropionyl-CoA.

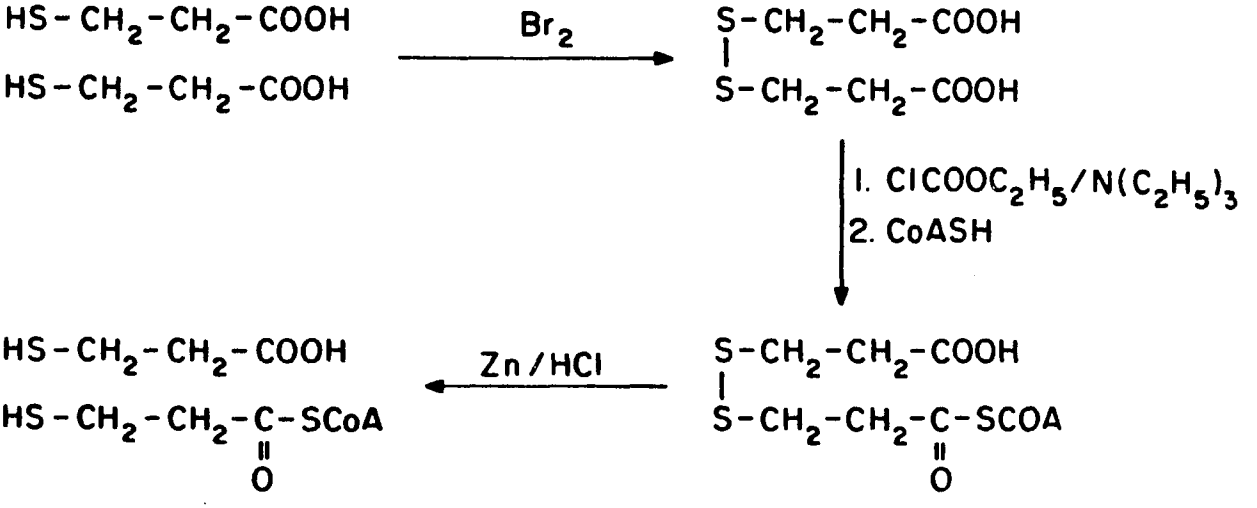

Figure 7

HPLC analysis of 3-mercaptopropionyl-CoA and its reaction products.

A, chemically synthesized 3-mercaptopropionyl-CoA . B, 3-mercaptopropionyl-CoA after reacting for 4 min with an equimolar amount of N-ethylmaleimide. C, the material shown in *panel B* after having been kept for 50 min at 25 °C and pH 10. D, the material shown an *panel C* after reacting with an excess of N-ethylmaleimide. For details see experimental section. The following peaks were identified by use of authentic materials: *III*, CoASH; *IV*, oxidized CoA (CoAS-SCoA)); *V*, reaction product of CoASH with N-ethylmaleimide.

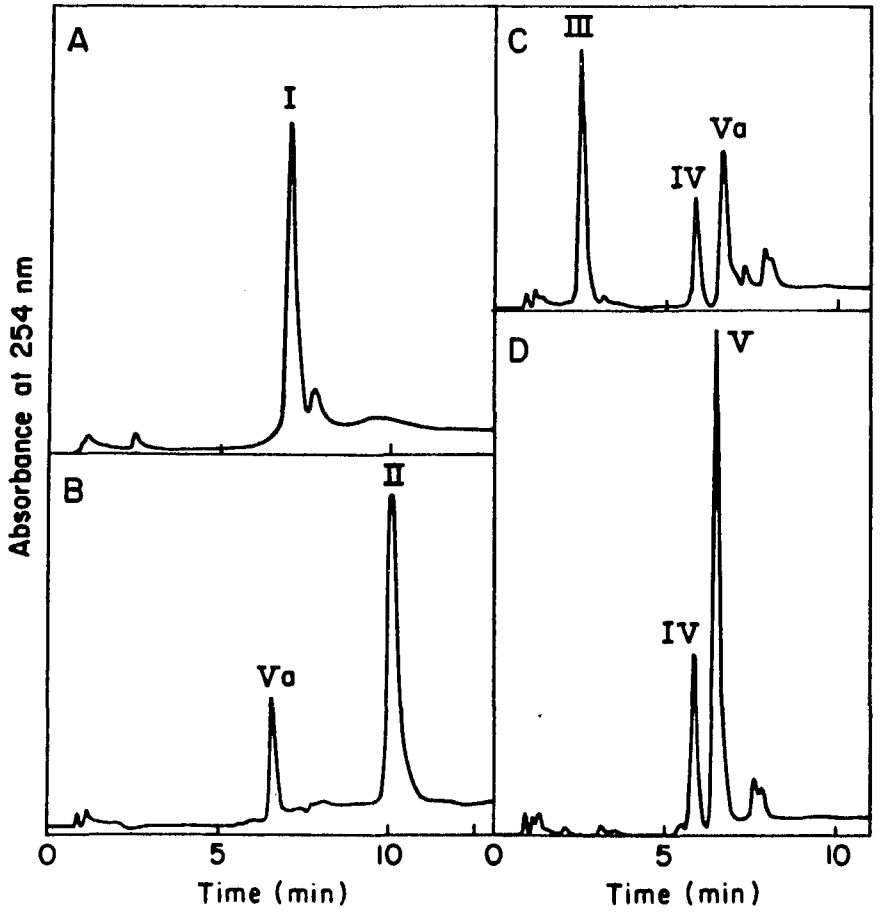

Figure 8

HPLC analysis of enzymatically formed 3-mercaptopropionyl-CoA. A, chromatogram obtained after incubating 3-mercaptopropionic acid with CoASH, ATP, $MgCl_2$, and soluble mitochondrial protein in 20 mM Tris-HCl (pH 8) for 50 min. B, chromatogram obtained after incubating 3-mercaptopropionyl-CoA and $MgCl_2$ in 20 mM Tris-HCl (pH 8) for 10 min. C, chromatogram obtained after incubating 3-mercaptopropionyl-CoA, $MgCl_2$, and soluble mitochondrial protein in Tris-HCl (pH 8) for 10 min. For experimental details see experimental section. Peaks identified by use of authentic materials; *I*, CoASH; *III*, oxidized CoA (CoAS-SCoA); *IV*, 3-mercaptopropionyl-CoA.

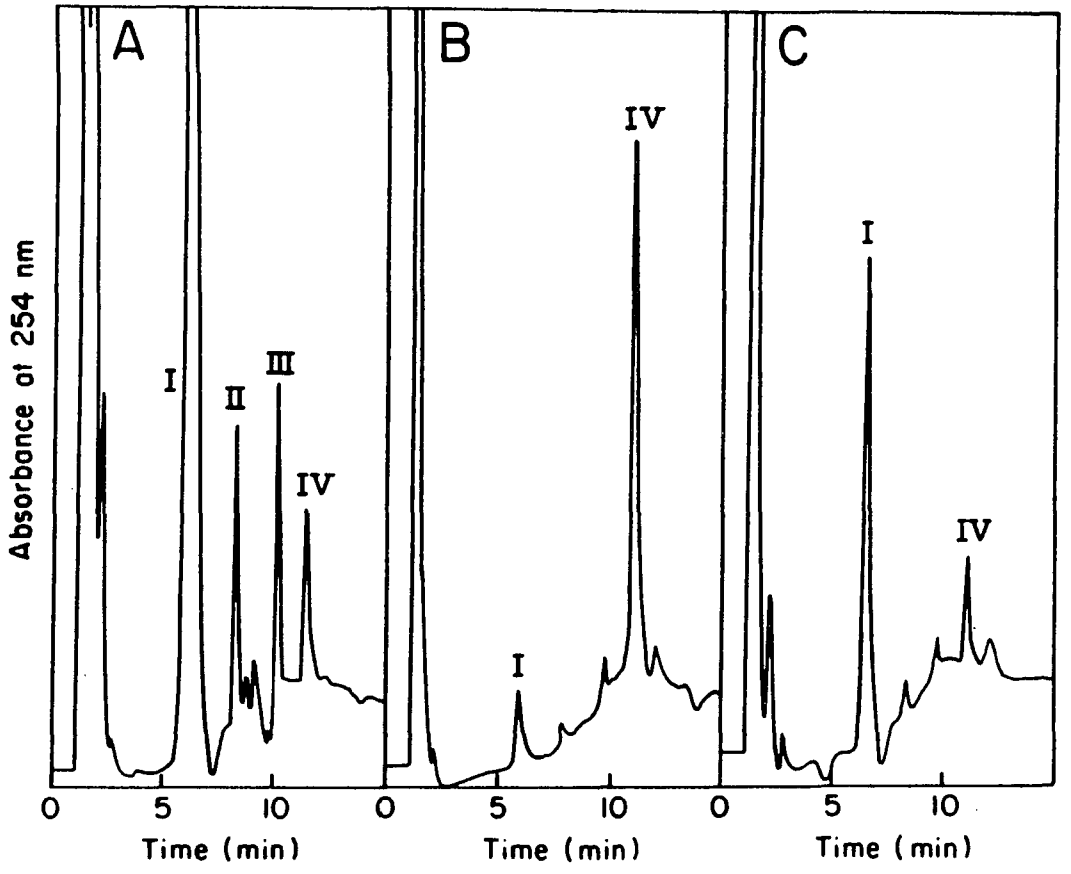

Figure 9

HPLC analysis of the products formed in the thiolase-catalyzed reaction between 3-mercaptopropionyl-CoA and acetoacetyl-CoA.

The reaction mixture contained 106 μM 3-mercaptopropionyl-CoA, 140 μM acetoacetyl-CoA, and pig heart 3-ketoacyl-CoA thiolase (16 milliunits) in 0.25 ml of 0.1 M KP_i (pH 8). The reaction was terminated after 90 s by the addition of 1.2 N HCl (50 μl). The solution was filtered after 5 min, and the pH was adjusted to 3 with 1 N KOH (20 μl). A, chromatograph obtained before thiolase was added. B, chromatogram obtained 90 s after the addition of enzyme. Peaks identified by use of authentic materials: *I*, acetoacetyl-CoA; *II*, 3-mercaptopropionyl-CoA; *III*, acetyl-CoA; *IV*, S-acetyl-3-mercaptopropionyl-CoA.

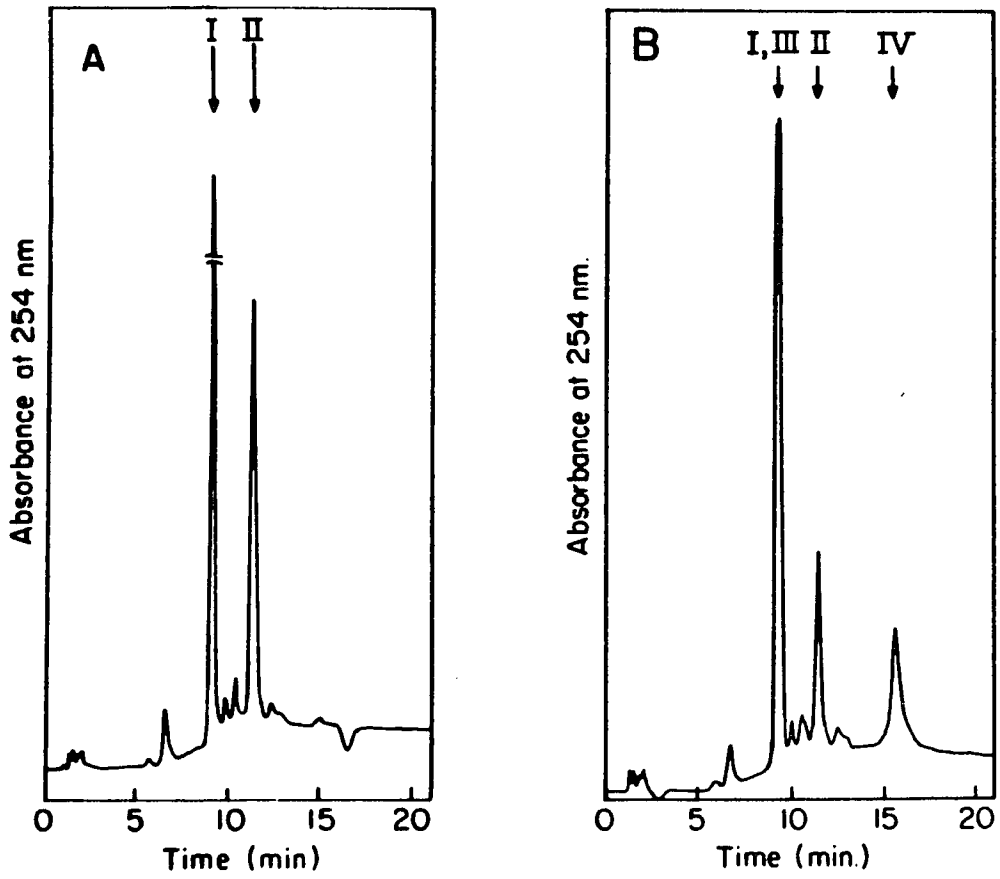

Figure 10

Kinetics of the reaction between acetoacetyl-CoA and either CoASH or 3-mercaptopropionyl-CoA catalyzed by 3-ketoacyl-CoA thiolase.

Data are plotted according to Hanes-Woolf. For experimental details see experimental section.

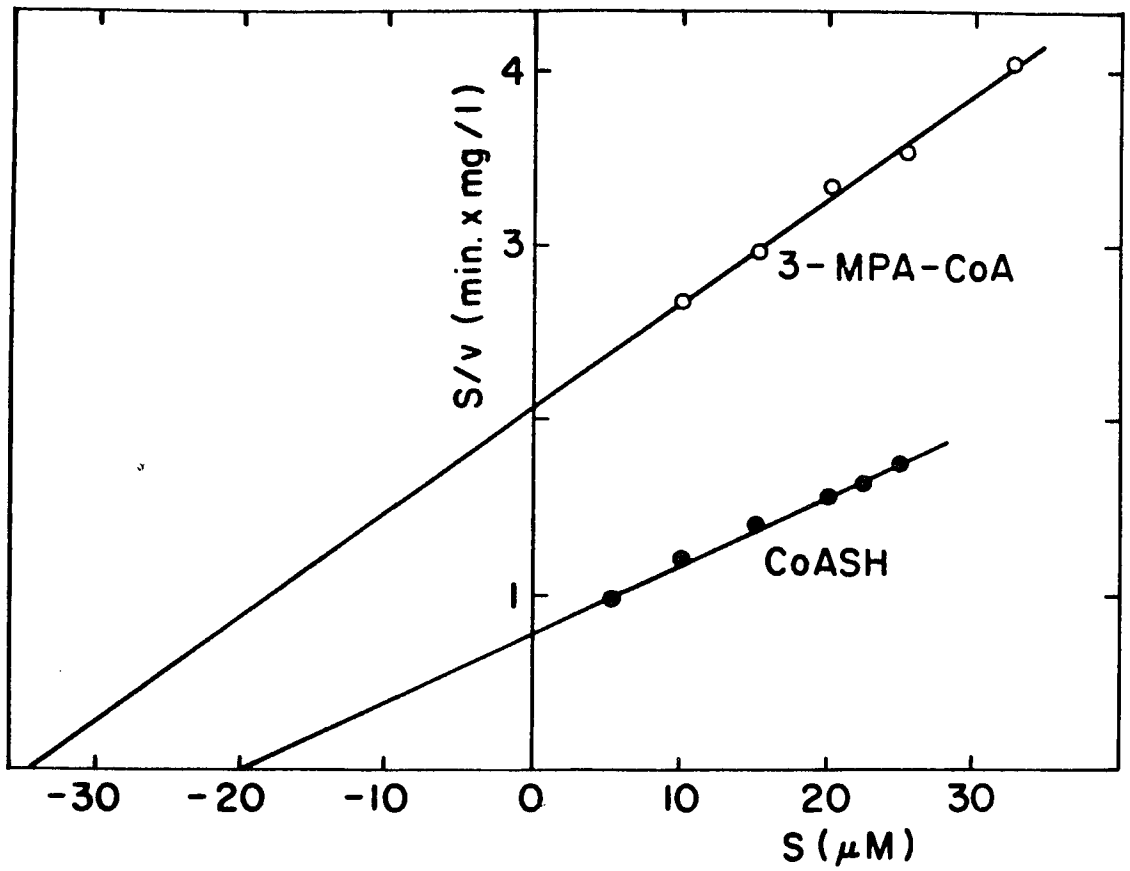

Figure 11

Inhibition of 3-ketoacyl-CoA thiolase and 3-hydroxyacyl-CoA dehydrogenase by S-myristoyl-3-mercaptopropionyl-CoA or palmitoyl-CoA.

A, 3-ketoacyl-CoA thiolase. B, 3-hydroxyacyl-CoA dehydrogenase. Circle, palmitoyl-CoA; triangle, S-myristoyl-3-mercaptopropionyl-CoA. 3-Ketoacyl-CoA thiolase was assayed spectrophotometrically at 303 nm as described in the experimental section. 3-Hydroxyacyl-CoA dehydrogenase was assayed spectrophotometrically at 340 nm as described in the experimental section except that 50 μM D,L-3-hydroxydodecanoyl-CoA was used as a substrate.

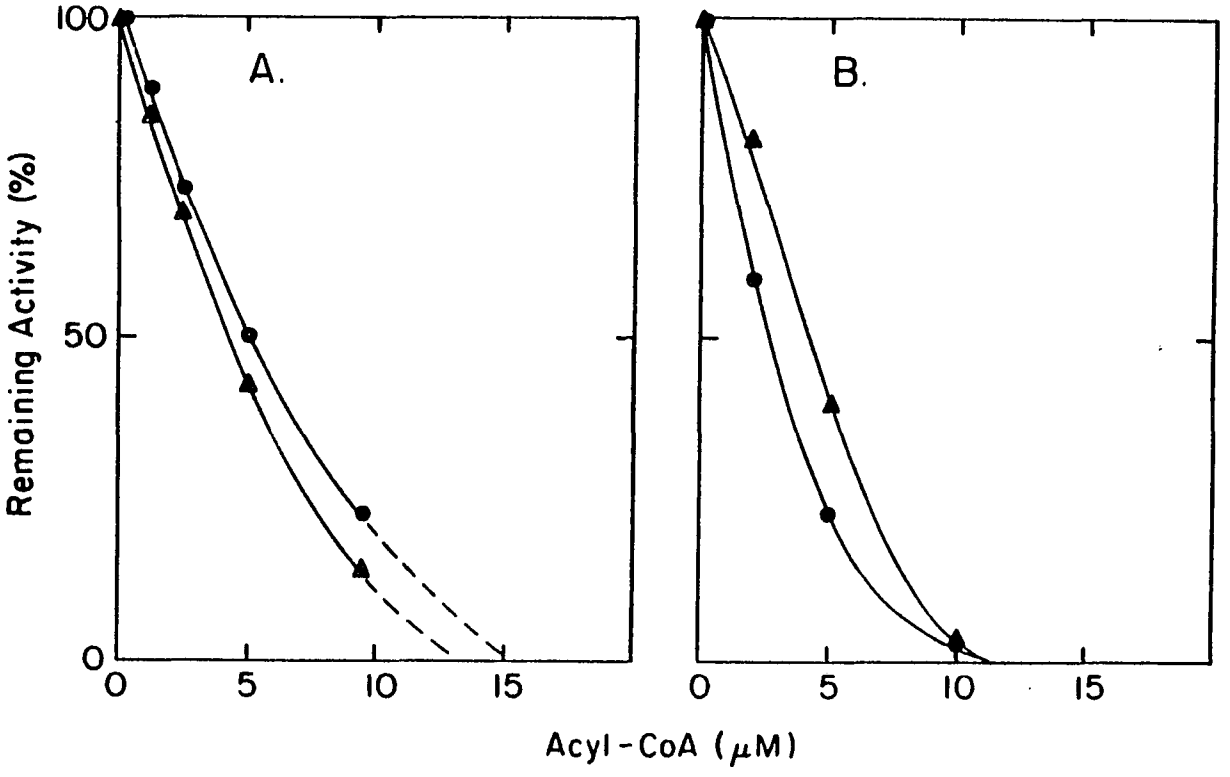

Figure 12

Inhibition of medium-chain acyl-CoA dehydrogenase by S-myristoyl-3-mercaptopropionyl-CoA.

The enzyme was assayed with 32 μM octanoyl-CoA as a substrate as described in the experimental section.

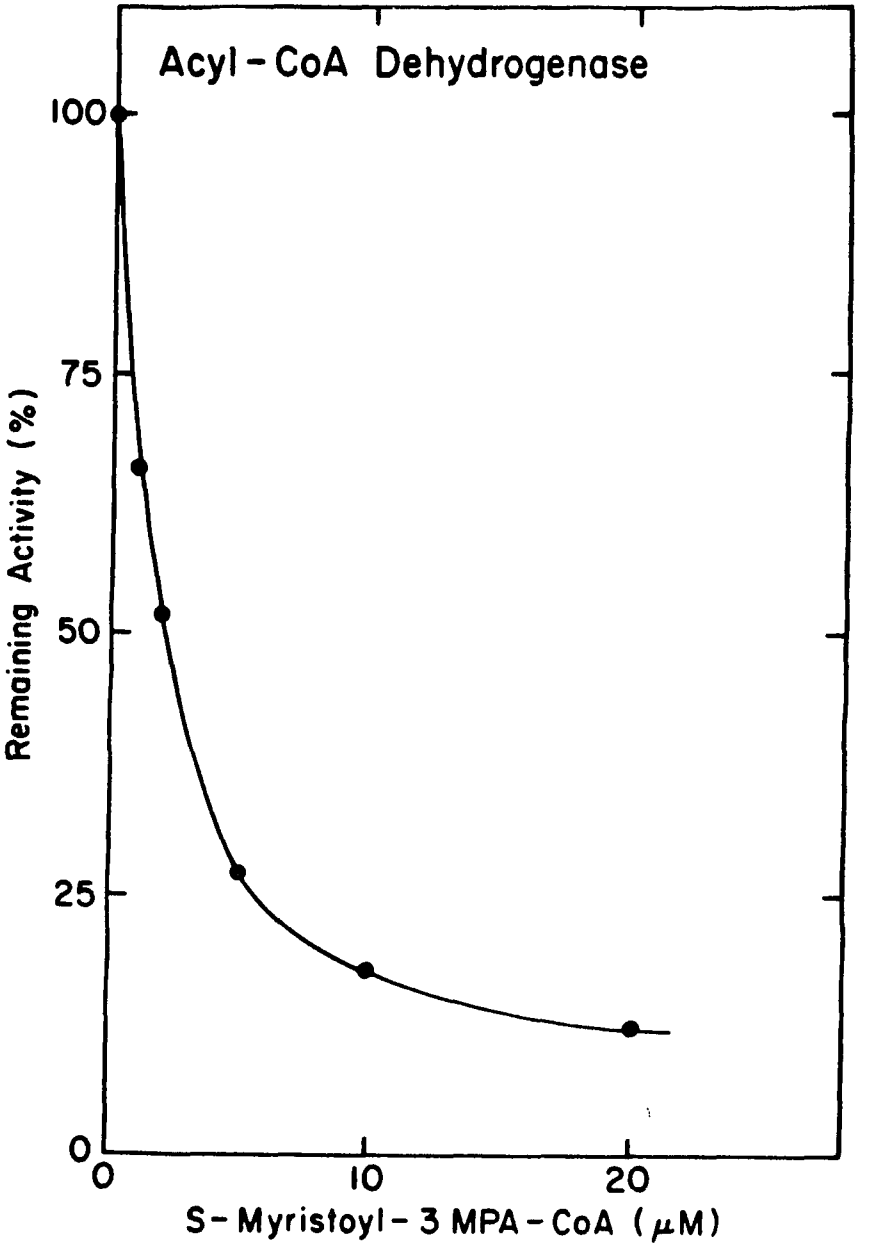

Figure 13

Mitochondrial metabolism of 3-mercaptopropionic acid.

I, 3-mercaptopropionic acid; *II*, 3-mercaptopropionyl-CoA; *III*, S-acyl-3-mercaptopropionyl-CoA; *IV*, S-acyl-3-mercaptopropionic acid. Enzymes involved in the mitochondrial metabolism of 3-mercaptopropionic acid are: A, acyl-CoA synthetase; B, thioesterase; C, 3-ketoacyl-CoA thiolase and acetoacetyl-CoA thiolase; D, acyl-CoA dehydrogenase; E, carnitine acyltranferase.

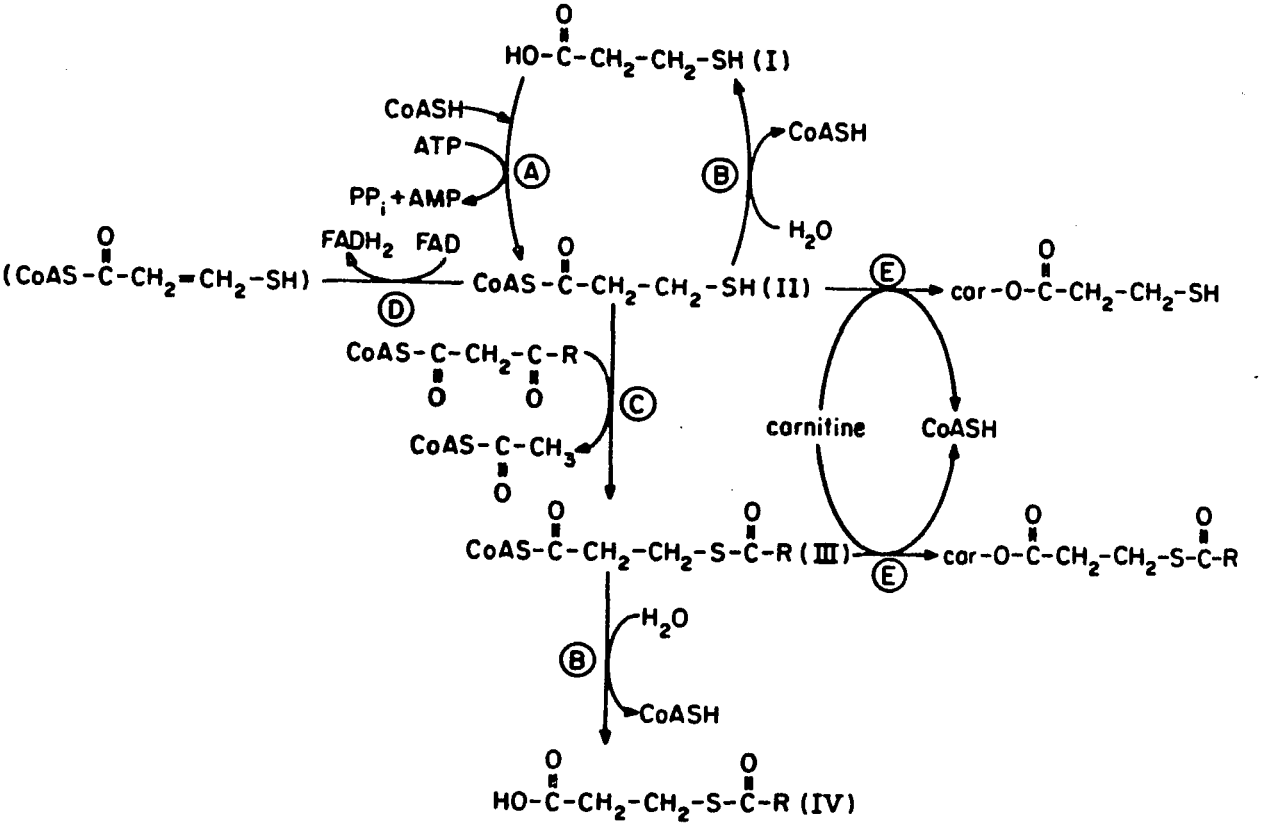

Figure 14

The pH dependence of the equilibrium of the 3-hydroxyacyl-CoA dehydrogenase-catalyzed oxidation of 3-hydroxy-4-*trans*-decenoyl-CoA and 3-hydroxybutyryl-CoA.

Circles, 3-hydroxy-4-*trans*-decenoyl-CoA; crosses, 3-hydroxybutyryl-CoA. The curves represent the theoretical predictions of the equilibrium position of the 3-hydroxyacyl-CoA dehydrogenase-catalyzed reaction using the experimentally determined equilibrium constant. For experimental details see the experimental section.

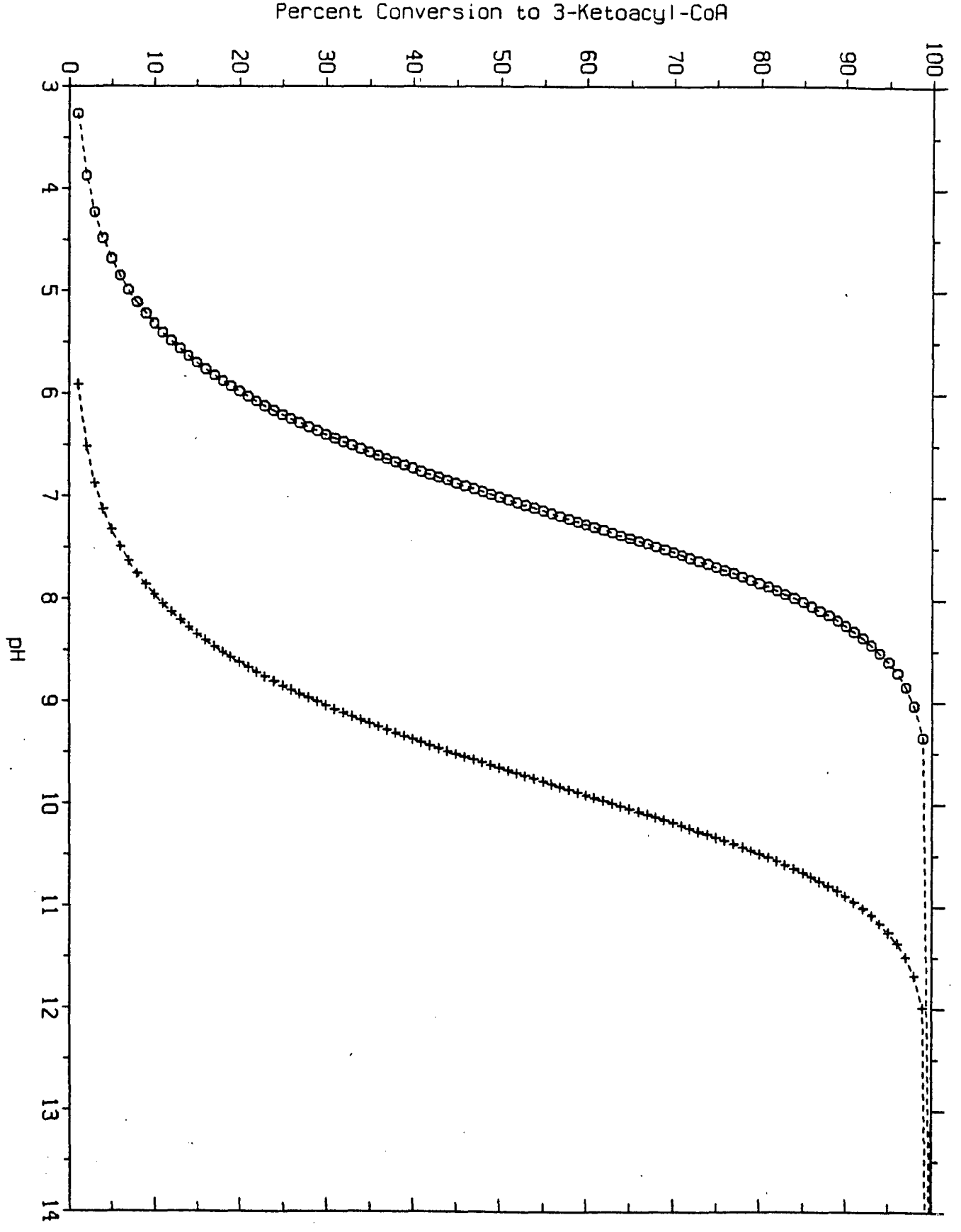
Percent Conversion to 3-Ketoacyl-CoA
0
10
20
30
40
50
60
70
80
90
100
pH
3
4
5
6
7
8
9
10
11
12
13
14

Figure 15

The dependence of the velocity of the coupled reaction on the ratio of the concentration of coupling enzyme to its Km for the intermediate.

The equations used to generate this plot assume that the equilibrium constant of the primary enzyme reaction is very low, and therefore [Pss] << K1f and K2f, and that the concentration of primary enzyme is much less than the concentration of the initial substrate. For details of kinetic parameters, see experimental section.

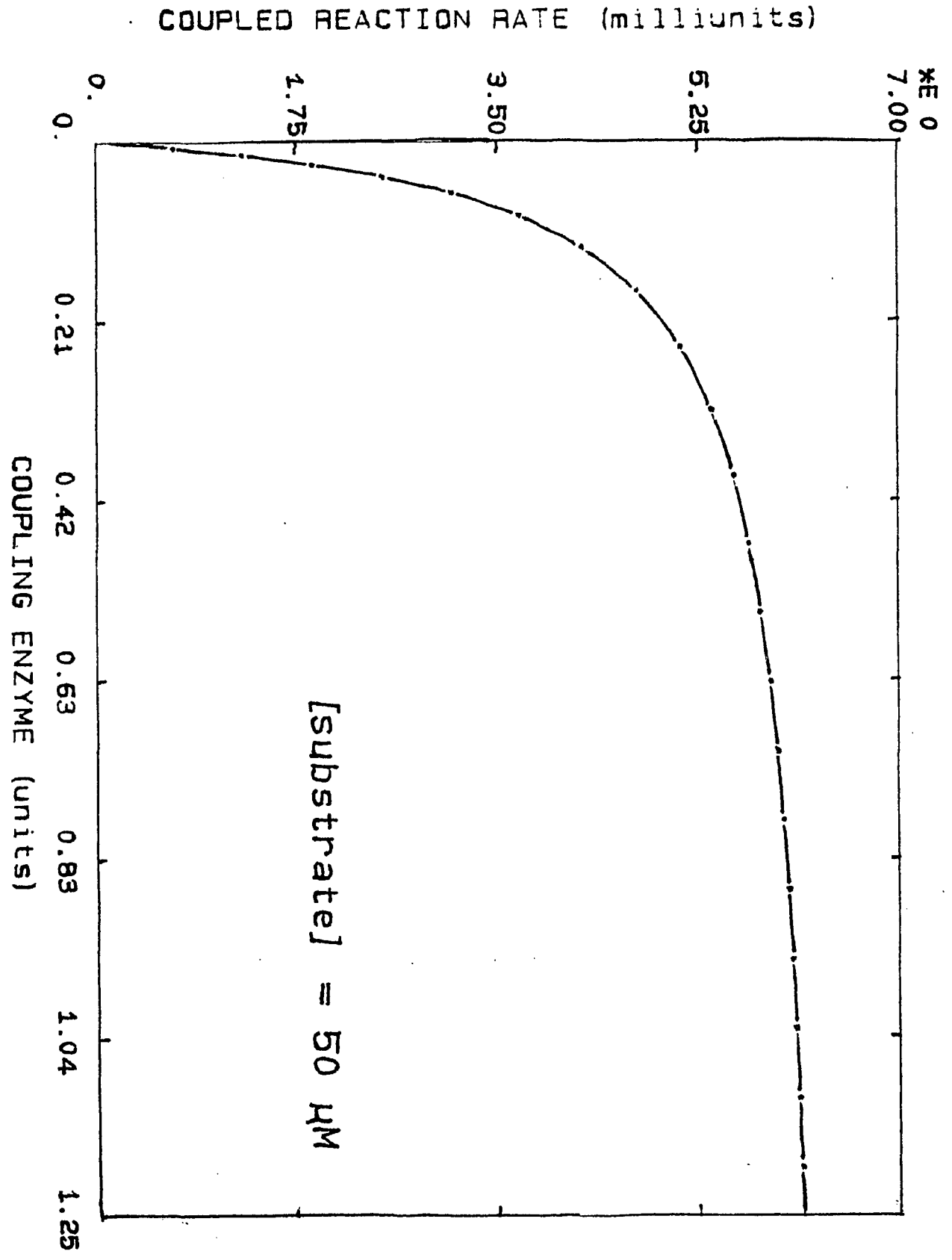
COUPLED REACTION RATE (milliunits)
0.
1.75
3.50
5.25
*E 0
7.00
0.
0.21
0.42
0.63
0.83
1.04
1.25
COUPLING ENZYME (units)
[substrate] = 50 μM

Figure 16

Eadie-Scatchard plot for the determination of the equilibrium constant of the primary reaction in coupled enzyme assays.

Lines 1-5 represent linearly increasing concentrations of primary enzyme from 0.1-0.5 μM. For details of the kinetic parameters, see the experimental section.

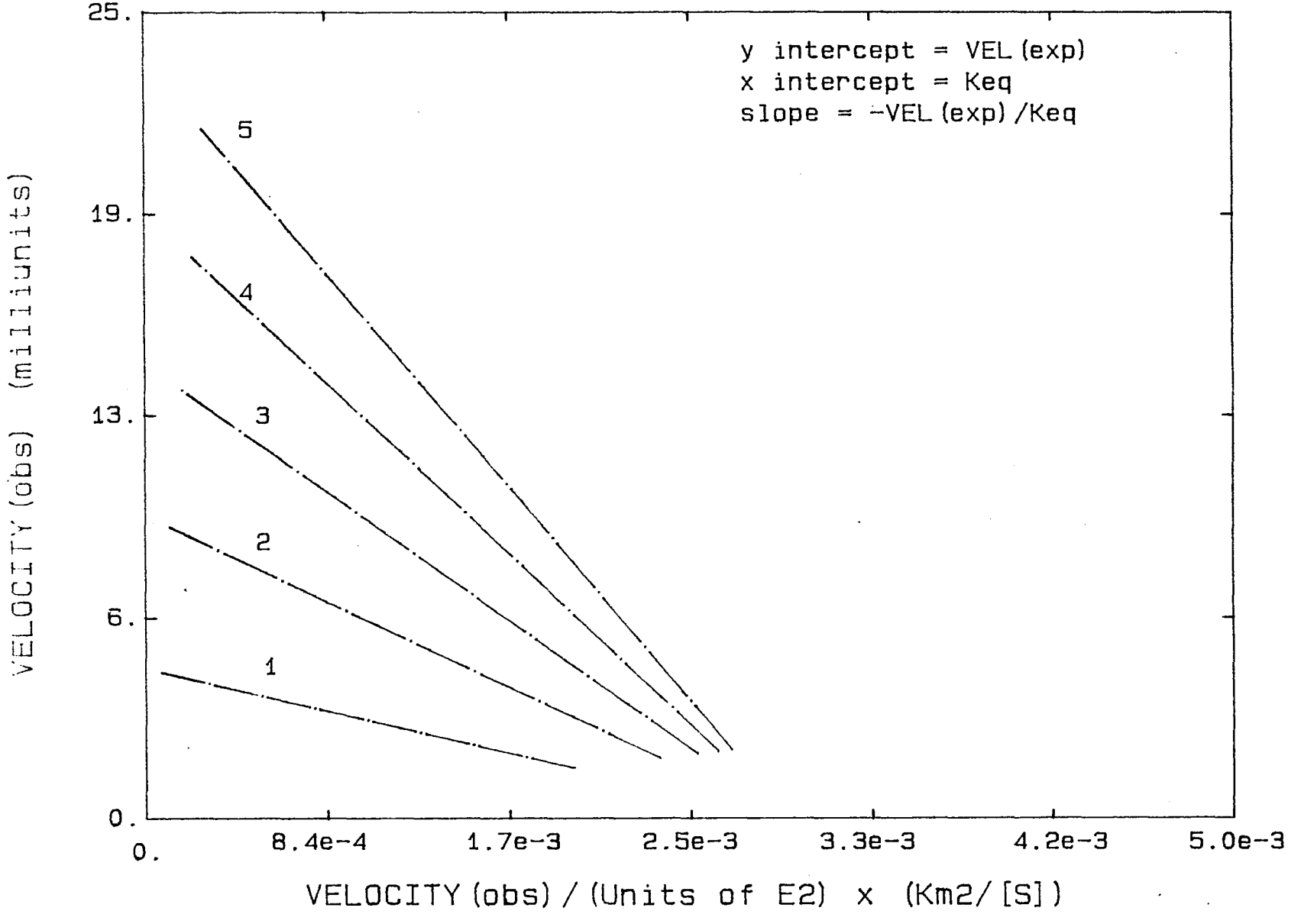
y intercept = VEL (exp)
x intercept = Keq
slope = -VEL (exp) /Keq
5
4
3
2
1
25.
19.
13.
6.
0.
0.
8.4e-4
1.7e-3
2.5e-3
3.3e-3
4.2e-3
5.0e-3
VELOCITY (obs) (milliunits)
VELOCITY (obs) / (Units of E2) x (Km2/[S])

Figure 17

The percent error between the use of equations (3) and (11) as a function of the [E2t]/Km2 ratio at two different substrate concentrations.

Curve 1 represents the theoretical error when the substrate concentration is 20 μM, and curve 2 is the error when the substrate concentration is 200 μM. For detail of kinetic parameters, see text and the experimental section.

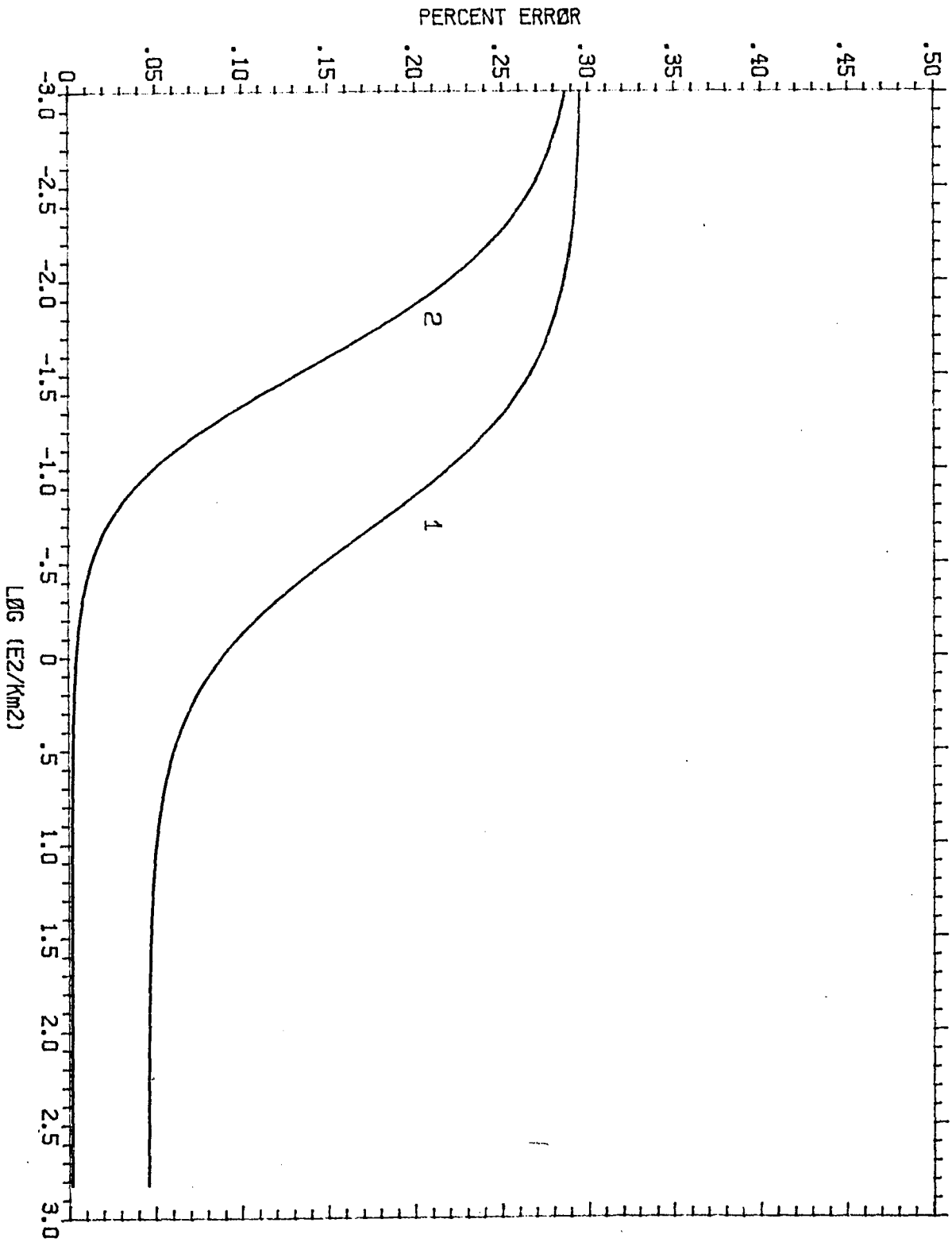
PERCENT ERRØR
0
.05
.10
.15
.20
.25
.30
.35
.40
.45
.50
-3.0
-2.5
-2.0
-1.5
-1.0
-.5
0
.5
1.0
1.5
2.0
2.5
3.0
LØG (E2/Km2)
2
1

Figure 18

The percent error between the use of equations (3) and (11) as a function of the [E2t]/Km2 ratio at various concentrations of primary enzyme.

Curves 1-10 represent linearly increasing concentrations of primary enzyme from 0.532-5.32 μM. For detail of kinetic parameters, see text and experimental section.

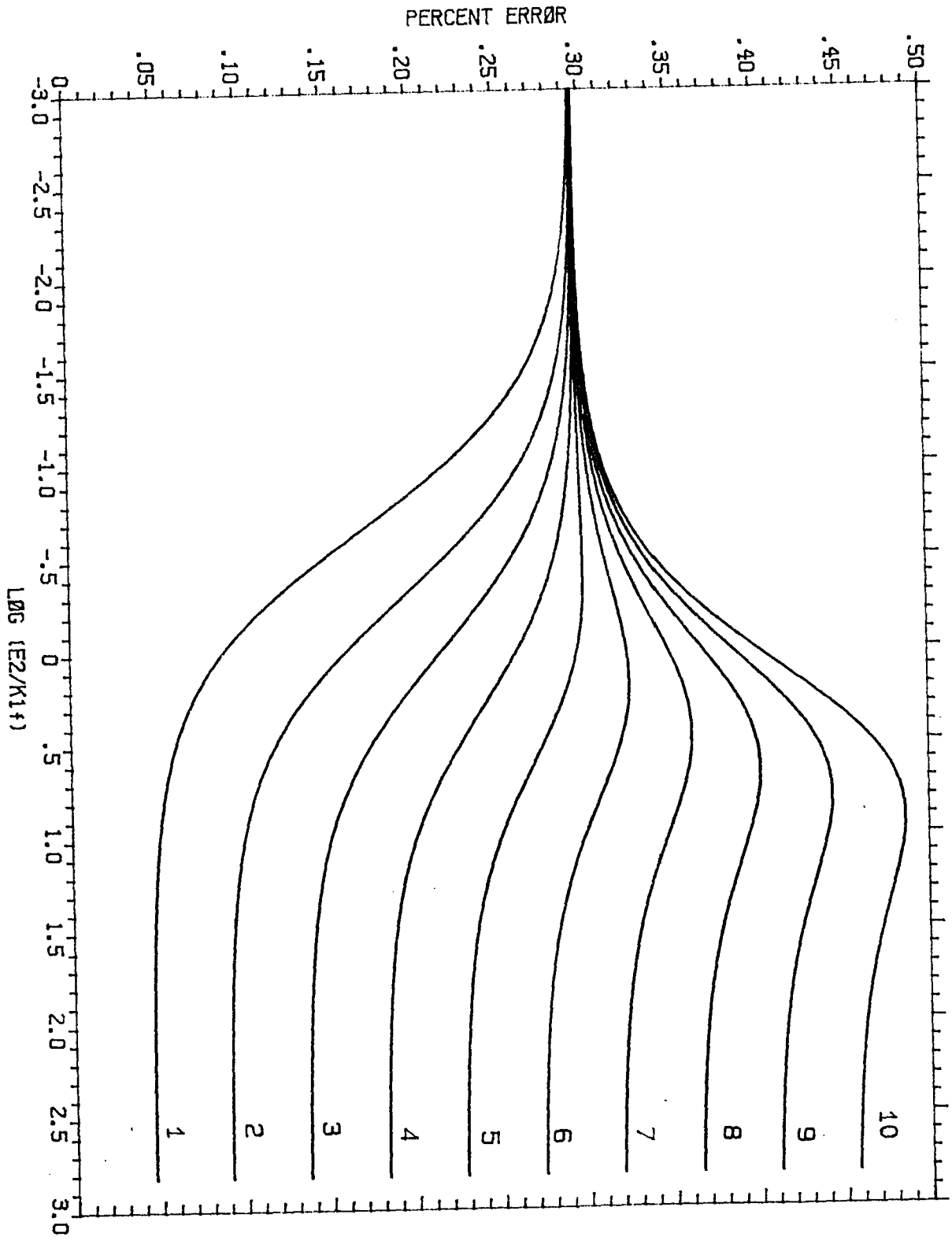
PERCENT ERRØR
.05
.10
.15
.20
.25
.30
.35
.40
.45
.50
0
-3.0
-2.5
-2.0
-1.5
-1.0
-.5
0
.5
1.0
1.5
2.0
2.5
3.0
LØG (E2/K1+)
1
2
3
4
5
6
7
8
9
10

Figure 19

The percent error between use of equations (3) and the true cubic polynomial rate equation as a function of the [E2t]/Km2 ratio at various concentrations of primary enzyme.

The log of the percent error is shown as a function of the log of the [E2t]/Km2 ratio at logarithmically increasing ratios of [E1t]/K1f from 1.0×10^{-2} to 1.0×10^{2}. For details of kinetic parameters, see text and experimental section.

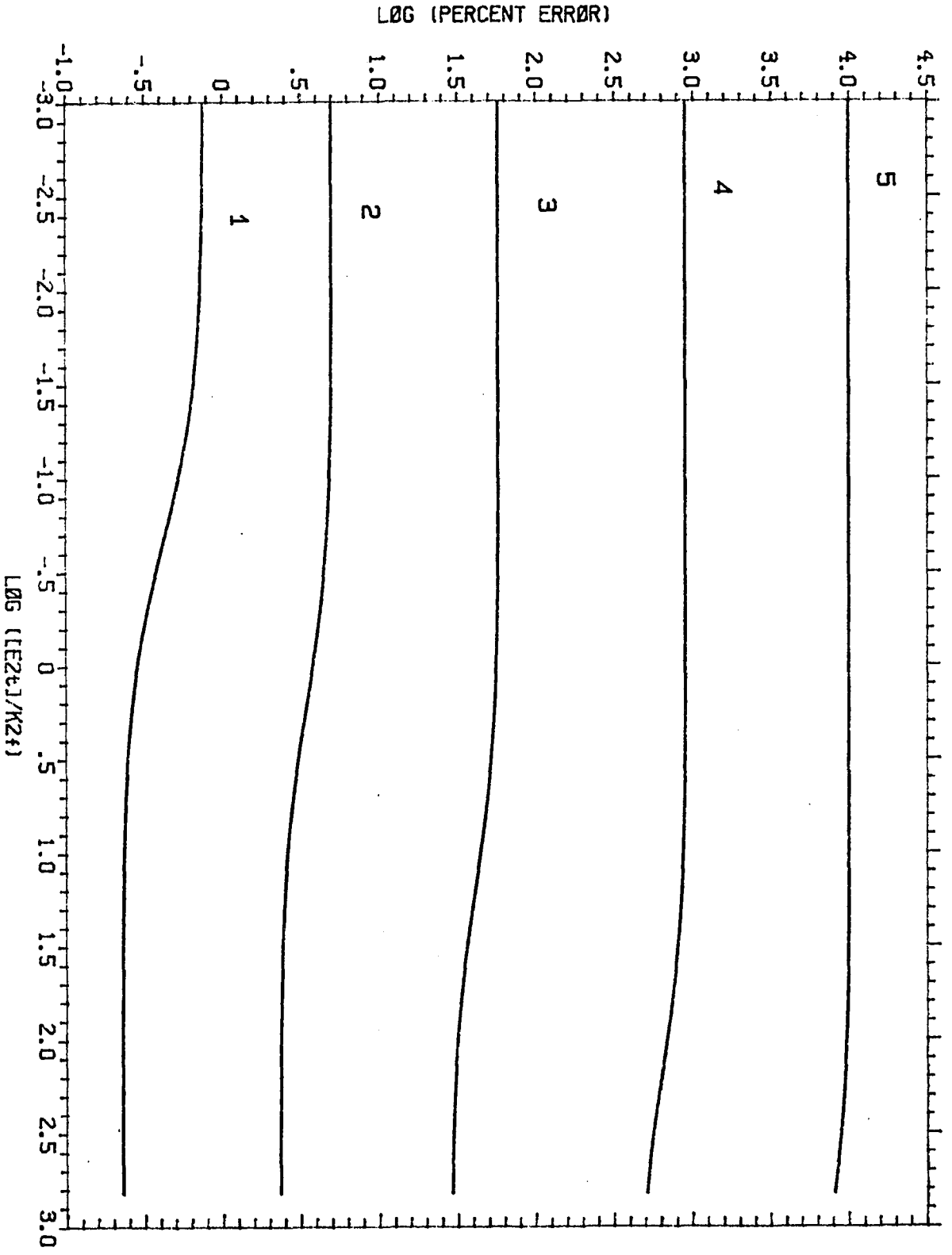
LØG (PERCENT ERRØR)
4.5
4.0
3.5
3.0
2.5
2.0
1.5
1.0
.5
0
-.5
-1.0
-3.0
-2.5
-2.0
-1.5
-1.0
-.5
0
.5
1.0
1.5
2.0
2.5
3.0
1
2
3
4
5
LØG (LE2t]/K2t)

Figure 20

The percent error between use of equations (3) and the true cubic polynomial rate equation as a function of the [E2t]/Km2 ratio at various concentrations of primary enzyme.

The percent error is shown as a function of the log of the [E2t]/Km2 ratio at logarithmically increasing ratios of [E1t]/K1f from 1.0×10^{-2} to 1.0. Curve 1, [E1t]/K1f = 0.01; curve 2, [E1t]/K1f = 0.1; curve 3, [E1t]/K1f = 1.0. The concentration of substrate is 200 μM. For details of kinetic parameters, see text and experimental section.

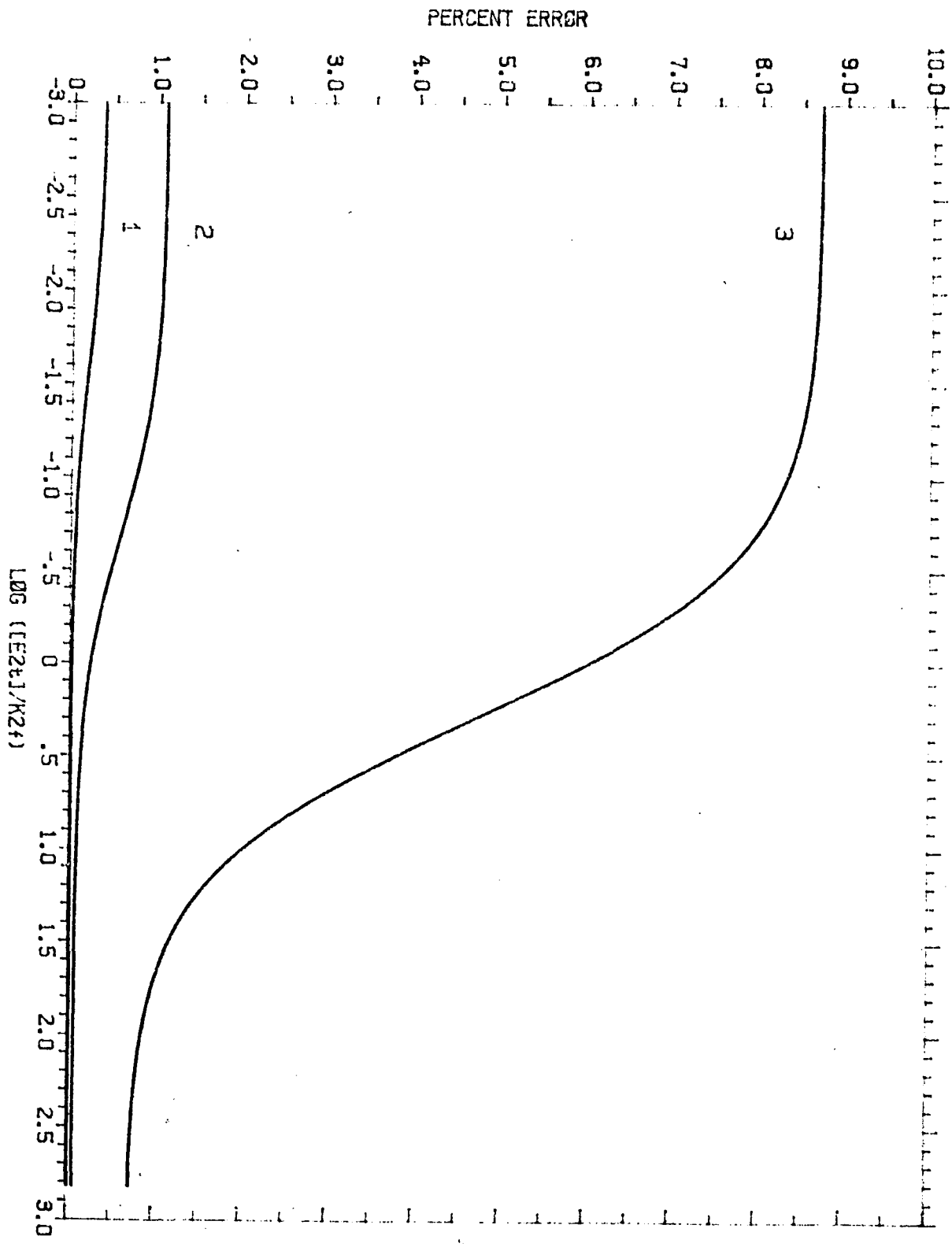
PERCENT ERROR
10.0
9.0
8.0
7.0
6.0
5.0
4.0
3.0
2.0
1.0
0
1
2
3
-3.0
-2.5
-2.0
-1.5
-1.0
-.5
0
.5
1.0
1.5
2.0
2.5
3.0
LOG ((E2+)/K2+)

References

1. DiMauro, S., Trevisan, C., and Hays, A., *Muscle and Nerve*, vol. 3, pp. 369-388, 1980.

2. Rhead, W. J., Amendt, B. A., Fritchman, K. S., and Felts, S. J., *Science*, vol. 221, pp. 73-75, 1983.

3. Lynen, F., *Harvey Lectures*, vol. Ser. 48, pp. 210-244, 1952-1953.

4. Dakin, H., *J. Biol. Chem.*, vol. 6, pp. 203-219, 1909.

5. Schulz, H., "Oxidation of Fatty Acids," in *Biochemistry of Lipids and Membranes*, ed. Vance, J. E., pp. 116-142, Benjamin-Cummings, Menlo Park, CA., 1985.

6. El-Aleem, S. A. and Schulz, H., *Federation Proceedings*, vol. 45, p. 1595, 1986.

7. McGarry, J. D. and Foster, D., *Ann. Rev. Biochem.*, vol. 49, pp. 395-420, 1980.

8. Olowe, Y. and Schulz, H., *J. Biol. Chem.*, vol. 257, pp. 5408-5413, 1982.

9. Schulz, H. and Fong, J. C., *Methods Enzymol.*, vol. 72, pp. 604-610, 1981.

10. Billington, D., Osmundsen, H., and Sherratt, H. S. A., *Biochem. Pharmacol.*, vol. 27, pp. 2879-2900, 1978.

11. Mahadevan, S. and Sauer, F., *J. Biol. Chem.*, vol. 246, pp. 5862-5867, 1971.

12. Chase, J. F. A. and Tubbs, P. K., *Biochem. J.*, vol. 129, pp. 55-65, 1972.

13. Turnbull, D. M., Bartlett, K., Younan, S. I. M., and Sherratt, H. S. A., *Biochem. Pharmacol.*, vol. 33, pp. 475-481, 1984.

14. Sherratt, H. S. A., *Biochem. Biophys. Res. Commun.*, vol. 117, pp. 653-657, 1983.

15. Kiorpes, T. C., Hoerr, D., Ho, W., Weaner, L. E., Inman, M. G., and Tutwiler, T. C., *J. Biol. Chem.*, vol. 259, pp. 9750-9755, 1984.

16. Tutwiler, G. F. and Dellevigne, P., *J. Biol. Chem.*, vol. 254, pp. 2935-2941, 1979.

17. Sabourault, D., Bauche, F., Giudicelli, Y., Nordmann, J., and Nordmann, R., *FEBS Lett.*, vol. 108, pp. 465-468, 1979.

18. Bauche, F., Sabourault, D., Giudicelli, Y., Nordmann, J., and Nordmann, R., *Biochem. J.*, vol. 206, pp. 53-59, 1982.

19. Bauche, F., Sabourault, D., Giudicelli, Y., Nordmann, J., and Nordmann, R., *Biochem. J.*, vol. 196, pp. 803-809, 1981.

20. Bauche, F., Sabourault, D., Giudicelli, J., Nordmann, J., and Nordmann, R., *Biochem J.*, vol. 215, pp. 457-464, 1983.

21. Sabbagh, E., Cuebas, D., and Schulz, H., *J. Biol. Chem.*, vol. 260, pp. 7337-7342, 1985.

22. Sprince, H., Parker, C. M., Josephs, J. A., and Magazino, J., *Ann. N. Y. Acad. Sci.*, vol. 166, pp. 323-325, 1969.

23. Karlson, A., Fonnum, F., Malthe-Soressen, D., and Storm-Mathisen, J., *Biochem. Pharmacol.*, vol. 23, pp. 3053-3061, 1974.

24. De Lores Arnaiz, G. R., de Esteves, B. R., and de Pacheco, M. M., *Biochem. Pharmacol.*, vol. 24, pp. 2307-2309, 1975.

25. Davidoff, F. and Korn, E., *J. Biol. Chem.*, vol. 240, pp. 1549-1558, 1965.

26. Struijk, C. and Beerthuis, R. K., *Biochim. Biophys. Acta*, vol. 116, pp. 12-22, 1966.

27. Stoffel, W., Ditzer, R., and Caesar, H., *Hoppe-Seyler's Z. Physiol. Chem.*, vol. 339, pp. 167-181, 1964.

28. Miesowicz, F. M. and Bloch, C., *J. Biol. Chem.*, vol. 254, pp. 5868-5877, 1979.

29. Stoffel, W. and Grol, M., *Hoppe-Seyler's Z. Physiol. Chem.*, vol. 359, pp. 1777-1782, 1978.

30. Stoffel, W. and Caesar, H., *Hoppe-Seyler's Z. Physiol. Chem.*, vol. 341, pp. 76-83, 1965.

31. Kunau, W. H. and Dommes, P., *Eur. J. Biochem.*, vol. 91, pp. 533-544, 1978.

32. Kunau, W. H. and Bartnik, F., *Eur. J. Biochem.*, vol. 48, pp. 311-318, 1974.

33. Dommes, V. and Kunau, W. H., *J. Biol. Chem.*, vol. 259, pp. 1781-1788, 1984.

34. Dommes, V., Luster, W., Cvetanovic, M, and Kunau, W. H., *Eur. J. Biochem.*, vol. 125, pp. 335-341, 1982.

35. Moreno de la Garza, M., Schultz-Borchard, U., Crabb, J. W., and Kunau, W. H., *Eur. J. Biochem.*, vol. 148, pp. 285-291, 1985.

36. Osmundsen, H., Cervenka, J., and Bremer, J., *Biochem. J.*, vol. 208, pp. 749-757, 1982.

37. Kunau, W. H. and Lauterbach, F., *Febs Letters*, vol. 94, pp. 120-123, 1978.

38. Cuebas, D. and Schulz, H., *J. Biol. Chem.*, vol. 257, pp. 14140-14144, 1982.

39. Lazarow, P. B., *J. Biol. Chem.*, vol. 253, pp. 1522-1528, 1978.

40. Osmundsen, H., Neat, C. E., and Norum, K. R., *Febs Letters*, vol. 99, pp. 292-296, 1979.

41. Lazarow, P. B. and De Duve, C., *Proc. Natl. Acad. Sci. USA*, vol. 73, pp. 2043-2046, 1976.

42. Osumi, T. and Hashimoto, T., *Arch. Biochem. Biophys.*, vol. 203, pp. 372-383, 1980.

43. Binstock, J. F., Pramanik, A., and Schulz, H., *Proc. Natl. Acad. Sci. USA*, vol. 74, pp. 492-495, 1977.

44. Yang, S-Y. and Schulz, H., *J. Biol. Chem.*, vol. 258, pp. 9780-9785, 1983.

45. Wakil, S. J. and Hubscher, G., *J. Biol. Chem.*, vol. 235, pp. 1554-1558, 1960.

46. Holland, P. C., Senior, A. E., and Sherratt, H. S. A., *Biochem. J.*, vol. 136, pp. 173-184, 1973.

47. Yang, S-Y., Bittman, R., and Schulz, H., *J. Biol. Chem.*, vol. 260, pp. 2862-2868, 1985.

48. Yang, S-Y., Cuebas, D., and Schulz, H., *J. Biol. Chem.*, 1986. in press

49. Cha, S., *J. Biol. Chem.*, vol. 215, pp. 4814-4818, 1970.

50. Straus, O. H. and Goldstein, A., *J. Gen. Physiol.*, vol. 26, pp. 559-585, 1943.

51. Reiner, J. M, *Behavior of Enzyme Systems*, Van Nostrand Reinhold, New York, 1968. 2nd edn.

52. Cornish-Bowden, A., *J. Mol. Biol.*, vol. 101, pp. 1-9, 1976.

53. Griffith, J. W., *Biochem. Soc. Trans.*, vol. 7, pp. 429-439, 1979.

54. Staack, H., Binstock, J. F., and Schulz, H., *J. Biol. Chem.*, vol. 253, pp. 1827-1831, 1978.

55. Steinman, H. and Hill, R. L., *Methods Enzymol.*, vol. 35, pp. 136-151, 1975.

56. Davidson, B. and Schulz, H., *Arch. Biochem. Biophys.*, vol. 213, pp. 155-162, 1982.

57. Osumi, T. and Hashimoto, T., *Biochem. Biophys. Res. Commun.*, vol. 83, pp. 479-485, 1978.

58. Osumi, T. and Hashimoto, T., *Biochem. Biophsy. Res. Commun.*, vol. 89, pp. 580-584, 1979.

59. Chappell, J. B., Hansford, R. G., and (Birnie, G. D., ed.), *Subcellular Components*, pp. 77-91, Butterworth, London, 1969. 2nd Ed.

60. Jacobs, E. E., Jacob, M, Sanadi, D. R., and Bradley, L. D., *J. Biol. Chem.*, vol. 223, pp. 147-156, 1956.

61. Goldman, P. and Vagelos, P. R., *J. Biol. Chem.*, vol. 236, pp. 2620-2623, 1961.

62. Weeks, G. and Wakil, S. J., *J. Biol. Chem.*, vol. 243, pp. 1180-1189, 1968.

63. Seubert, W. and (Lardy, H. A.), *Biochemical Preparations*, 7, p. 80, John Wiley and Sons, New York, 1960.

64. Seubert, W., Lamberts, I., Kramer, R., and Ohly, B., *Biochim. Biophys. Acta*, vol. 164, pp. 498-517, 1968.

65. Ellman, G. L., *Arch. Biochem. Biophys.*, vol. 82, pp. 70-77, 1959.

66. Drabowicz, J. and Mikolajczyk, M, *Synthesis*, vol. 1, pp. 32-34, 1980.

67. Stout, E. I., Shasha, B. S., and Doane, W. M, *J. Org. Chem.*, vol. 39, pp. 562-563, 1974.

68. Holmberg, B. and Schjanberg, E., *Ark. Mineral. Geol.*, vol. 14A, 1940. Article 7

69. Ruppert, J. F. and White, J. D., *J. Org. Chem.*, vol. 39, pp. 269-270, 1974.

70. Stoffel, W., Caesar, H., and Ditzer, R., *Hoppe-Seyler's Z. Physiol. Chem.*, vol. 339, pp. 182-189, 1964.

71. Thomason, S. C. and Kubler, D. G., *J. Chem. Ed.*, vol. 45, pp. 546-547, 1968.

72. Hoskins, D. D., *Methods Enzymol.*, vol. 14, pp. 110-114, 1969.

73. Beckmann, J. D. and Frerman, F. E., *J. Biol. Chem.*, vol. 258, pp. 7563-7569, 1983.

74. Schulz, H. and Staack, H., *Methods Enzymol.*, vol. 71, pp. 398-403, 1981.

75. Duncombe, G. R. and Frerman, F., *Arch. Biochem. Biophys.*, vol. 176, pp. 159-170, 1976.

76. Chase, J. F. A., *Methods Enzymol.*, vol. 13, pp. 387-393, 1969.

77. Shepard, D. and Garland, P. B., *Methods Enzymol.*, vol. 13, pp. 11-16, 1969.

78. Binstock, J. F. and Schulz, H., *Methods Enzymol.*, vol. 71, pp. 403-411, 1981.

79. Cuebas, D., Beckmann, J. D., Frerman, F. E., and Schulz, H., *J. Biol. Chem.*, vol. 260, pp. 7330-7336, 1985.

80. Hansford, R. G. and Johnson, R. N, *J. Biol. Chem.*, vol. 250, pp. 8361-8375, 1975.

81. Mahler, H. M., Wakil, S. J., and Bock, R. M, *J. Biol. Chem.*, vol. 204, pp. 453-468, 1953.

82. Clark, P. R. H. and Bieber, L. L., *J. Biol. Chem.*, vol. 256, pp. 9861-9868, 1981.

83. Wakil, S. J., "β-Hydroxyacyl-CoA Dehydrogenases," in *The Enzymes*, vol. 7, pp. 97-103, Academic Press, New York, 1960.

84. Kimura, C., Kondo, A., Koeda, N, Yamanaka, H., and Mizugaki, M, *J. Biochem.*, vol. 96, pp. 1463-1469, 1984.

85. Pullman, M. E., *Anal. Biochem.*, vol. 54, pp. 188-198, 1973.

86. Rickards, G. and Weiler, L., *J. Org. Chem.*, vol. 43, pp. 3607-3609, 1978.

87. Mizugaki, M., Kimura, C., Nishimaki, T., Yamamoto, H., Sagi, M., Nishimura, S., and Yamanaka, H., *J. Biochem.*, vol. 92, pp. 1671-1674, 1982.

88. Crombie, L., *J. Chem. Soc: London*, pp. 1007-1025, 1955.

89. Easterby, J. S., *Biochem. Biophys. Acta*, vol. 293, pp. 552-558, 1973.

90. Storer, A. C. and Cornish-Bowden, A., *Biochem. J.*, vol. 141, pp. 205-209, 1974.

91. Easterby, J. S., *Biochem. J.*, vol. 199, pp. 155-161, 1981.

92. Cleland, W. W., *Anal. Biochem.*, vol. 99, pp. 142-145, 1979.

93. Kuchel, P., "Chapter 7," in *Organized Multienzyme Systems: Catalytic Properties*, ed. Welch, G. R., Academic Press, Inc., New York, 1985.

94. Varfolomeev, S. D., *Mol. Biol.*, vol. 11, pp. 790-880, 1977. (English trans. pp. 430-443)

95. Cleland, W. W., *Biochim. Biophys. Acta*, vol. 67, p. 104, 1963.

96. Chaplin, M. F., *Trends Biochem. Sci.*, vol. 6, 1981. VI

97. Robson, B., *Trends Biochem. Sci.*, vol. 6, 1981. XII-XIV